SEISMIC SIMULATION OF THREE-STOREY GLULAM FRAMED STRUCTURES WITH MORTISE AND TENON DESIGN

GERALDINE CHUA JIA XUAN

A project report submitted in partial fulfilment of the requirements for the award of Master of Engineering (Civil)

Lee Kong Chian Faculty of Engineering and Science
Universiti Tunku Abdul Rahman

September 2023

DECLARATION

I hereby declare that this project report is based on my original work except for citations and quotations which have been duly acknowledged. I also declare that it has not been previously and concurrently submitted for any other degree or award at UTAR or other institutions.

Signature : _____

Name : Geraldine Chua Jia Xuan
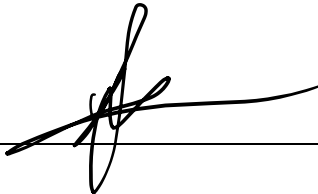
ID No. : 23UEM01762

Date : 05 April 2024

APPROVAL FOR SUBMISSION

I certify that this project report entitled **"SEISMIC SIMULATION OF THREE-STOREY GLULAM FRAMED STRUCTURES WITH MORTISE AND TENON DESIGN"** was prepared by **GERALDINE CHUA JIA XUAN** has met the required standard for submission in partial fulfilment of the requirements for the award of Master of Engineering (Civil) at Universiti Tunku Abdul Rahman.

Approved by,

Signature   :

Supervisor   :   Ir. Ts. Dr. Yip Chun Chieh

Date   :   6/4/2024

ACKNOWLEDGEMENTS

I would like to express my deepest appreciation to my supervisor, Ir. Ts. Dr. Yip Chun Chieh, for his invaluable guidance, mentorship, and unwavering support throughout the duration of this thesis. His expertise, insightful feedback, and encouragement have been pivotal in shaping the direction and quality of this research.

ABSTRACT

This thesis investigates the seismic behaviour of glulam framed structures utilising mortise and tenon joinery, aiming to analyse stress concentration areas and compare the seismic performance with reinforced concrete (RC) buildings. The study focusses on evaluating the strength and weaknesses of glulam structure during earthquake events. A comprehensive analysis of stress distribution and structural integrity is conducted using finite element modelling techniques. The glulam framed structures are designed with fixed supports and incorporate mortise and tenon design without additional components such as slabs and footings. Through detailed simulations and seismic analysis, this research aims to provide insights into the performance of glulam framed structures and their comparative advantages and limitations in seismic conditions.

TABLE OF CONTENTS

CHAPTER

LIST OF TABLES

LIST OF FIGURES

LIST OF SYMBOLS / ABBREVIATIONS

f_{ck}	characteristic compressive cylinder strength of concrete at 28 days, N/mm^2
f_{yk}	characteristics yield strength of reinforcement, N/mm^2
tet	Tetrahedral
hex	Hexahedral
ASTM	American Society for Testing and Materials
BCs	Boundary Condition
BS 4449	British Standard on steel for the reinforcement of concrete
BS 6399-2	Code of Practice for Assessing Wind Loading on Buildings
BS 8500	British Standard for concrete production, providing guidelines and requirements for concrete use in construction
BS 8100	British Standard for the design of concrete structures
BS 8666	British Standard for scheduling, dimensioning, bending, and cutting of steel reinforcement for concrete
BS EN 1991	Eurocode 1, Actions on Structures
CBD	Central Business District
CBF	Concentrically Braced Frame
CLT	Cross-Laminated Timber
DMRF	Ductile Moment Resisting Frame
DOF	Degree of Freedom
EBF	Eccentrically Braced Frames
EN 1992	Eurocode 2, part of the European Standards for structural design, focused on concrete structures
EN 1998	Eurocode 8, part of the European Standards for structural design, focus on earthquake resistance design
ETABS	Extended Three-Dimensional Analysis of Building System
FEA	Finite Element Analysis
FPS	Friction Pendulum System
GGJB	Galeri Glulam in Johor Bahru
GLT	Glued-Laminated Timber
MTIB	Malaysian Timber Industry Board
ML	Machine Learning

MMI   Modified Mercalli Intensity

MS 1553   Code of Practice on Wind Loading for Building Structure

MS 1714   Visual Strength Grading for Sawn Hardwood Timber

MS 544: Part 3 2001 Code of Practice for Structural Use of Timber: Permissible Stress Design of Glued Laminated Timber

MS 758:2001 Glued Laminated Timber – Performance Requirements and Minimum Production Requirements (First Revision)

PML   Probable Maximum Loss

PMM   Plastic Moment Modifier

RC   Reinforced Concrete

RP   Reference Point

TSC   Turkish Seismic Code-2018

LIST OF APPENDICES

CHAPTER 1

INTRODUCTION

1.1   Background

Timber has been utilised as a building material for centuries, owing to its abundance, sustainability, and relative ease of construction, as well as its strength, durability, lightweight nature, ease of workability, insulation properties, versatility for indoor and outdoor applications, and its renewable and sustainable qualities (Birketts Bog Mats, n.d.). Throughout history, timber framed structures have adorned urban landscapes and rural areas alike, showcasing the versatility and resilience of wood in architectural design. However, with the advent of modern construction materials like reinforced concrete, the prevalence of timber in structural engineering has somewhat diminished.

The seismic performance of buildings is a critical aspect of structural design, particularly in earthquake-prone areas. Timber framed structures, including those constructed with engineered wood products like glulam, have shown remarkable resilience during earthquakes due to their inherent flexibility and ability to withstand deformation (Eduardo, 2021). Glulam, a composite material made from bonded layers of lumber, combines the structural strength of wood with enhanced stability and uniformity, making it an increasingly popular choice in seismic design. Timber, including glulam, performs extremely well in seismic events, with its lateral force resisting systems often exhibiting high levels of ductility, allowing them to absorb significant deformation before fracture (Eduardo, 2021). Additionally, timber framed construction is characterised by its lightweight nature and multiple nailed connections, offers flexibility to adapt to movement and redundant load paths, making it a preferred choice in earthquake-prone areas (Southern Pine, 2023).

In the recent years, there has been a resurgence of interest in timber construction, driven by advancements in engineering techniques, sustainable building practices, and the recognition of wood as a viable alternative to traditional materials. One such advancement is the innovative mortise and

tenon joinery, a traditional method of connecting timber elements that has been reinvigorated through modern design principles and computational analysis.

The mortise and tenon joint, when executed with precision and ingenuity, offers several advantages over conventional fastening methods. Its reliability and strength, whether used independently or reinforced with glue or pins, make it difficult to separate (Dan, 2023). The blind mortise and tenon joints conceal the end grain of the tenon, preserving the material's natural beauty, while showcasing craftsmanship with their distinct appearance through the mortise and tenon joint (Dan, 2023). These versatile joints can be used in many types of projects, further adding to their appeal.

The combination of these advantages, coupled with advancements in timber engineering, has sparked interest in exploring the potential of mortise and tenon joints for seismic resistance. By incorporating innovative design principles and computational simulations, researchers aim to enhance the seismic performance of timber framed structures, challenging the dominance of reinforced concrete buildings in earthquake-prone regions.

This study seeks to delve into the seismic behaviour of glulam framed structures utilising mortise and tenon design, with a focus on analysing their performance under earthquake loading conditions. By investigating stress concentration areas, evaluating structural integrity, and comparing the strengths and weaknesses of glulam structures against reinforced concrete buildings, this research endeavours to contribute to the advancement of seismic resistant construction practices.

Through a comprehensive exploration of engineered wood, computational modelling, and seismic analysis, this study aims reveal the potential of engineered wood as a sustainable, resilient, and aesthetically pleasing alternative in earthquake-resistant construction.

1.2   Importance of the Study

The significance of this research lies in its potential to address several pressing challenges in this field of structural engineering and earthquake-resistant construction, particularly with regards to glulam framed structures utilising mortise and tenon joinery. One notable gap in current research is limited exploration of mortise and tenon joinery with the context of engineered wood

products like glulam. While mortise and tenon joinery have traditionally been associated with solid timber construction, their application in glulam structures presents a novel area of investigation. By bridging this gap, exploring the integration of mortise and tenon joinery in glulam construction, this study contributes to advancing timber engineering techniques and promoting the use of glulam as a renewable and sustainable building material.

Secondly, the study aims to enhance the seismic resistance of buildings, particularly in earthquake-prone regions worldwide, through the utilisation of glulam framed structures with mortise and tenon joinery. Understanding the seismic behaviour of these structures is essential for improving their seismic resistance. By evaluating stress concentration areas and analysing structural responses under seismic loading conditions, this study informs the development of guidelines for robust seismic design guidelines for timber construction.

Furthermore, the research promotes sustainable construction practices by advocating for the wider adoption of glulam framed structures. Glulam buildings offer inherent benefits such as carbon sequestration, energy efficiency, and recyclability (Simone, 2022). By demonstrating the seismic performance of glulam structures with mortise and tenon design, this study encourages the adoption of sustainable construction practices in seismic prone regions.

Additionally, the interdisciplinary nature of the study fosters collaboration between architects, engineers, and craftsmen. By integrating joinery techniques with computational analysis, the research bridges the gap between traditional craftsmanship and modern engineering methodologies. This holistic structural design approach leverages both traditional wisdom and cutting-edge technology, leading to innovative solutions in seismic resistant construction.

Finally, the findings of this study have the potential to inform policy and industry practices governing earthquake-resistant construction. By providing empirical evidence of the seismic performance of glulam framed structures with mortise and tenon joinery, policymakers and industry stakeholders can make informed decisions regarding building codes, regulations, and industry standards.

In summary, this study addresses the critical need for sustainable, resilient, and aesthetically pleasing structural solutions in earthquake-resistant

construction. By advancing our understanding of glulam engineering principles and seismic behaviour, it contributes to the broader goal of creating safer and more sustainable built environments for future generations.

1.3   Problem Statement

Despite the potential advantages of glulam framed structures with mortise and tenon joinery, several challenges and uncertainties that require focused investigation. One primary concern is the internal seismic performance of glulam buildings compared to the reinforced concrete structures, particularly in earthquake-prone regions.

Traditional timber construction techniques may not fully exploit on the structural benefits of engineered wood products like glulam, leading to uncertainties regarding their seismic resilience. The lack of comprehensive research on the seismic behaviour of glulam structures with joinery further exacerbates these uncertainties, hindering the wider adoption of glulam construction in earthquake-prone areas.

Moreover, the complex interaction between various factors, including material properties, joint configurations, and structural dynamics, poses challenges in accurately predicting the seismic response of glulam framed structures. The dynamic nature of earthquakes introduces additional complexities, such as non-linear behaviour and localised stress concentrations, which may compromise the performance of glulam buildings under seismic loading conditions.

Furthermore, the existing body of research predominantly focuses on conventional construction materials such as reinforced concrete, with limited emphasis on engineered wood products and innovative joinery techniques. This knowledge gap inhibits the development of comprehensive design guidelines and performance-based criteria for glulam framed structures in earthquake-resistant construction.

Addressing these challenges requires a systematic investigation into the seismic behaviour of glulam framed buildings with mortise and tenon design. By identifying critical issues and uncertainties, this study aims to provide valuable insights into the structural performance and elasticity of glulam structures under seismic loading conditions.

Ultimately, the goal is to bridge the gap between theory and practice, informing the design, construction, and regulatory frameworks for glulam construction in earthquake-prone regions. Through rigorous analysis and experimentation, this study contributes to the advancement of earthquake-resistant construction practices, thereby enhancing the safety and sustainability of built environments worldwide.

1.4   Aim and Objectives

The main aim of this study is to assess the seismic performance of glulam framed structures with mortise and tenon joinery, comparing them to reinforced concrete buildings.

The objectives are shown as following:

i.   To analyse the seismic behaviour of glulam framed structures with mortise and tenon design.

ii.   To evaluate stress concentration areas within these structures during earthquakes.

iii.   To compare the strengths and weaknesses of glulam structures and reinforced concrete buildings in terms in their seismic performance.

1.5   Scope of the Study

The scope of this study encompasses the seismic behaviour analysis of glulam framed structures utilising mortise and tenon joinery. This research will investigate the structural performance and resilience of these timber structures under seismic loading conditions. The study will focus on the design, modelling, and simulation of glulam framed buildings using ABAQUS software. Specific aspects to be addressed include the development of mortise and tenon joint configurations, evaluation of material properties, assessment of structural integrity, and analysis of seismic response. The study will also compare the seismic performance of glulam structures with mortise and tenon joinery to conventional reinforced concrete buildings.

1.6   Limitations of the Study

The study is subject to several limitations that should be considered when interpreting the results, as shown as following:

1. Finite element analysis (FEA) assumptions may oversimplify real-world seismic events.
2. Lack of experimental validation for simulation results.
3. Simplified boundary conditions in finite element models may not fully represent real-world structural support conditions and constraints.
4. Variations in foundation types, soil properties, and building configurations are not fully accounted for, which could influence structural response to seismic forces differently than simulated.

1.7   Contribution of the Study

This research significantly contributes to timber engineering and earthquake-resistant construction by providing insights into the seismic performance of glulam framed structures with mortise and tenon design. It provides practical guidance for structural design, advances sustainable construction practices, and facilitates evidence-based decision making for policymakers and industry stakeholders. By integrating traditional joinery techniques with modern engineering methodologies, the study fosters interdisciplinary collaboration and innovation in earthquake-resistant construction practices, ultimately enhancing the safety, sustainability, and resilience of built environments.

1.8   Outline of the Report

This report is structured into five main chapters, each serving a distinct purpose and contributing to the overall understanding of seismic simulation of three-storey glulam framed structures with mortise and tenon design.

Chapter 1 includes an introduction to the study, covering aspects such as the background, importance, problem statement, aim, objectives, scope, limitation, contribution, and outline of the report.

In Chapter 2, the literature review provides an extensive review of the relevant literature, elucidating topics ranging from earthquakes and structural

damage to seismic-resistant devices, simulation methods, material properties, modelling techniques, and analysis approaches.

Moving forward to Chapter 3, the methodology and work plan outline the research approach, including the flowchart, specification, material properties, modelling techniques, boundary conditions, applied loads, and procedures for job creation.

In Chapter 4, the results and discussions chapter present the findings from simulations and analyses their implications within the context of the research objectives, particularly focusing on the structural performance of timber framed structures under seismic loading conditions.

Finally, Chapter 5, the conclusion and recommendation chapter, encapsulates the conclusions drawn from the research findings, along with recommendations for future studies and practical applications in the field of seismic resistant construction of glulam framed structures.

CHAPTER 2

LITERATURE REVIEW

2.1 Introduction

In this chapter, the emphasis shifts towards seismic simulation for three-storey glulam framed structures, incorporating with mortise and tenon design. The aim is to provide an overarching perspective on the context, importance, and foundation of this research by exploring the various dimensions of seismic events, structural damage, seismic resistance devices, and simulation techniques, with a specific emphasis on glulam framed structures and the mortise and tenon design.

Seismic events have historically presented a substantial threat to structures worldwide, resulting in considerable loss and damage, particularly in earthquake-prone regions. This chapter provides an in-depth exploration of the existing literature and research pertinent to seismic events, their impact on structures, methods for enhancing seismic resilience, and the tools for simulating such phenomena.

A comprehensive understanding of the global impact of seismic activities is essential to the evaluation of the significance of research in seismic simulation and innovative structural design. Earthquake are natural disasters that affect countries and regions around the world, causing massive casualties, economic losses, and structural damage.

Furthermore, a key aspect of this exploration is the focus on the Asia region, which is known as one of the most seismically active areas in the world. This region along with the Pacific Ocean's circum-Pacific seismic belt, known as the "Ring of Fire", experiences a significant frequency of earthquakes and volcanic activity, with about 81 percent of the Earth's largest earthquakes occurring in this area (USGS, n.d.). This emphasises the importance of understanding seismic phenomena for research in seismic simulation and structural design. The high frequency of earthquakes in the Asia region has resulted in numerous casualties and extensive structural damage, highlighting

the importance of enhancing seismic resistance, especially in timber framed constructions.

Structural damage resulting from seismic events is a multifaceted challenge, influenced by a variety of building materials and construction methodologies. Within this literature review, an analysis is conducted on the structural performance of various building materials, including reinforced concrete, timber, steel, masonry, and infrastructure. Understanding the advantages and disadvantages of each material is essential to evaluate the feasibility and effectiveness of innovative construction techniques.

Anti-seismic mechanisms are essential to protect structures from earthquake damage. This chapter delves into a variety of these mechanisms, encompassing dampers, tuned mass dampers, base isolators, bracing systems, and other innovative approached.

Simulation tools are indispensable for the assessment of structural performance under seismic loading conditions. In this literature review, several software tools commonly used in seismic research will be introduced.

In summary, the objective of this literature review is to provide a comprehensive understanding of the global impact of earthquakes, including the structural damage they cause and the methods used to assess and enhance seismic resistance. This chapter serves as a foundation overview of the multifaced components central to the thesis, laying the groundwork for a comprehensive examination of seismic simulation and innovative structural design in timber framed constructions.

2.2   Earthquake

One type of natural disaster that can cause significant damage to a particular area is an earthquake, which is often unpredictable. There are four types of earthquakes: tectonic earthquakes occur due to movement of tectonic plates, induced earthquakes are triggered by human activities such as mining or reservoir filling, volcanic earthquakes are associated with volcanic activity, and collapse earthquakes happen as a result of the collapse of underground structures or caverns (Swiss Seismological Service, n.d.).

Tectonic earthquakes, the majority of earthquakes in the world, which are brought on by the relative motion of tectonic plates within the interior of the Earth, where this motion causes stress to build up along faults (USGS, n.d). When the stress surpasses the rock's strength, the rock fractures along the fault, frequently occurs in pre-existing weak areas within the rock, as shown in Figure 2.1. As a result, the stored energy is abruptly discharged, manifesting as an earthquake.
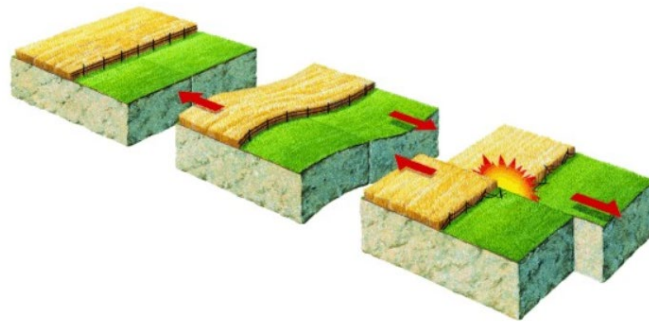
Figure 2. 1: Crustal stress on rocks during earthquakes.

The vibrations that occur during an earthquake is referred to seismic waves. Seismic waves are shaped like ripples on a pond, spreading from the initial rupture point, as shown in Figure 2.2. These waves can be of substantial magnitude, and resulting in their high destructive potential close to the focus point.
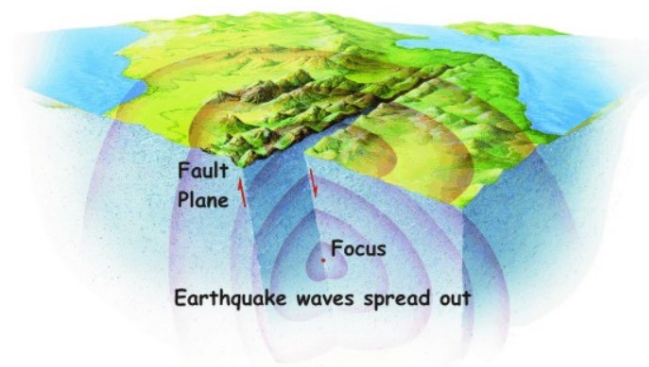
Figure 2. 2: Diagram of seismic waves.

Seismologists found that a sudden movement on a fault produces two different types of seismic waves: P-waves and S-waves. The interaction of P-

and S-waves with the Earth's interior and surface is considered a third type of seismic wave. The velocity of the waves is determined by the type of wave and the characteristics of the rock; denser rocks exhibit faster wave propagation. Based on research findings, P-waves travel approximately at a speed of 6 - 7 km/s within the Earth's crust, whereas S-waves travel at a speed of approximately 3.5 – 4 km/s (British Geological Survey, 2008).

The mechanics of faulting can vary depending on the type of fault involved, such as strike-slip, normal, or reverse faults, each exhibiting distinct characteristics in terms of fault movement and stress distribution (Wu, et al., 2023).

The effects of earthquakes encompass various occurrences, including ground shaking, surface faulting, ground failure, and occasionally tsunamis, especially in coastal areas (USGS, n.d.). Ground shaking refers to the ground's vibration caused by seismic waves, intensifying with magnitude and diminishing with distance from the fault. Surface faulting involves the differential movement of the Earth's surface along fractures, resulting from deep-seated forces, causing damage to structures within the affected zones. Ground failure encompasses liquefaction-induced processes like lateral spreads, flow failures, and loss of bearing strength, damaging infrastructure and causing casualties (USGS, n.d.). Tsunamis are caused by sudden vertical movement of undersea earthquakes, and are destructive water waves rapidly propagating across oceans, causing widespread devastation in coastal areas and distant regions from the earthquake's epicentre.

Magnitude and intensity scales are essential tools in earthquake research and can provide valuable insights into the intensity, impact, and frequency of seismic events. These scales help quantify the energy released by earthquakes and assess their effects on the ground and human-made structures. The Richter scale, developed in the 1935 by Charles F. Richter and Beno Gutenberg, is a quantitative measure used to assess earthquake size based on the amplitude of seismic waves recorded by seismographs (John, 2024). However, modern techniques have led to the adoption of more accurate measurement methods, like the moment magnitude scale, which considers the seismic moment and rupture area of an earthquake, thus providing a more reliable assessment of its

magnitude. Table 2.1 offers a comprehensive overview of earthquake magnitude, intensity, and their corresponding effects, providing valuable insights into the seismic characteristics and their impacts.

Table 2. 1: Earthquake magnitude, intensity, and effects (Skymet Weather Team, 2017).

Magnitude	Intensity	Earthquake Effects
1.0 – 3.0	I	Generally not felt
3.0 – 3.9	II – III	Quite noticeable by people on rest, particularly by people on upper floors
4.0 – 4.9	IV – V	Usually felt indoors. Breaking down of window panes and dishes
5.0 – 5.9	VI – VII	Felt by mostly all, movement of furniture expected, negligible damages to property likely
6.0 – 6.9	VII – IX	Considerable damage in ordinary substantial buildings with partial collapse, great damages to poorly constructed buildings. Threat to life
7.0 and higher	VIII or higher	Total damage, objects thrown into air, massive destruction and threat to human life

Additionally, the Modified Mercalli Intensity Scale evaluates the impact of earthquakes on people, buildings, and the environment at specific locations, providing qualitative measures of intensity based on observed damage and human perception. Figure 2.3 compares measurements on the Modified Mercalli Intensity Scale with magnitudes on the moment magnitude scale, providing valuable insights into the relationship between intensity and magnitude.

CIIM Intensity	People's Reaction	Furnishings	Built Environment	Natural Environment
I	Not felt			Changes in level and clarity of well water are occasionally associated with great earthquakes at distances beyond which the earthquakes felt by people.
II	Felt by a few.	Delicately suspended objects may swing.		
III	Felt by several; vibration like passing of truck.	Hanging objects may swing appreciably.		
IV	Felt by many; sensation like heavy body striking building.	Dishes rattle.	Walls creak; window rattle.	
V	Felt by nearly all; frightens a few.	Pictures swing out of place; small objects move; a few objects fall from shelves within the community.	A few instances of cracked plaster and cracked windows with the community.	Trees and bushes shaken noticeably.
VI	Frightens many; people move unsteadily.	Many objects fall from shelves.	A few instances of fallen plaster, broken windows, and damaged chimneys within the community.	Some fall of tree limbs and tops, isolated rockfalls and landslides, and isolated liquefaction.
VII	Frightens most; some lose balance.	Heavy furniture overturned.	Damage negligible in buildings of good design and construction, but considerable in some poorly built or badly designed structures; weak chimneys broken at roof line, fall of unbraced parapets.	Tree damage, rockfalls, landslides, and liquefaction are more severe and widespread wiht increasing intensity.
VIII	Many find it difficult to stand.	Very heavy furniture moves conspicuously.	Damage slight in buildings designed to be earthquake resistant, but severe in some poorly built structures. Widespread fall of chimneys and monuments.	
IX	Some forcibly thrown to the ground.		Damage considerable in some buildings designed to be earthquake resistant; buildings shift off foundations if not bolted to them.	
X			Most ordinary masonry structures collapse; damage moderate to severe in many buildings designed to be earthquake resistant.	

Figure 2. 3: The Modified Mercalli Intensity (MMI) scale (Volcano Hazards Program, n.d.).

Seismic risk assessments play a vital role for engineers in predicting how structures will withstand earthquakes and estimating the resulting financial impact, known as probable maximum loss (PML), in the aftermath of significant seismic events (David, 2019). These assessments encompass various factors, including the stability of buildings and sites, potential damage to structures and contents, and the potential for business interruption, as depicted in Figure 2.4 within the flow chart method. ASTM international has developed standards for understanding seismic risk assessments and comparing them to other assessments. Notable standards include ASTM E2026, which outlines the terminology and processes for assessments, addressing inconsistencies in quality and reporting. ASTM E2557 supplements E2026, providing levels of investigation based on user tolerance for uncertainty and seismic activity. These standards define four study levels, from simple desktop assessments (Level 0) to detailed seismic analyses (Level 3). Although they do not set acceptability thresholds, building purchasers or lenders often establish them. Updates ensure assessments are conducted by qualified engineers and adhere to clear scope statements and ASCE 41 Tier 1 guidelines (David, 2019).
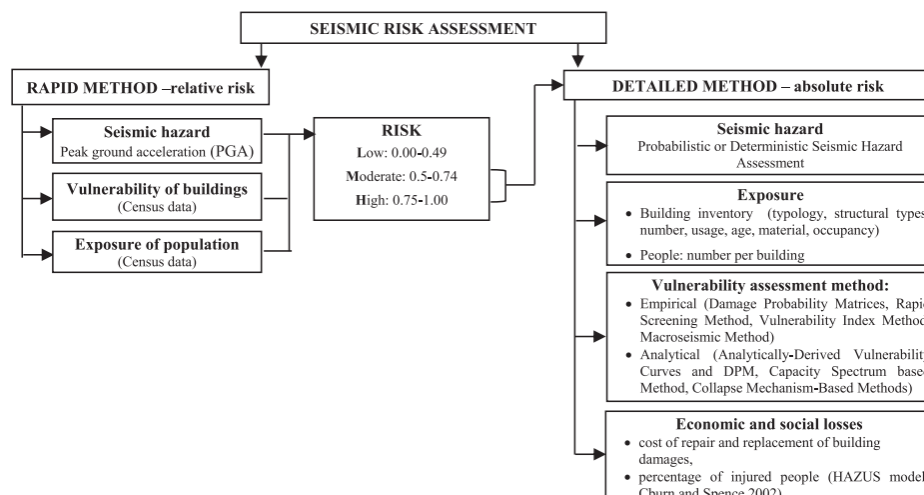
Figure 2. 4: Overview of seismic risk assessments: rapid vs. detailed (Tanja, et al., 2017).

2.2.1 Global disaster impact

The impact of an earthquake can be significant and wide-ranging. It can be observed in both short term and long term. Short term impacts of an earthquake include a significant loss of life and injuries due to collapsing structures and failing debris (Pishva, 2016). The infrastructure, such as buildings, bridges, and roads, can be severely damaged, disrupting transportation and essential services. As a result, a significant number of individuals may find themselves displaced from their homes, leading to either temporary or long-term homelessness. Urgent humanitarian response efforts, including search and rescue operations and medical aid, are necessary to address the immediate crisis. Survivors also grapple with psychological trauma and emotional distress stemming from the event and the loss of loved ones. In the long term, earthquakes leave a lasting impact. The economic consequences are substantial, requiring the rebuilding and repair of infrastructure, revitalization of businesses, and restoration of economic activities (BBC, n.d.). Social disruption occurs, affecting community dynamics, population distribution, and social cohesion. Environmental changes arise, including landscape alterations, land subsidence, and shifts in watercourses, which affect ecosystems, agriculture, and water resources. Measures are taken to improve infrastructure resilience and implement stricter building codes and regulations to mitigate future earthquake risks. Ongoing

support and mental health services are necessary to address persistent psychological and emotional challenges faced by individuals and communities.

According to World Vision (2023), Haiti experienced devasting earthquakes in 2010 and 2021. The 2010 earthquake, with a powerful magnitude of 7.1, struck near the capital, Port-au-Prince, claiming approximately 300,000 lives. Similarly, in 2021, a 7.2 magnitude earthquake near Petit-Trou-de-Nippes resulted in over 2,000 fatalities and affected more than 1.2 million people, including 540,000 children, according to UNICEF. These earthquakes highlighted the ongoing vulnerability of Haiti to seismic events and the critical need for effective disaster response and recovery efforts. Despite not initially operating in the areas most affected by earthquakes, World Vision swiftly responded to assist over 155,000 individuals impacted by the disasters. Their efforts included providing health and nutrition support to 150,000 people, offering cash assistance to 11,120 individuals for essential needs, and reaching over 71,000 people with food security and livelihood programs after the 2021 earthquake.

Following the devastating 2010 earthquake, World Vision, present in Haiti for 30 years, distributed emergency supplies immediately and supported nearly 2 million people in the first 90 days. Over the subsequent years, their initiatives treated 300,000 for cholera, fed 250,000 students across 800 schools, provided shelter to over 200,000, and facilitated access to clean water for 90,000 displaced individuals for almost two years. Additionally, they trained 19,000 farmers, established 30 children-friendly spaces benefiting nearly 8,000 children, and constructed 10 schools. World Vision continues its commitment to empowering Haitian communities toward long-term recovery and resilience.

2.2.2 Casualties in the Asia region

According to World Vision (2023), approximately 18 million people in Turkey and Syria have been affected by the disaster on February 6, 2023, resulting in a tragic loss of over 55,000 lives and nearly 130,000 injuries. The destruction has left millions displaced, with over 10 million individuals requiring urgent assistance. Numerous cities in the region have been extensively damaged, leaving approximately 50,000 buildings, including residential complexes,

schools and hospitals, either in ruins or too damaged to occupied. Access to vital healthcare services is severely limited, with only 1 in 7 health centres operating partially. The loss of secure housing and disrupted access to education have left children highly vulnerable to exploitation, abuse, and separation from their families.

Similarly, the devastating Sichuan earthquake in China resulted in the destruction of a staggering 5 million buildings and the cost of restoring infrastructure was estimated at $75 million (GCSE Geography, n.d.). Besides, the earthquake that struck Sabah, Malaysia in 2015 took everyone by surprise, as the region was not known for being prone to seismic activity. The event was unexpected and caught both the local population and authorities off guard. The lack of prior experience with such earthquakes in the area meant that people were unprepared for the potential consequences and challenges that followed. A powerful 6.0 magnitude earthquake lasting 30 seconds, claimed the lives of 18 individuals on Mount Kinabalu (Sarah, 2015). Following the earthquake, the Meteorological Department recorded around 100 aftershocks, which along with rainfall, triggered mudslides impacting 1000 residents in Kundasang, Ranau, and Kota Belud.

The Asia region, characterised by its high population density and vulnerability to seismic activity, has experienced numerous devastating earthquakes throughout history.

2.2.3   Casualties and damage coverage

The socio-economic consequences of earthquakes extend beyond immediate casualties and infrastructure damage, encompassing long-term impacts on communities, economies, and governance structures. After the 2010 earthquake in Haiti, the country faced extensive challenges in rebuilding infrastructure and restoring livelihoods. Despite international aid efforts, long-term socio-economic impacts remain and many communities struggling to recover from the devastation. This highlighted the importance of effective disaster preparedness and recovery strategies, including robust insurance mechanisms and government policies to support reconstruction efforts.

Following the 2011 earthquake and tsunami in Japan, the government implemented comprehensive disaster risk management measures to mitigate future risks and enhance resilience. This included the establish of stricter building codes, early warning systems, and community training programs (Arnold, n.d.). These initiatives helped minimise casualties and damage during subsequent seismic events, demonstrating the effectiveness of proactive disaster preparedness and response measures.

Similarly, in Indonesia, the 2004 Indian Ocean earthquake and tsunami exposed vulnerabilities in disaster management systems and highlighted the need for improved recovery strategies. The estimated cost of damage resulting from the disaster was approximately 10 billion (Vasudha, 2021). Meanwhile, according to the government's assessment, the estimated cost for repairing damaged buildings and infrastructure in the affected regions following the earthquake in Mount Kinabalu is projected to exceed RM100 million (Malay Mail, 2015). These staggering figures highlighted the urgent need for enhanced disaster preparedness and response measures to mitigate future risks and socio-economic impacts.

2.3 Structural damage

The complex issue of structural damage arising from seismic events involves various building materials and construction methods. It is imperative to assess the performance of these materials to gauge their appropriateness and capacity to withstand earthquakes.

2.3.1 Reinforced concrete

Reinforced concrete structures are widely used in civil engineering due to their excellent combination of strength, durability, and versatility. However, these structures are susceptible to various forms of damage under different loading conditions, necessitating a thorough understanding of their behaviour and failure mechanisms.

The research study conducted by Onder and Mehmet (2023) investigated the structural damage resulting from two large earthquakes with magnitudes of 7.7 and 7.6 in the Pazarcik and Elbistan districts of Kahramanmaras Province in

Turkey. These earthquakes caused extensice damage to building and resulted in casualties. A 2016 building situated in the Yesilturt district of Malatya has been examined, as shown in Figure 2.5. The building consists of one level of basement, ground floor, mezzanine and roof floor each, and 12 normal floors, with floor heights ranging from 2.75m to 4.35m. Its overall height from ground level is 41.5m. A summary of the building's geometric characteristics is provided in Table 2.2 of the study.

Figure 2. 5: Facade view of the building.

Table 2. 2: General geometric properties of the building.

Slab System	Bi-directional Slabs, 15-18 cm Thick
Horizontal Structural System	RC frames and shear-walls
RC Column Dimensions	35 x 50 cm, 40 x 50 cm, 50 x 50 cm etc.
RC Beam Dimensions	20 x 60 cm, 30 x 60 cm, 30 x 100 cm etc.
RC Shear-wall Thickness	25 cm
Plan Dimensions on Normal Floors	38.20 m x 20.45 m

The research finding indicate significant damage to infill walls within the building, as shown in Figure 2.6, likely due to inadequate reinforcement with RC shear walls in the structural system. Despite meeting regulatory limits for period and storey drift, the building experienced high relative storey drifts, leading to unexpected damage infill walls up to the 7th normal floor. Moreover, inadequate mortar joints in these infill walls compromised their adherence within the structural system, exacerbating the damage.

Figure 2. 6: Infill wall damages.

Performance analysis and on-site examinations were conducted to identify critical elements within the building. Damage was observed in some beams, particularly those located in weak areas such as the ground and mezzanine floors, as depicted in Figure 2.7. These beams, designed with a length of 95 cm and situated around the elevator shear wall, experienced significant earthquake forces due to their inadequate cross-sectional capacities relative to their dimensions. Serious damages were observed in these beams, especially those adjacent to the elevator shear walls, up to the 7th normal floor.

Damage initiation from the ground and mezzanine floors and decreasing severity with height was consistent with expectations based on the structural design and seismic loading pattern.
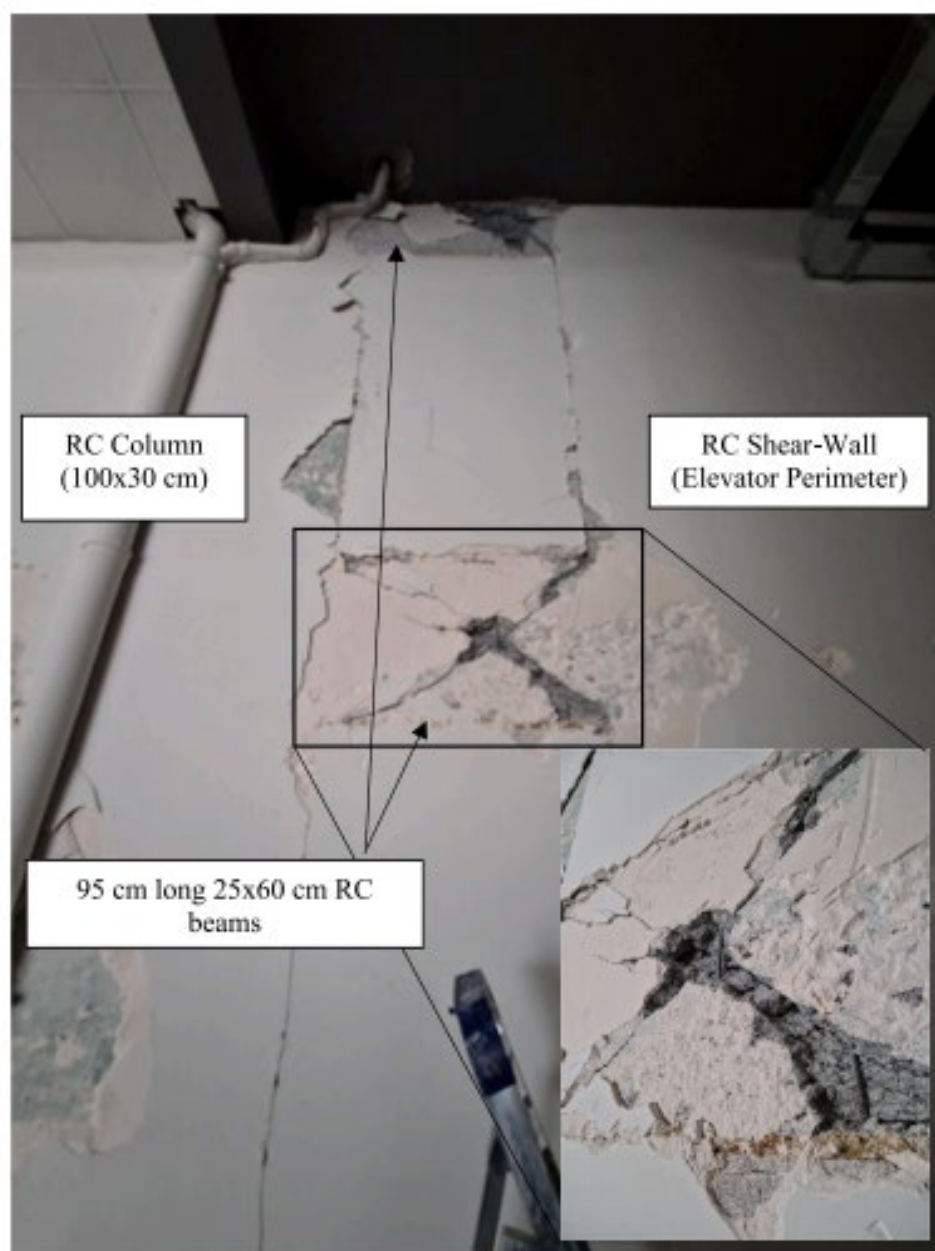

Figure 2. 7: 95cm long beams damaged on the ground and mezzanine floor.

After identifying the structural issues and damages, a proposed solution involves a repair and strengthening design. Priority is given to repair the damaged beams, for which cement-based self-compacting thixotropic repair mortars with high adhesion and strength properties are recommended. The

building's low stiffness, attributed to the absence of RC walls in the structural system is noted. Although the building meets the relative inter-storey drift limitation specified by TSC, it was not deemed necessary to add RC shear walls to increase stiffness. Instead, the addition of steel members between the repaired beams and certain main corridor beam-columns is suggested to enhance horizontal load transfer. The selection of members to be added to the structure aim to support the damaged beams and facilitate load transfer in the beam free zone within the corridor.

In reviewing reinforced concrete structures' vulnerabilities and repair strategies, it is clear that seismic resilience remains a paramount concern. These findings underscore the need for innovative solutions, such as the mortise and tenon design explored in this study, to address seismic challenges effectively in glulam framed constructions.

2.3.2   Timber

A research study shows that building can suffer significant damage in the face of earthquakes. Alih, et al. (2019) addresses the behaviour of RC and wooden structures building in Sabah earthquakes and the factors that lead to different types of damage. Figure 2.8 shows that the side elevation view and plan view of non-seismic building in Sabah. By referring to Figure 2.8, the shortest columns were failed through shear, which means that shear cracks will be created in the face of earthquakes. However, the earthquake did not cause any major damage to the wooden structure building. This is because of the arrangement of wooden boards shown in Figure 2.9 and the connection shown in Figure 2.10 provide flexibility to the structure to experience shaking during the earthquake. Therefore, it can be summarized that RC buildings showed the less ductility behaviour and poor detailing compared to wooden structure.

However, despite the insights gained from studies on RC and wooden structures, there remains a research gap in understanding the behaviour of glulam structures, such as Glued-laminated timber (GLT) and Cross-laminated timber (CLT), during seismic events. Addressing this gap is crucial for advancing our knowledge of timber construction and enhancing seismic resilience of buildings, which forms the primary objective of this research.
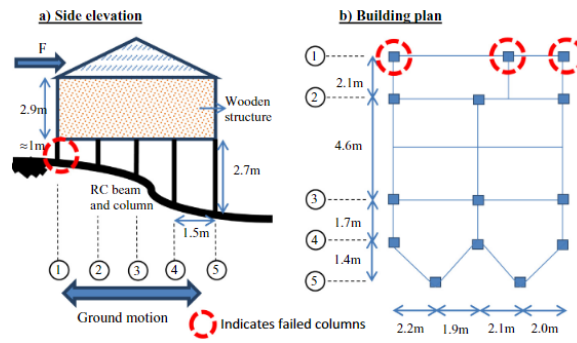
Figure 2. 8: Building configuration measured on site and columns' grid as reference: (a) Side elevation, (b) Building plan (Alih S., et al., 2019).
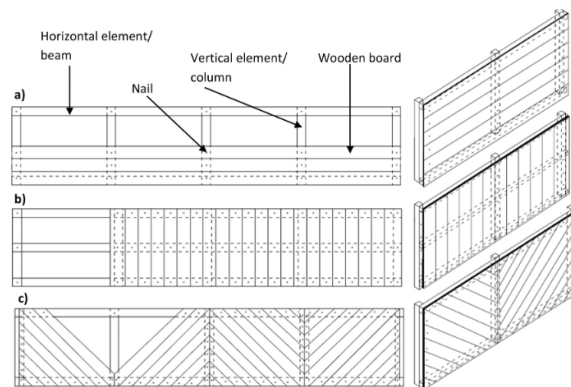

Figure 2. 9: Arrangement of wooden boards as infill: (a) horizontal direction, (b) vertical direction, (c) diagonal direction (Alih S., et al., 2019).

Figure 2. 10: Connection in wooden structures (Alih S., et al., 2019).

2.3.3   Steel

In the context of structural engineering, steel is a widely used material due to its strength, ductility, and versatility. However, like any material, steel structures can suffer from various forms of damage and deterioration over time, especially when subjected to external forces such as seismic events or environmental factors like corrosion.

The study conducted by Charles, et al. (2011) provides preliminary field observations on the performance of selected steel structures in Christchurch during the earthquake series of 2010 to 2011, comprised six damaging earthquakes occurring at different time. The most notable event was the earthquake of magnitude 7.1, followed by one of magnitude 6.3.

During the earthquake series, two multi storey buildings in the CBD equipped with eccentrically braced frames (EBFs) as part of their lateral load resisting system received green tags, indicating they were safe for occupancy with minor repairs required.

The Club Tower Building features EBFs positioned on three sides of an elevator core to the west side, along with a ductile moment resisting frame (DMRF) on the east façade, as shown in Figure 2.11. During inspection, significant yielding was observed in the EBFs, with peak shear strains estimated between 3% and 4%. However, the metallurgical properties of the active links were deemed robust, eliminating the need for replacement. The fractures link at a lower level of the EBF occurs at the parking structure, as shown in Figure 2.12, indicating ductile overload failure rather than brittle fracture.
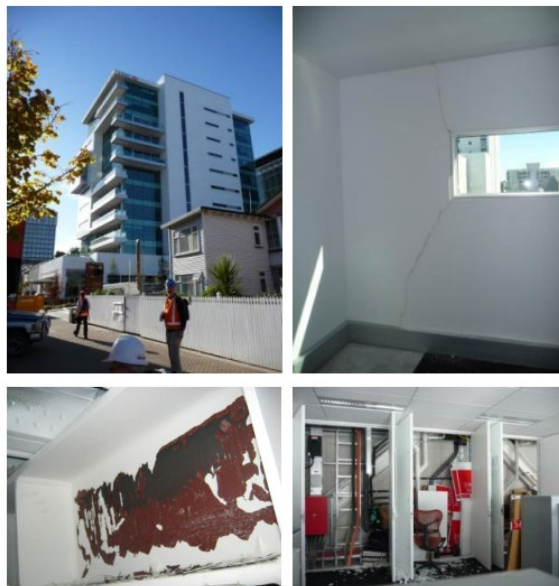
Figure 2. 11: Club Tower: from top down and left to right: (a) Global view; (b) cracking of partition in cantilevering portion of story; (c) point flaking of partially hidden EBF link; (d) global view of EBF braces obstructed by various utility runs.

Figure 2. 12: Fractured link at lower level of the EBF.

Additionally, a historical building, constructed before 1910, the Regent Theater building reveals a bracing frame with partial out-of-plane failure around top dome, as shown in Figure 2.13. However, the welded appearance of the CBFs suggests they may be newer additions, possibly incorporated during subsequent renovations. In some cases, steel braced frames were utilised to retrofit unreinforced masonry structure, as illustrated in Figure 2.14. Design

considerations for these instances prioritise drift limits to prevent unreinforced masonry failure, explaining the substantial member sizes of those frames in proportion to the reactive mass and their elastic response.

Figure 2. 13: Braced dome at top of Regent on Worchester Building.

Figure 2. 14: Braced frame as a retrofit to unreinforced masonry building.

The examination of steel structures under seismic conditions provides valuable insights into their performance and resilience. Observations of steel buildings in seismic zones underscore the critical role of lateral load resisting systems, such as eccentrically braced frames (EBFs), mitigating earthquake damage. Additionally, the study reveals the importance of material properties and design considerations in ensuring structural integrity during seismic events. These findings contribute to the broader understanding of seismic resistant construction practices and inform the investigation into enhancing the seismic resilience of glulam framed constructions.

2.3.4   Masonry

Masonry, a traditional construction material, involves the assembly of individual units such as bricks, stones, or concrete blocks using mortar to form structures. Masonry structures offer durability, fire resistance, and aesthetic appeal, making them prevalent in various architectural styles and construction practices.

Manjip, et al. (2021) conducted a research study focusing on the heavy damage inflicted on public residential buildings in Bhaktapur due to the Gorkha earthquake in 2015. The study involved a rapid visual damage assessment of 3979 buildings post-earthquake, aiming to identify vulnerable parameters in traditional masonry construction practices to inform future construction practices for safer buildings. The buildings with different damage grades were further analysed, and the results were provided in Appendix A.

Following the rapid visual screening, several factors contributing to the increase damaged of buildings were identified. These included sloping landforms and the lack of repair and intervention works, which exacerbated the damage to buildings. Figure 2.15 compares the damage grades of RC buildings and masonry buildings, revealing that masonry building were more vulnerable. Approximately 64% of masonry buildings suffered heavy (D3) to very heavy damage (D4) compared to RC buildings.

Figure 2. 15: Buildings based on structure type: (a) masonry buildings; (b) RC buildings.

Furthermore, Figure 2.16 demonstrates that the vulnerability of buildings increases with the number of storeys. The study highlighted the characteristics of each structural system, noting that masonry structures tend to be brittle with low strength, while RC structures are ductile with high capacity.

Various deficiencies were identified in masonry construction practices in Bhaktapur, including deficient bonding at corner continuous vertical joints, flexible floor diaphragms, unsupported sloping roofs, inadequate or absent passing-through connections in multi-leaf masonry assemblages, absence of sill and lintel bands, unsymmetrical building plans and elevations, excessively high and narrow walls, and imbalanced sizes and positions of wall openings among others. These vulnerabilities underscored the inefficiency of non-engineered masonry construction practices compared to engineered RC building practices in Bhaktapur.

Figure 2. 16: Building types based on nos. of floor: (a) one storey; (b) two storey; (c) three storey; (d) four storey; (e) five storey.

Investigating structural damage in masonry building post-earthquake reveals vulnerabilities in traditional construction methods, such as deficient bonding and inadequate support. This emphasises the need for improved engineering standards to enhance seismic resilience. Comparing masonry with reinforced concrete structures underscores the importance of robust structural systems. These insights inform strategies for bolstering the seismic resilience of glulam framed constructions.

2.3.5 Infrastructure

Infrastructure plays a fundamental role in supporting societal functions and economic activities, serving as the backbone of modern civilisation. It encompasses a wide range of systems and facilities essential for the functioning of communities, including transportation networks, utilities, telecommunications, and public amenities. The quality and resistance of infrastructure are crucial for ensuring the safety, efficiency, and sustainability of urban and rural environments.

The study conducted by Nanako, Aaron, and Chiho (2024) focuses on infrastructure rebuilding and social recovery efforts following the Great East Japan Earthquake and Tsunami in 2011. This catastrophic event, characterised by a magnitude 9 earthquake followed by a 40m tsunami, led to unprecedented destruction and loss of life. The subsequent nuclear accident further compounded the humanitarian crisis, resulting in a staggering death toll, injuries, and displacement of hundreds of thousands of people.

Kesennuma City, one of the hardest-hit areas, experienced extensive damage from the tsunami, with significant loss of life and destruction of structures. The city bore the third-highest number of fatalities, reflecting the severity of the disaster. A staggering 25,420 structures, including over 15,000 houses, were either destroyed or damaged, as illustrated in Figure 2.17.

Figure 2. 17: Damage of tsunami in Kesennuma.

The study highlights the importance of rebuilding infrastructure, addressing structural damage, and aiding social recovery in the aftermath of

disasters. It examines the challenges, strategies, and outcomes of these efforts, offering insights into communities' resilience.

2.4 Seismic resistance device

In this section, multiple devices designed to enhance the seismic resistance in structures are discussed. Each device serves a specific purpose and can mitigate the impact of seismic events on buildings and infrastructure. The discussion will encompass various types of seismic resistance devices, including damper, tuned mass damper, base isolator, bracing system, and the innovative mortise and tenon design. Examples of practical applications of these devices are provided to illustrate their effectiveness in improving the seismic resistance of structures.

2.4.1 Viscous Damper

Viscous dampers are devices designed to absorb and dissipate energy during seismic events, reducing the structural response and minimising damage to buildings (Agrawal, et al, 2022). These devices typically consist of hydraulic, friction, or viscous dampers strategically installed within the structural system to mitigate the effects of seismic forces, as shown in Figure 2.18.
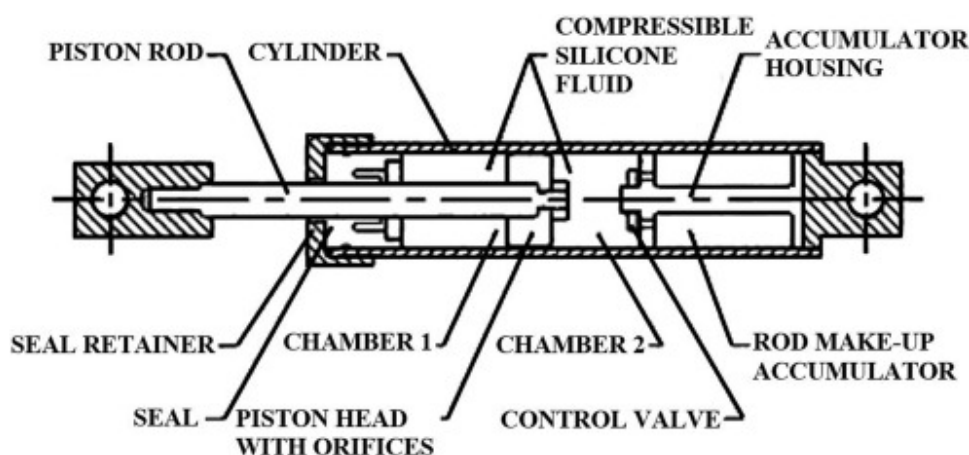
Figure 2. 18: A typical fluid viscous damper (Agrawal, et al, 2022).

According to Lupoi and Greco (2022), the efficacy of viscous damper in reducing base shear on bridge piers was highlighted. The study demonstrated the viscous dampers were effective in improving the seismic response on structures, particularly bridges, as evidenced by their successful application in

a seismic retrofitting project of an Italian cantilever bridge located on the A14 highway in the Abruzzo Region. In this project, viscous dampers were chosen for their considerable damping and yield capacity, enabling them to dissipate energy induce by seismic action and mitigate stresses in structural elements.

However, it is worth noting that these dampers could introduce some rigidity to the structure during high frequency vibrations and exhibit viscoelastic characteristics beyond a certain frequency threshold. One notable application of viscous dampers was the retrofit of the San Francisco-Oakland Bay Bridge in California, USA, following the 1989 Loma Prieta earthquake. To address seismic vulnerability, the bridge was strengthened with 96 new viscous dampers strategically placed at critical points to damp movement and mitigate potential damage from future seismic events (Roumen, et al, n.d.).

2.4.2　Tuned mass damper

Tuned mass dampers (TMD), alternatively known as a "harmonic absorber", are passive vibration control devices employed to counteract the effects of dynamic forces on structures, particularly in response to seismic activity. These devices utilise the principle of dynamic vibration absorption, whereby a mass-spring system is tuned to resonate at the frequency of the structure's oscillations, thereby reducing structural vibrations and enhancing stability (Michael, 2017). Tuned mass dampers have been extensively studied and implemented in tall buildings and other structures to improve their seismic performance.

According to Kang (2022), the efficacy of tuned mass dampers in reducing structural vibrations has been extensively studied and implemented in various structures, including tall buildings. The study demonstrated that the attachment of a tuned mass damper significantly reduced vibration amplitudes in seismic resistant construction.

One example of tuned mass dampers is found in the Taipei 101 skyscraper in Taiwan. Taipei 101 features a massive tuned mass damper, weighing 730 tons, suspended between the 87th and 91st floors. This damper effectively reduces building sway caused by wind and seismic forces, ensuring the stability and safety of the structure during extreme conditions, shown in Figure 2.19.
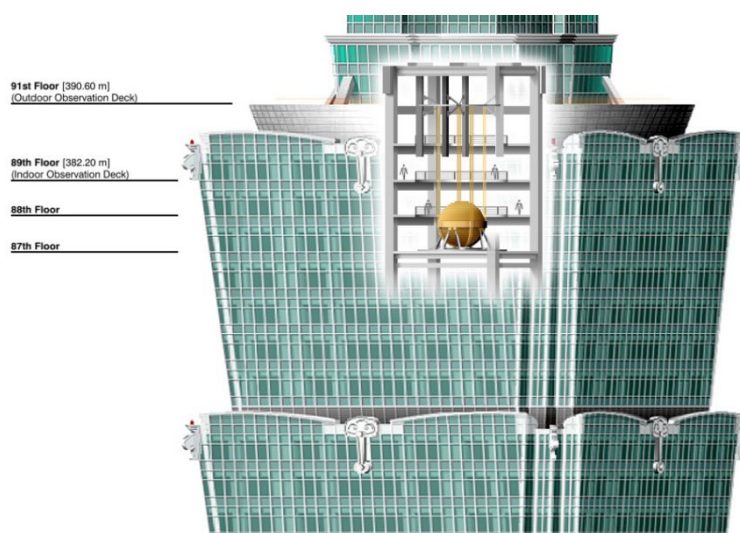
Figure 2. 19: Location of Taipei 101's tuned mass damper between 87th and 91st floor.

2.4.3   Base isolator

Base isolators are seismic mitigation devices installed a building's foundation and superstructure to isolate them from ground movement during earthquakes, shown in Figure 2.20 (Anand, 2016). By isolating the structure from the ground vibrations, base isolators effectively reduce seismic forces transmitted to the building, thereby minimising structural damage and enhancing occupant safety.

Figure 2. 20: Base isolation for a building (Anand, 2016).

The study conducted by Raden and Ibnu (2023), focused on the application of base isolators, particularly the Friction Pendulum System (FPS), in the design of the Universitas Islam Malang Hospital structure. The research

highlighted the effectiveness of base isolators in reducing interstorey drift significantly compared to fixed bases, indicating their potential to enhance the seismic resilience of the structures.

The Los Angeles City Hall in California, USA, is an example of applying base isolators to enhance its seismic resistance. During the retrofit, 414 base isolators were strategically placed within the building's columns and beneath the walls, just below the existing basement level and foundation system (Acmartin, n.d.). This proactive measure significantly reduces the seismic forces affecting the building, thereby reducing damage and ensuring the safety of the occupants.

2.4.4 Bracings

Bracing systems are structural elements designed to increase the lateral stiffness and strength of buildings, thereby improving their resistance to seismic forces (Meena, n.d.). These systems typically consist of diagonal or cross-braces installed within the building's framework to resist lateral movement and redistribute seismic loads.

Nandona (2022) analysed different types of bracing, such as X, V, and knee bracing, to assess their effectiveness in reducing displacements and increasing stiffness during earthquakes. The research concluded the bracing systems, particularly buckling restrained braces, are more effective in seismic strengthening for small buildings, as they increase base shear and provide more resistance during earthquakes. This highlights the importance of bracing systems in reducing the impact of lateral loads on high rise buildings during seismic events.

For instance, the Burj Khalifa in Dubai, United Arab Emirates, is one of the well-known iconic skyscrapers designed to withstand earthquakes. Engineers utilised a cross- bracing system to enhance its resistance to lateral forces, including those generated by seismic activity, shown in Figure 2.21 (Samsung C&T Global PR Manager, 2017). The tower features a combination of reinforced concrete shear walls and outrigger trusses strategically distributed throughout its height to provide lateral stiffness and strength, ensuring stability and structural integrity during seismic events.

Figure 2. 21: Bracing design for Burj Khalifa's building.

2.4.5   Mortise and tenon design

The mortise and tenon joint are a traditional woodworking technique used to join timber elements in timber framed structures. This method involves cutting a slot (mortise) into one piece of timber and inserting a projecting piece (tenon) from another piece to create a strong and durable connection (Dan, 2023). There are four types of mortise and tenon joints, each with its unique characteristics and application, shown in Figure 2.22.
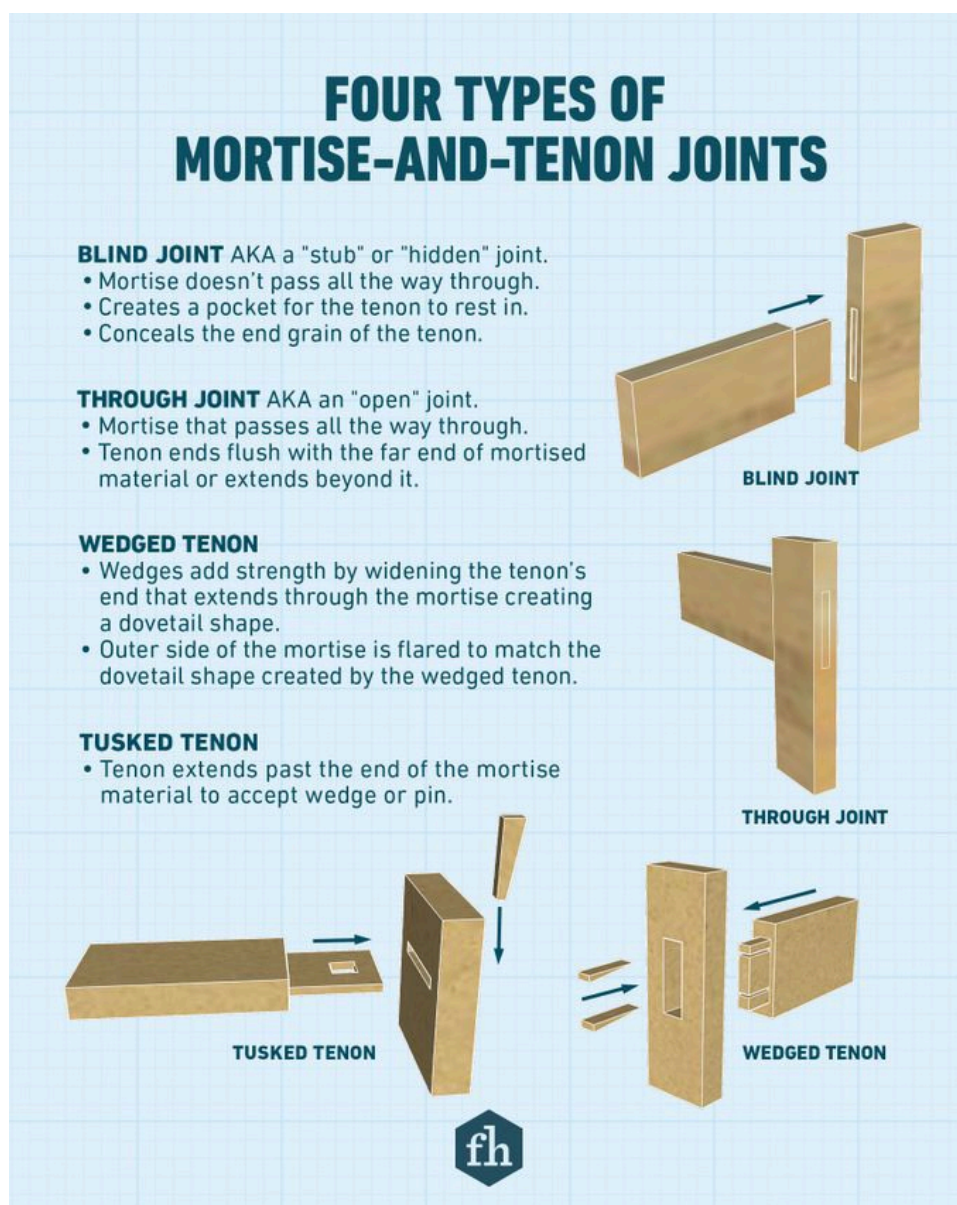
Figure 2. 22: Type of mortise and tenon joints (Dan, 2023).

Wang (2020) introduces a specialised mortise and tenon structure designed for T-shaped wall constructional columns, emphasising stability, integrity, and safety by connecting prefabricated concrete members with aligned tenon holes and longitudinal bars during assembly. While my discussion primarily focuses on traditional mortise and tenon joints in timber construction, Wang's findings underscore the broader importance of this structural element in construction projects.

Traditional mortise and tenon joints, provide robust and reliable connections between structural members, contributing to the longevity and

resilience of timber structures. When creating mortise and tenon joints, it is essential to ascertain the dimensions of the mortise slot for a suitable fit and structural integrity. Typically, the mortise holes should not exceed one-third the width of the width of the mortise material. Besides, the length of the mortise hole can vary depending on the design but should typically range between one and four times the width of the hole. This can result in square or rectangular mortise, or a circular to oval shape. If the mortise hole length exceeds four times its width, it is advisable to split it into multiple tenons for better stability. For blind mortises, the depth should generally be between one-half to two-thirds of the mortised material's depth. In the case of through mortise, where the hole extends completely through the material, there is no specific depth required. The dimensions of the tenon should correspond to those of the mortise hole.

These considerations highlight the precision craftsmanship required in traditional mortise and tenon joinery, ensuring a secure and durable connection between timber elements. Historical structures like Horyu-ji Temple in Nara, Japan, shown in Figure 2.23, exemplify the effectiveness of mortise and tenon joints in ensuring structural stability and resilience against earthquakes. Incorporating these principles into contemporary timber construction practices can further enhance the seismic resilience of structures, aligning with the primary objective of this study.
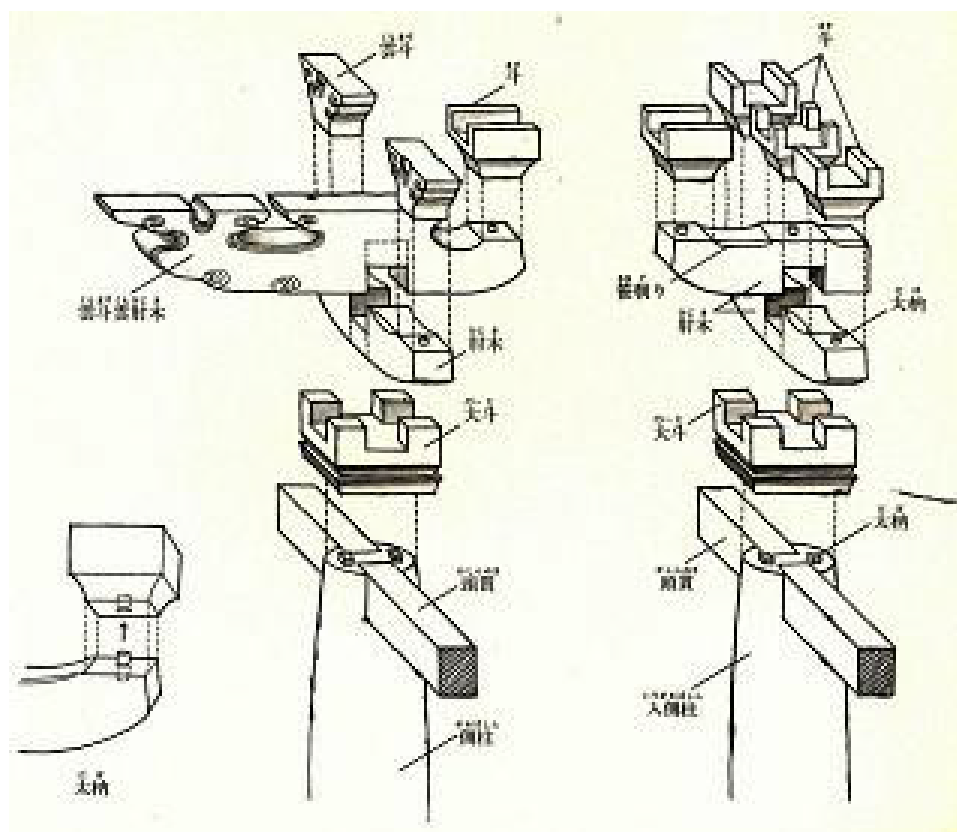
Figure 2. 23: Mortise and tenon design of Horyu-ji Temple.

2.5   Simulation

This section discussed the different simulation software commonly used in structural analysis will be discussed. Specifically, ANSYS, ETAB, and ABAQUS highlighted their capabilities and features in simulating seismic behaviour and structural response. Each software offers unique advantages and functionalities for modelling and analysing complex structures subjected to seismic loads.

2.5.1   ANSYS

ANSYS software is a dynamic and versatile tool widely used for finite element analysis (FEA) across various engineering disciplines. Offering a comprehensive range of analysis tools, ANSYS provides engineers and researchers with as user-friendly interface and a powerful integrated platform for simulating structural behaviour, including responses to seismic loading conditions. With its persistent and dependable solver technology, ANSYS software enables accurate predictions of structural responses under dynamic

forces, making it an essential tool for assessing safety and performance level of buildings and infrastructure. Moreover, ANSYS software offers powerful non-linear and linear solvers, allowing for detailed analyses of complex structural systems (Wilde Pdsvision, n.d.). Its dynamic environment facilitates the preparation of geometry for analysis and the integration of additional physics, enhancing fidelity in simulation results. As a multipurpose tool, ANSYS software stands out as preferred choice in the field of structural engineering for seismic analysis and design projects.

2.5.2 ETABS

Extended Three-Dimensional Analysis of Building System (ETABS) is an engineering software designed for the analysis and design of multi-storey buildings. Its features include modelling tools, code-based load prescriptions, and various analysis methods tailored for the unique grid-like geometry of such structures. Users can evaluate both basic and advanced systems under static or dynamic conditions. For a detailed assessment of seismic performance, ETABS offers modal and direct-integration time-history analyses coupled with P-Delta and Large Displacement effects (Ondrej, 2022). It also includes non-linear links and features like concentrated PMM or fiber hinges to capture material non-linearity, whether under monotonic or hysteretic behaviour. The software is intuitive interface and integrated functionalities make it practical for implementing applications of any complexity. Additionally, its interoperability with a range of design and documentation platforms enhances productivity, making it suitable for designs ranging from simple 2D frames to complex modern high-rises.

2.5.3 ABAQUS

ABAQUS is a powerful finite element analysis (FEA) software renowned for its versatility in tackling complex engineering simulations across various industries. With its wide array of element types and material models, ABAQUS can effectively simulate stress and deformation in diverse materials such as metals, rubber, polymers, composites, concrete, and even biological tissues (Simulia, n.d.). Moreover, ABAQUS goes beyond stress analysis, enabling the

simulation of heat transfer, mass diffusion, acoustics, piezoelectricity, and more, either independently or fully coupled with stress analyses. Its modularity and flexibility allow engineers to model any combination of elements, materials, procedures, and loading sequences, making it a go-to tool for simulating real-world scenarios.

In addition, ABAQUS is lauded for its robust finite element analysis algorithms, which enable the simulation of various seismic phenomena like non-linear material behaviour, large deformations, and dynamic effects. This makes it an ideal platform for conducting seismic analysis and design studies, optimising structural performance, and enhancing resilience against seismic hazards.

Importantly, ABAQUS will play a key role in this research, as it will be utilised to investigate stress concentration within timber framed structures during earthquakes.

2.6 Material properties and design codes

In this section, the natural properties of concrete, steel bars, and timber, as well as their relationship to applicable design codes will be examined. Understanding the inherent characteristics of these materials is crucial for structural design and analysis, as they directly influence the behaviour and performance of buildings and infrastructure.

2.6.1 Concrete

Concrete is a widely used construction material known for its strength, durability, and versatility. Its natural properties, including compressive strength, tensile strength, modulus of elasticity, and density, play an important role in determining the performance of concrete structures. These properties influence how concrete structures behave under different loading conditions, such as axial compression, bending, and shear.

In structural engineering, the use of concrete is governed by various design codes and standards to ensure the safety and reliability of structures. In Malaysia, concrete design is typically guided by standards such as BS 8500 for concrete production and BS 8100 for design and construction of concrete

structures. These codes provide specifications for concrete mixtures, reinforcement detailing, structural analysis, and construction practices, ensuring that concrete structures meet the required performance criteria and adhere to safety standards.

Additionally, Eurocode standards, such as Eurocode 2 (EN 1992), are also followed in Malaysia, providing unified design principles for concrete structures across European countries. These standards cover various aspects of concrete design, including material properties, structural analysis, durability, and construction techniques. By adhering to both British and Eurocode standards, engineers in Malaysia ensure that concrete structures are designed, constructed, and maintained to withstand diverse environmental conditions and loading scenarios, while upholding safety standards and structural integrity.

2.6.2 Steel bar

Steel bars, also known as reinforcing bars or rebars, are important components in reinforced concrete structures, providing tensile strength and enhancing the overall structural integrity. Steel bars are characterised by their material properties, including yield strength, ultimate tensile strength, elongation, and ductility, which determine their performance in resisting applied loads and deformations.

In Malaysia, the design and use of steel bars in construction are governed by various design codes and standards, including both British and Eurocode. Standards such as BS 4449 and BS 8666 provide specifications for the manufacturing, testing, and detailing of steel reinforcement, ensuring compliance with quality and safety requirements. Eurocode standards, such as Eurocode 2 (EN 1992) and Eurocode 8 (EN 1998), offer design guidelines for steel reinforcement in concrete structures, covering aspects such as material properties, detailing, and construction practices.

Steel bars come in various shapes and sizes, including round bars, deformed bars, and welded wire mesh, each suited for specific structural applications. The selection of steel bars depends on factors such as the structural design, loading conditions, and environmental considerations.

Understanding the material properties and design standards of steel bars is essential for ensuring the structural performance and safety of reinforced concrete structures. By adhering to established codes and standards and using high quality steel reinforcement, engineers can effectively enhance the durability, resilience, and longevity of concrete structures in diverse construction projects.

2.6.3   Glulam

Glulam, a type of glued laminated timber, is increasingly being utilised in Malaysia's construction sector. It is crafted by bonding individual layers of solid timber together, resulting in larger and more durable members than traditional sawn logs. Renowned for its versatility and reliability, glulam offers architects and engineers a wide range of design possibilities.

A key advantage of glulam lies in its flexibility, as it can be tailored to various dimensions and shapes, including straight, curved, or cambered profiles. Additionally, glulam boasts exceptional strength and fire resistance, outperforming conventional timber materials. Its compact dimensions and superior fire-retardant properties make it an attractive choice for structural applications.

Beyond its practical attributes, glulam is aesthetically pleasing and easy to work with, allowing for efficient machining and assembly processes. From an environmental standpoint, glulam is highly sustainable, as timber is a renewable resource that stores carbon and requires minimal energy for processing.

Compliance with Malaysian standards such as MS 758: 2001, MS 544: Part 3, MS 1714, and MS 1553 / BS 6399-2 / BS EN 1991 ensures that glulam products meet stringent performance and safety criteria.

A notable project highlighting the use of glulam in Malaysia is the Galeri Glulam in Johor Bahru (GGJB). This initiative, spearheaded by the Malaysian Timber Industry Board (MTIB), showcases glulam's potential in load-bearing structures. Utilising locally sourced hardwoods like resak and keruing, the GGJB project demonstrated the innovative application of glulam in architectural

design, aligning with the nation's efforts to promote sustainable timber practices and domestic timber utilisation (Construction Plus Asia, 2016).

2.7 Modelling

The process of modelling structural elements for seismic analysis is elucidated, covering various component crucial for accurate simulation and assessment of seismic behaviour.

2.7.1 Beam

Beam are important structural elements in construction, providing a secure pathway for loads and ensuring optimal weight distribution across building's foundation. They support the building's floors, ceilings, and roofs, transferring the load to the vertical load bearing framework. Transfer beams, larger and heavier, are employed to manage combined weight and effectively transfer support loads. Modelling beams involves defining their geometric and material properties, including length, depth, cross-sectional shape, stiffness, and strength. Boundary conditions, such as supports or connections to other elements, are specified for accurate representation of the structural system's response to seismic force. When loads such as the weight of floors, ceilings, or roofs act on a beam, they create bending forces that cause the beam to bend or deform. The beam's cross-sectional shape and material properties, including stiffness and strength, determine its ability to resist these bending forces. By generating internal stresses within their material, beams counteract bending moments and maintain their structural integrity. Therefore, in addition to providing a secure pathway for loads and ensuring optimal weight distribution across the building's foundation, beams also play an important role in resisting bending moments to maintain structural stability and safety.

2.7.2 Column

Columns is also an important vertical structural element in construction, primarily tasked with transferring compressive load from the structure's slab, such as the roof or upper floors to its foundation and the ground below, effectively counteracting the gravitational forces acting upon the building.

These loads may originate from various sources, including beams, ceilings, or roof slabs. In essence, columns provide essential support to the entire structure, ensuring its stability and integrity, as well as determining the clearance height of a building. Modelling columns involves defining their geometric properties, such as height and cross-sectional shape, as well as material properties like strength and stiffness. Additionally, boundary conditions at the column ends, such as connections to other structural elements or the foundation, are specified to accurately represent their behaviour under different loading conditions.

2.7.3   Frame

In structural engineering, frame structures consist of interconnected beams and columns designed to support and stabilise buildings. They are important in distributing loads, resisting lateral forces like wind or seismic loads, and maintaining structural stability. Frame structures are versatile and can be constructed from various materials such as reinforced concrete, steel, and wood (Kumar, 2023).

Modelling a frame involves specifying the arrangement and properties of its components, including beams, columns, and connections. Geometric properties like lengths, depths, and cross-sectional shapes of beams and columns are defined, along with material properties such as stiffness and strength. Boundary conditions at beam-column connections are also determined to accurately depict the frame's behaviour under different loads.

Frame structures can withstand both lateral and gravitational loads due to their combination of beams, columns, and slabs. They are particularly effective in overcoming large moments generated by applied loads, ensuring structural stability and safety (Kumar, 2023). Different types of frame structures exist, including portal frames, rigid frames, and braced frames, each offering specific benefits in terms of load resistance and structural performance.

Designing and analysing frame structures adhere to engineering codes and standards, which establish criterial for structural integrity, safety, and performance. Factors like load combinations, material properties, and structural detailing are carefully considered to meet strength and serviceability requirements.

Overall, frame structures are indispensable components in building construction, providing stability, support, and resilience against various loads, thus ensuring the safety and functionality of the built environment.

2.7.4   Multi storey

Multi storey structures are buildings consist of multiple floors or levels, typically designed to accommodate various functions such as residential, commercial, or industrial spaces. In addition to columns, beams, and floor systems, multi storey buildings often incorporate various structural elements such as shear walls, flat slabs, and other lateral load resisting systems to enhance their stability and performance. These elements play a crucial role in distributing loads, resisting lateral forces such as wind and seismic loads, and providing overall structural integrity to the building. Therefore, when modelling multi storey structures, it is important to include these elements to accurately capture their behaviour under different loading conditions. The modelling of multi storey buildings involves simulating the entire structure, including its floors, columns, beams, and connections, to accurately represent its behaviour under different loading conditions, including gravity loads, lateral loads, and seismic forces. Additionally, consideration for factors such as building height, floor layout, material properties, and structural configurations are crucial in the modelling process to ensure structural integrity, stability, and safety. Multi storey buildings are subjected to complex loading scenarios, and effective modelling techniques are essential for assessing their performance and ensuring compliance with design standards and regulations.

2.8   Parameters

Various parameters critical to seismic analysis are described, including dynamic loads, constraints, surface or embedded contacts, and EI Centro. These parameters play a key role in accurately modelling and analysing structural behaviour under seismic loading conditions. By comprehensively understanding and properly defining these parameters, engineers and researchers can ensure the reliability and effectiveness of seismic analysis

results, ultimately contributing to the safety and resilience of structures in earthquake-prone regions.

2.8.1   Dynamic loads

Dynamic loads refer to transient forces or accelerations acting on structures during seismic events, leading to dynamic responses and potentially causing structural damage. Modelling dynamic loads involves specifying their magnitude, frequency content, and directionality based on seismic hazard assessments and design criteria. Consideration is given to various types of dynamic loading, including ground shaking, inertial forces, and dynamic excitations from nearby structures or machinery, to accurately simulate the seismic response of the structure.

Understanding the importance of dynamic loads is crucial as they can significantly influence the structural behaviour, often resulting in complex nonlinear responses that cannot be adequately captured by static analysis alone. While static loads exert a constant force on the structure, dynamic loads vary with time and can induce vibrations, resonance, and structural amplification effects, thereby posing risks of instability and failure. The equation of force (Force = mass x acceleration) explains the greater impact of dynamic loads on structures compared to static loads, as they vary with time.

Advanced computational tools like finite element analysis (FEA) and dynamic analysis software such as Abaqus, ANSYS, or OpenSees are commonly used to simulate dynamic loads. These tools empower engineers to capture the dynamic behaviour of structures under seismic loading, considering factors like material properties, geometric configurations, and boundary conditions. For example, in seismic analysis of RC buildings, dynamic loads can be emulated by applying ground motion records from seismic hazard assessments as excitation input to finite element models. This approach facilitates the assessment of a structural responses to dynamic loads, enabling the assessment of seismic performance and identification of vulnerabilities requiring mitigation measures.

2.8.2   Constraints

Constraints in seismic analysis refer to boundary conditions or limitations imposed on structural degrees of freedom (DOF) to simulate realistic structural behaviour under seismic loading. These constraints may include fixed supports, roller supports, or prescribed displacements at specific locations to represent structural connections, foundation conditions, or structural discontinuities. Proper constraint modelling is essential to capture the interaction between structural elements and the surrounding environment during seismic events.

Structural constraints play a fundamental role in stabilising the structure and governing its response to seismic forces, thereby influencing the overall seismic performance and resistance of the structure. Additionally, design constraints such as architectural requirements, material limitations, and construction standards, need to be considered in conjunction with structural constraints to ensure a comprehensive seismic analysis.

Selecting suitable constraints requires a thorough understanding of the structural system, including its geometry, material properties, loading conditions, and expected behaviour under seismic excitation. It requires careful consideration of the types of constraints that best represent the physical behaviour of the structure while minimising computational complexity. In addition, the appropriateness of constraints should be verified through sensitivity analysis and benchmarking against experimental data or established analytical solutions to ensure the fidelity and reliability of seismic analysis results.

2.8.3   Surface or Embedded contact

Surface or embed contact refers to the interaction between structural components or between structural elements and their surrounding environment, such as soil or foundation systems, during seismic loading. Modelling surface or embedded contact involves defining contact interfaces, frictional properties, and contact behaviour to simulate realistic interaction and load transfer mechanisms. It is critical to ensure that surface or embedded contact are accurately model the response of structure and its underlying systems to seismic forces. Effective modelling of contact interfaces facilitates the transfer of forces

and moments between adjacent structural components, allowing accurate prediction of structural behaviour under seismic loading conditions.

Additionally, combining friction properties and contact behaviour parameters allows the simulation of sliding, separation, and reattachment phenomena prevalent in seismic events. This comprehensive representation of surface or embedded contact is essential for evaluating the structural integrity, stability, and performance of systems under seismic excitation. For example, in seismic analysis of bridge structures, the interaction between the bridge deck and supporting piers, as well as the interface between the piers and the underlying soil or foundation, must be accurately modelled to evaluate the structural response and ensure the safety and resistance of the bridge system.

2.8.4   El Centro

The EI Centro parameter is a key characteristic of structural elements representing their flexural stiffness distribution along their length. In seismic analysis, EI Centro plays a significant role in determining the structural response to bending and deformation under seismic loading. Modelling EI Centro involves defining the variation of flexural stiffness along the length of structural members, considering factors such as material properties, cross-sectional geometry, and support conditions. Accurate representation of EI Centro is essential for capturing the dynamic behaviour and deformation patterns of structural elements during seismic events.

The EI data serves as a fundamental input in finite element models, guiding the simulation of structural response under seismic excitation. The EI values significantly affect the overall stiffness and behaviour of the structure, influencing factors such as natural frequency, mode shapes, and deformation patterns. In seismic design, adjustment to EI data may be necessary based on specific structural configurations, loading conditions, and design requirements. For example, structures with irregular geometries or complex loading scenarios, customised EI distributions can be employed to better capture the structural response and ensure seismic resistance. Additionally, EI adjustments can be made to optimise structural performance, reduce potential vulnerabilities, and meet design objectives, such as enhancing ductility or reducing structural drifts.

Figure 2.24 illustrating the time history of ground acceleration. This graph provides insight into the dynamic forces acting on the structure over time during seismic event. Therefore, the accurate representation and adjustment of EI Centro data are important for the reliable assessment and design of structures subjected to seismic loading.
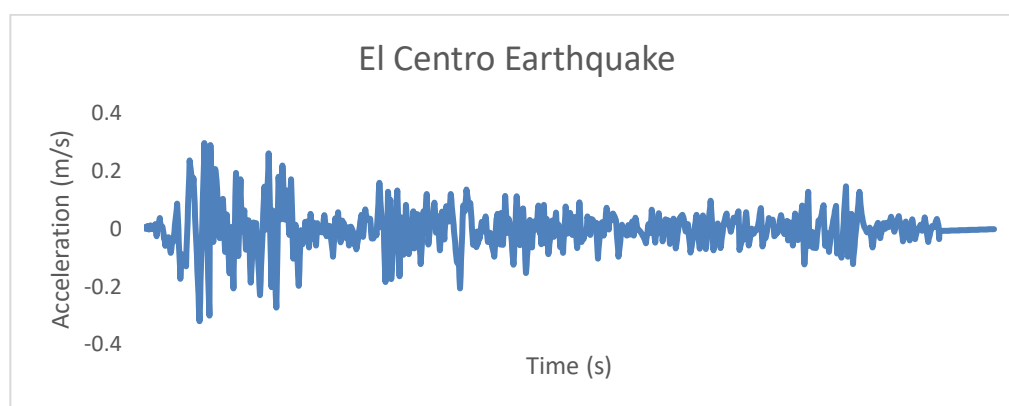
Figure 2. 24: EI Centro graph.

2.9   Meshing

In this section, the process of meshing, a crucial step in finite element analysis, is discussed, encompassing considerations such as the size and type of elements employed.

2.9.1   Size of element

The size of elements in the meshing process plays a important role in determining the accuracy and computational efficiency of the finite element model. General considerations for sizing elements include balancing between global size and local refinement to capture both overall structural behaviour and localized phenomena accurately. Mesh size is critical to the convergence of nonlinear analysis. Larger mesh sizes may not produce sufficiently accurate results, while smaller element sizes may cause issues such as rapid local damage or uneven damage distribution (Rahul, et al, 2017). Furthermore, reducing the mesh size below characteristic length of the problem should be avoided to prevent localised zero volume in the damaged region (Rahul, et al, 2017). The global size of elements influences the overall mesh density and computational cost, with finer meshes providing more detailed results but requiring higher

computational resources. Local refinement techniques, such as adaptive meshing or element size controls, are employed to enhance mesh resolution in critical regions of interest, such as areas of high stress concentration or geometric complexity, ensuring accurate representation of local behaviour without excessive computational overhead.

2.9.2   Type of element

The selection of element type in meshing is essential for accurately representing the structural geometry and behaviour in finite element analysis. Various types of elements, including tetrahedral (tet), hexahedral (hex), triangular, and quadrilateral elements, are available, each with distinct advantages and limitations based on the structural geometry, loading conditions, and analysis objectives.

Tetrahedral elements are commonly used for irregular geometries and complex structures due to their flexibility, while hexahedral elements are preferred for regular geometries and solid structures, offering higher computational efficiency and accuracy. Triangular and quadrilateral elements are employed for planar structures and surface meshes, providing efficient representation of two-dimensional behaviour.

The selection of element type depends on factors such as geometric complexity, mesh quality, numerical stability, and computational resources, with careful consideration given to optimizing the balance between accuracy and computational efficiency for the specific analysis requirements. Additionally, special-purpose elements such as beam, shell, and solid elements may be used to model specific structural components or behaviour, further enhancing the fidelity of the finite element model.

2.10   Plastic and elastic analysis

In this section, the focus is on plastic and elastic analysis, including discussions on stress-strain relationships, Von Mises stress, and principal stress.

2.10.1 Stress-strain analysis

Stress-strain analysis involves examining relationship between applied stresses and resulting strains in a material. As illustrated in Figure 2.25, the stress-strain curve provides information about how a material deforms under loading and helps to determine its mechanical properties, such as modulus of elasticity, yield strength, and ultimate tensile strength. Stress-strain analysis is important for understanding material behaviour under both elastic and plastic deformation and is widely used in material characterisation and structural design.
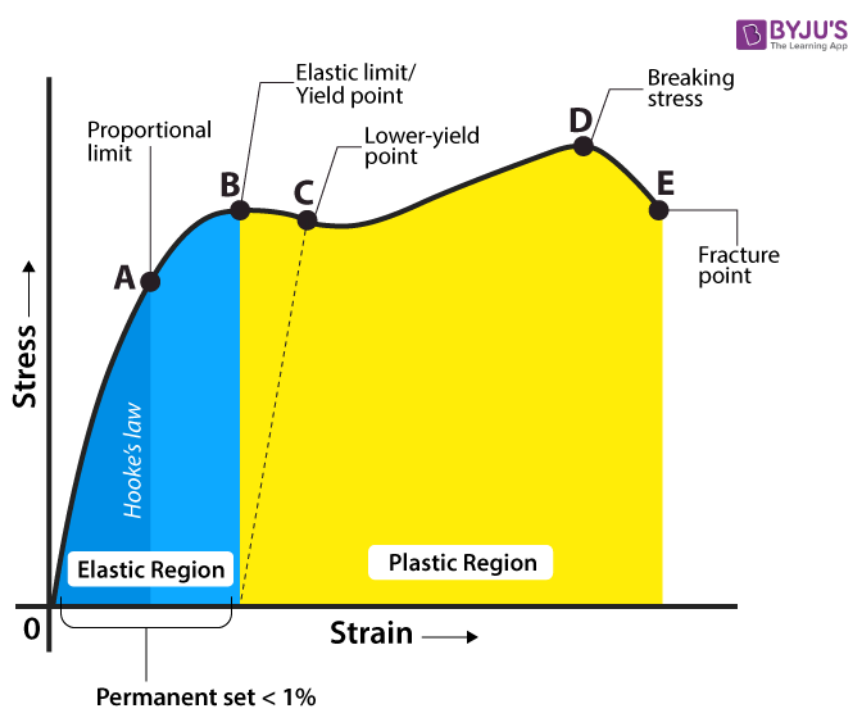
Figure 2. 25: Stress-strain graph (BYJU's, n.d.).

There are two primary types of stress experienced by materials: tensile stress, which occurs when a material is pulled apart, and compressive stress, which occurs when a material is push together. Stress is defined as the force applied per unit area, represented by the formula $\sigma = {F}/{A}$, where σ represents stress, F is the applied force, and A is the cross-sectional area. Similarly, tensile strain and compressive strain refer to the amount of deformation experienced by a material under tension or compression respectively. This deformation is

quantified by the equation $\varepsilon = \Delta L / L$, where ε represents strain, ΔL is the change in length, and L is the original length of the material.

Figure 2.25 illustrates the stress-strain curve for a material, showing the proportional limit where the material obeys Hooke's Law (BYJU's, n.d.). Hooke's Law states that stress is directly proportional constant, which is known as the Young's modulus. The elastic limit or yield point on the curve indicates the point at which the material returns to its original position upon removal of the applied load. However, beyond this limit, the material undergoes plastic deformation, meaning it does not return to its original shape after the load is removed.

The study by Jorge, et al. (2023) presents a Machine Learning (ML)-based framework aimed at predicting the stress-strain relationship of arc-direct energy deposited mild steel. Their dataset initially comprised 1000 raw stress-strain curves, ranging from 11 to 66 data points, representing the elasto-plastic response up to a total strain of 30%, as illustrated in Figure 2.26. These curves were redefined to 30 and 10 points for ML modelling purposes, as illustrated in Figure 2.27 and Figure 2.28 respectively.
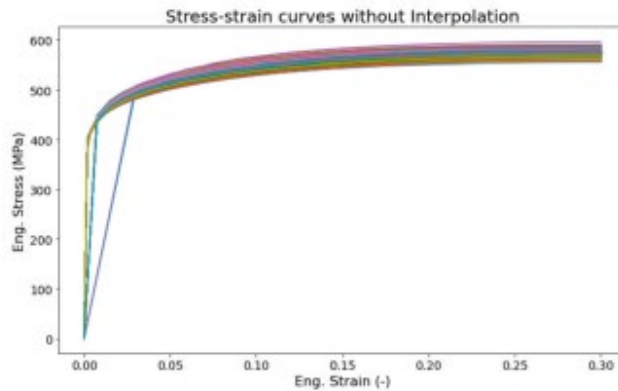
Figure 2. 26: 1000 raw stress-strain values obtained after simulating a tensile test in Abaqus CAE (Jorge, et al., 2023).
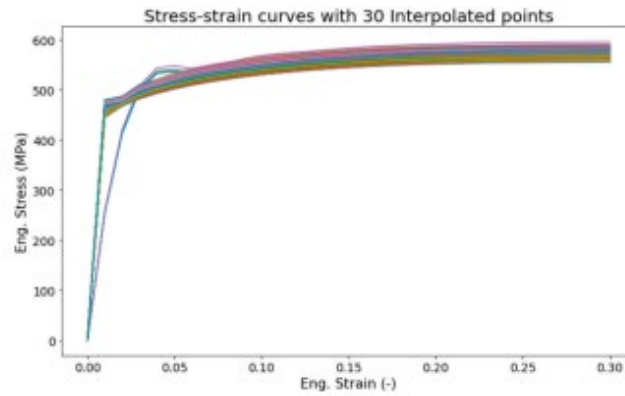
Figure 2. 27: A 2D plot of 1000 stress-strain values at 30 interpolated strain points (Jorge, et al., 2023).
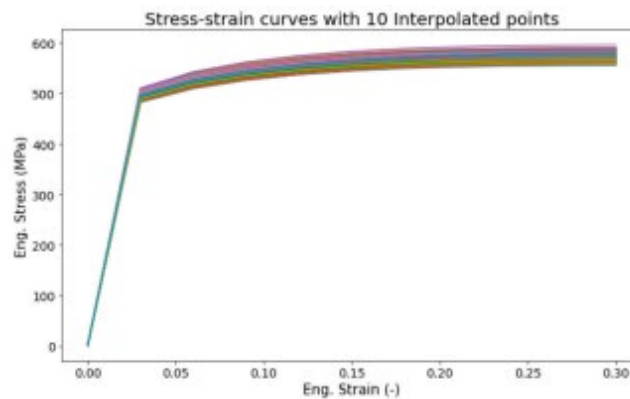
Figure 2. 28: A 2D plot of 1000 stress-strain values at 10 interpolated strain points (Jorge, et al., 2023).

2.10.2   Von mises stress

In mechanical engineering and materials science, Von Mises stress, also known as equivalent tensile stress or equivalent stress, is a measure of the combined effect of all normal and shear stresses in a material, representing a hypothetical tensile stress that would cause the same deformation as the actual combined stress state. It is particularly useful for assessing the yielding and failure of ductile materials, such as metals, under complex loading conditions where different types of stresses are present simultaneously (Simscale, 2023).

For steel materials, Von Mises stress is critical in determining their failure behaviour under loading. Steel exhibits ductile behaviour, meaning it can undergo significant plastic deformation before failure. Von Mises stress helps engineers assess the integrity of steel structures by indicating areas prone to

yielding or plastic deformation. The formula for Von Mises stress, denoted as σ_v , is given by:

$$\sigma_v = \sqrt{\frac{(\sigma_1 - \sigma_2)^2 + (\sigma_2 - \sigma_3)^2 + (\sigma_3 - \sigma_1)^2}{2}}$$

Where $\sigma_1, \sigma_2, \sigma_3$ are the principal stress in the material.

Similarly, for timber and concrete materials, Von Mises stress can be used to evaluate their integrity and failure behaviour. However, the application of Von Mises stress to these materials is not as straightforward as for metals. Timber exhibits orthotropic behaviour, meaning its properties vary with direction, and concrete is inherently brittle, exhibiting limited plastic deformation. Therefore, Von Mises stress may not be as directly applicable to these materials compared to metals.

Figure 2.29 illustrating the Von Mises criterion in 2D. Tresca criterion focuses on predicting yielding based on maximum shear stress present in the material, whereas Von Mises approach the assessment of yielding in complex stress states. While Tresca criterion is straightforward and easy to apply, Von Mises criterion provides a more accurate representation of material behaviour. This criterion is simpler to apply but may be overly conservative, especially in cases where the stress state is not purely shear-dominated.
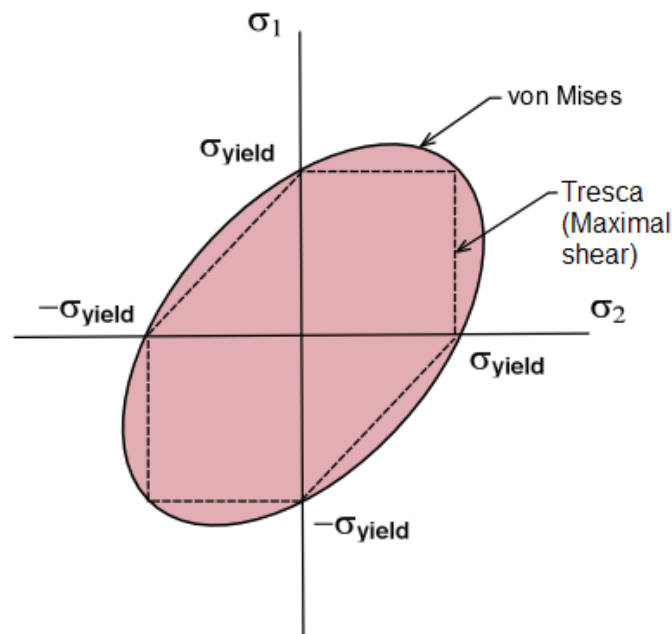
Figure 2. 29: Von Mises stress criterion in 2D.

In their study, Muthuveerappan and Sivarajan (2023) investigated the effects of process parameters on deformation and Von Mises stress in drilling using finite element analysis. Three key process parameters, namely the material of the drilling bit, cutting speed, and drill point angle were analysed. The researchers conducted their analysis using the static structural mode in ANSYS Workbench. Figure 2.30 presents the values of deformation obtained from the simulation. Additionally, the corresponding signal-to-noise (SN) ratios were computed and are depicted in Figure 2.31. These SN ratios provide insight into the variation of deformation across different parameter settings. Furthermore, the results were tabulated in table form, as shown in Figure 2.32, to facilitate a comprehensive comparison and analysis of the data obtained from simulations. This approach allowed researchers to evaluate the influence of each process parameter on deformation and Von Mises stress. Their finding revealed that Von Mises stress increases with higher cutting speeds, indicating a correlation between machining parameters and stress levels.

Simulation no	Total-deformation Max (m)	Von-Mises stress (Pa)
1	2.54E-12	189.73
2	1.02E-11	757.55
3	2.30E-11	1739.6
4	3.89E-11	425.75
5	1.33E-10	1692.6
6	2.99E-10	3803.2
7	3.46E-11	420.85
8	1.39E-10	1718.7
9	3.12E-10	3799

Figure 2. 30: Deformation and Von Mises stress.
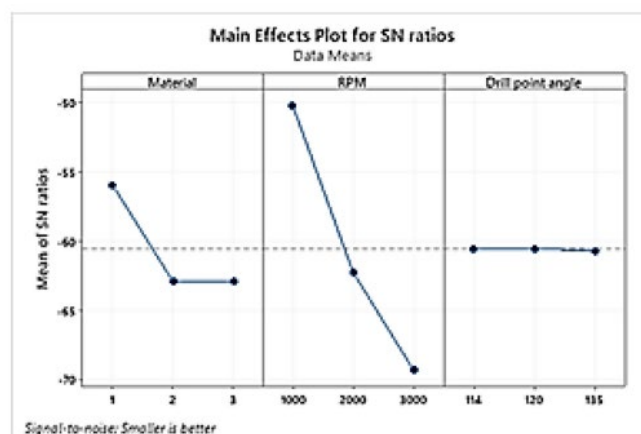
Figure 2. 31: SN graph for Von Mises stress.

Simulation no	Von-Mises	SN ratio
1	189.73	−45.5627
2	757.55	−57.5882
3	1739.6	−64.809
4	430.75	−52.6845
5	1692.6	−64.5711
6	3803.2	−71.603
7	420.85	−52.4825
8	1718.7	−64.704
9	3799	−71.5934

Figure 2. 32: SN ratio results for Von Mises stress.

2.10.3 Principal stress

Principal stresses represent the maximum and minimum normal stresses experienced by a material at a specific point in a structure, along with the direction in which these stresses act, as shown in Figure 2.33. These stresses are important in determining the structural integrity and failure modes of the materials under loading conditions. For ductile materials like steels, principal stress help to assess the potential for yielding and fracture, whereas for brittle materials like concrete, they aid in predicting crack initiation and propagation. The formula for determining principal stresses involves solving the eigenvalue problem of the stress tensor matrix, resulting in three principal stress values $(\sigma_1, \sigma_2, \sigma_3)$ and their corresponding direction, as illustrated in Figure 2.34.
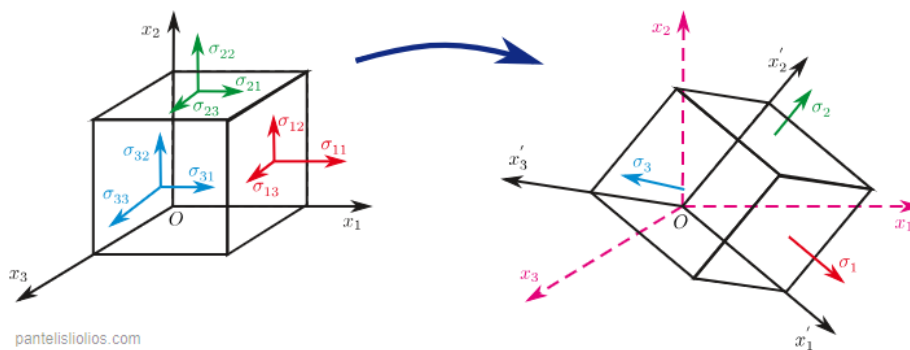
Figure 2. 33: Principal stresses and their direction with respect to the initial coordinate system (Pantelis, 2020).

$$|\sigma_{ij} - \sigma\delta_{ij}| = \begin{vmatrix} \sigma_{11} - \sigma & \sigma_{12} & \sigma_{13} \\ \sigma_{21} & \sigma_{22} - \sigma & \sigma_{23} \\ \sigma_{31} & \sigma_{32} & \sigma_{33} - \sigma \end{vmatrix} = 0$$

Figure 2. 34: Eigenvalue equation (Pantelis, 2020).

Concrete exhibits distinct behaviour under tensile and compressive loading due to its brittle nature. In tension, concrete is prone to cracking and failure, while in compression, it can withstand higher loads before failure occurs. The principal stresses in concrete provide understanding into the maximum and minimum stress states experienced by the material.

Understanding the distribution of principal stresses in concrete structures allows engineers to assess the risk of tensile cracking and compressive failure, guiding reinforcement and design decisions to enhance structural performance and durability.

2.11   Summary of literature review

This chapter provided a comprehensive review literature review to seismic analysis and finite element modelling of glulam framed structures. Key topics covered included structural damage, seismic resistant devices, material properties of structural elements, as well as the methodologies and tools used for finite element analysis in seismic engineering.

CHAPTER 3

METHODOLOGY AND WORK PLAN

3.1   Introduction

In this research, ABAQUS software serves as the primary tool for analysing and modelling three-storey glulam framed structures with mortise and tenon design. ABAQUS offers a comprehensive suite of visualisation tools and advanced finite element capabilities, making it an efficient choice for seismic simulation. However, proficiency in translating civil, structural, and architectural drawings into model structures is crucial for effective utilisation of the software. This chapter outlines the methodology and work plan for simulating the seismic behaviour of three-storey glulam framed structures with mortise and tenon design using ABAQUS, covering the modelling process and analysis result presentation.

3.2   Flow chart of research

Figure 3.1 illustrates the sequential steps involved in the seismic simulation of glulam framed structures with and mortise and tenon design. The process begins with the initial design phase, where the structure parameters and geometry are defined based on the research objectives and structural requirements. Once the design is finalised, the next step involves modelling the structure using ABAQUS software. This phase includes translating the design specifications into a digital model within the software environment.

Following the modelling phase, the boundary conditions are established to simulate the real-world constraints and loading conditions experienced by the structure. These boundary conditions define how the structure interacts with its environment and are crucial for accurately capturing its seismic response.

With the model prepared and boundary conditions set, the seismic analysis is conducted using ABAQUS. This involves subjecting the structure to seismic loads representative of those experienced during an earthquake event. The software calculates the structural response, including displacements,

stresses, and deformations, allowing for a comprehensive evaluation of its seismic performance.

After obtaining the simulation results, the next step is result interpretation. This involves assessing the acceptability of the results based on predefined criteria. If the results meet the desired objectives and performance standards, they are deemed acceptable, and the analysis proceeds to reporting and documentation. However, if the results are not satisfactory or require further optimisation, the process loops back to the modelling phase. This iterative process continues until acceptable results are achieved, ensuring the accuracy and reliability of the seismic simulation.
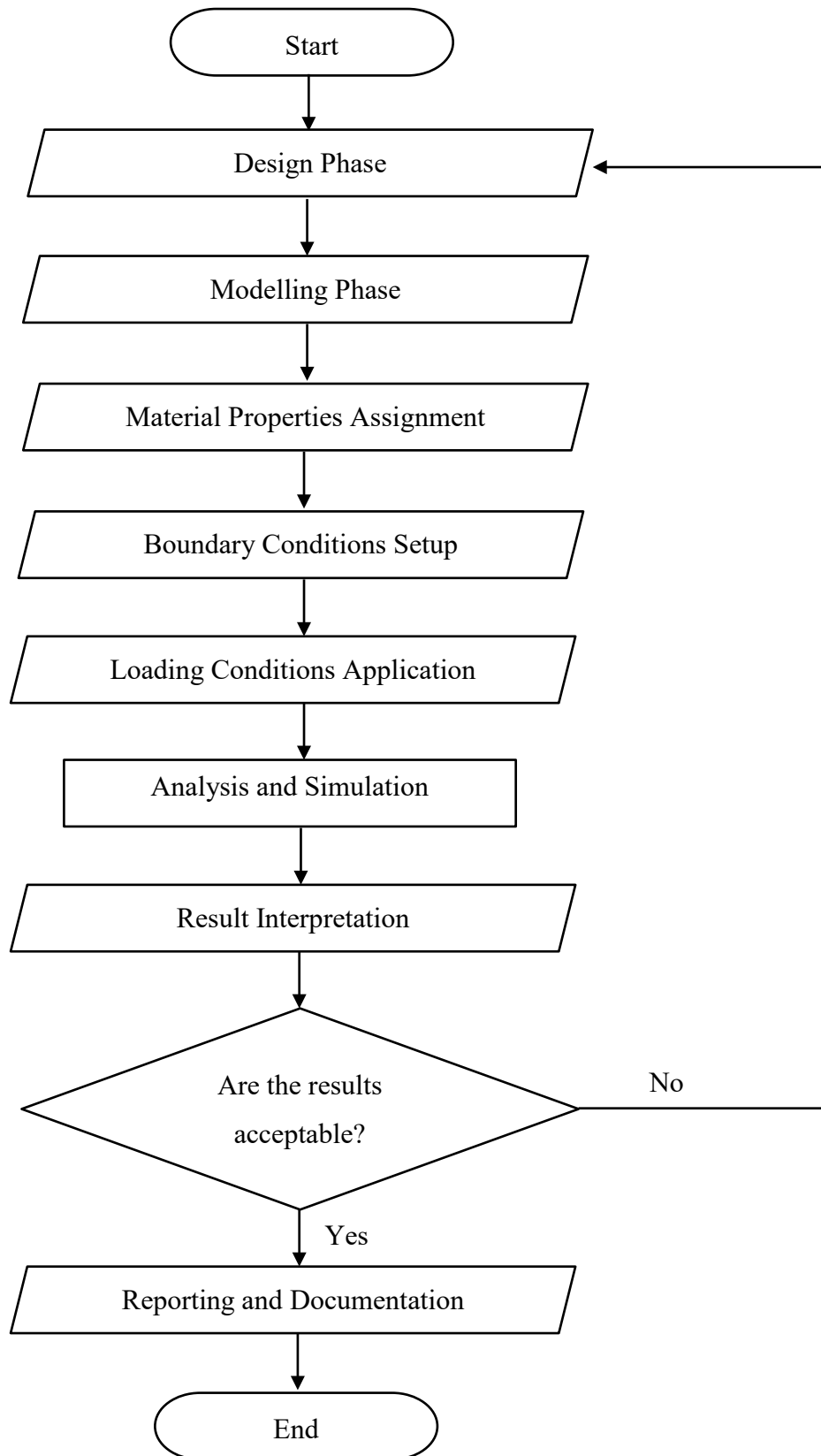
Figure 3. 1: Seismic simulation flowchart.

3.3 Specification

This section outlines the specifications related to concrete and glulam materials. Concrete elements, including beams and columns, will be discussed in detail, along with their respective properties and design parameters. Similarly, glulam components, particularly those featuring the mortise and tenon design, will be examined, with specific attention given to the structural characteristics and properties.

3.3.1 Concrete

In this section, concrete has been utilised in the design of a three-storey building. Concrete columns are specified with dimensions of 40 x 40, while beams are 31 x 75, as shown in Figure 3.2. The AutoCAD figure illustrates the layout of the concrete elements within the structure, highlighting the column and beam dimensions specified for the construction.
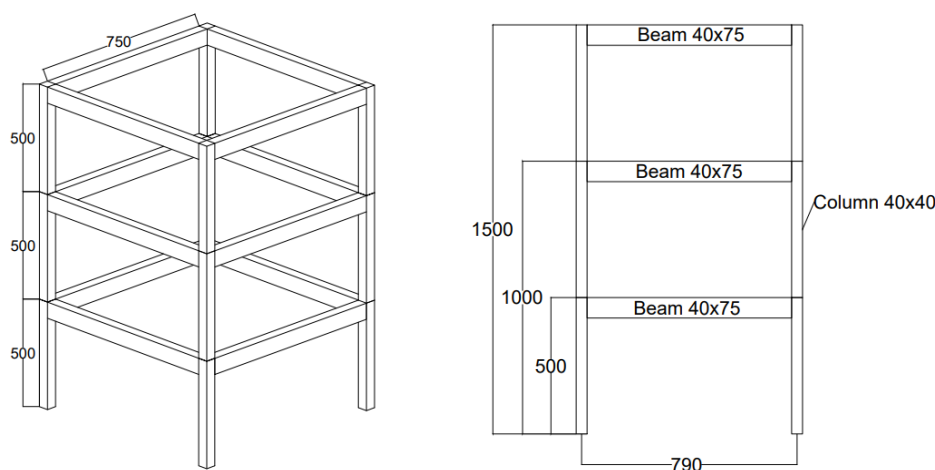
Figure 3. 2: 3D view of concrete modelled in AutoCAD.

3.3.2 Glulam

In this section, the use of mortise and tenon joinery in glulam design is explored. Glulam timber, specifically grade GL28h, is selected as the primary material for the construction of the three-storey building. Column dimensions are specified as 40 x 40, while beams are sized at 40 x 75. Given the emphasis on glulam construction, the connections between all structural components are achieved using the mortise and tenon method. at the first floor, glulam columns

incorporate both mortise and tenon connections, with mortise joints linking to the beams and tenon joints connecting to the columns of the second floor, as shown in Figure 3.4. Beams utilise tenon joints for connection to both columns. Moving to the second floor, columns feature mortise joints at the bottom and tenon joints at the top, facilitating connection to the columns of the third floor. Lastly, columns at the third floor exclusively incorporate mortise joints at the bottom to connect to the columns of the second floor. The design approach ensures robust connections and seamless integration of glulam elements through the structure. Figure 3.5 depicting the column and beam at the third floor with the mortise and tenon joint.
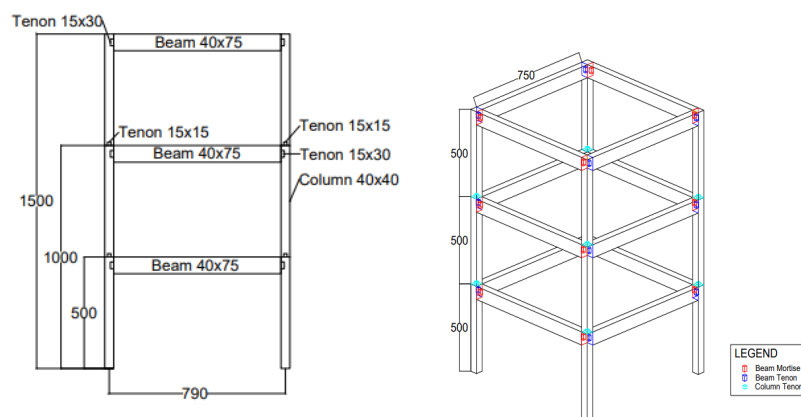
Figure 3. 3: 3D view of timber modelled in AutoCAD.
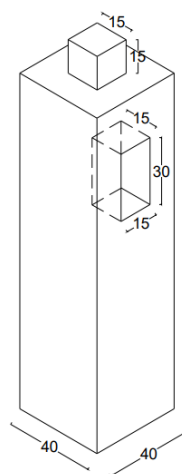
Figure 3. 4: Cut section of column at first floor.
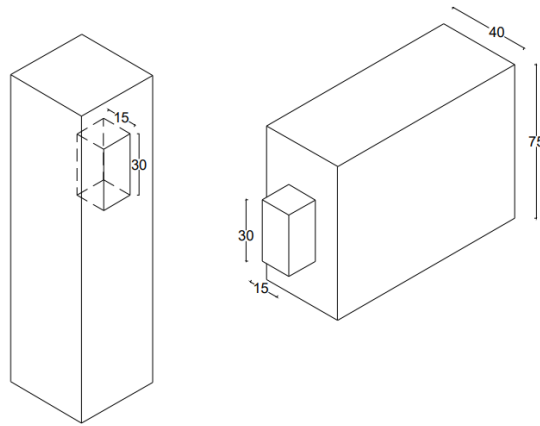
Figure 3. 5: Mortise and tenon joint between column and beam at third floor.

3.4   Material properties

This section covers the material properties of timber and concrete as pertinent to the seismic simulation of timber framed structures with innovative mortise and tenon designs.

3.4.1   Concrete grade

A specific grade of reinforced concrete, Class C25/30, has been selected for modelling the structure. This grade is commonly employed in both residential and commercial settings. It finds frequent use in house foundations and general concrete works due to its balanced properties of strength and workability. Furthermore, it is well-suited for applications such as residential house and shed slabs, footpaths and kerbs, as well as driveways and patios. The properties of C25/30 are summarised in Table 3.1, providing a comprehensive overview of the concrete material properties essential for the seismic simulation.

Table 3. 1: Summary of the material properties.

Materials	Material Properties	Value
	f_{ck}	25 N/mm^2
	Mass Density	2.4×10^{-9} tonne/mm^3
	Young's Modulus	30 000 N/mm^2
	Poisson's Ratio	0.2
C25/30 grade	Dilation Angle	31˚
concrete	Eccentricity	0.1
	f_{b0}/f_{c0}	1.16
	k	0.667
	Compression yield stress	25 N/mm^2
	Tension yield stress	2.25 N/mm^2

3.4.2 Rebar amount

A concrete building inherently requires reinforcement to enhance its strength and structural integrity. The three-storey building was designed with a total height of 1500mm and a single bay spacing at 790mm center to center, incorporates steel reinforcement to ensure its robustness. Concrete cover for the reinforcement in beams and columns is set at 5mm to provide adequate protection. For this research, steel grade S275 has been chosen for the reinforcement material due to its favourable properties. S275 steel is renowned for its exceptional strength and toughness, rendering it well-suited for applications demanding increased durability and resilience against impacts (Yena Engineering BV, 2023). Moreover, its remarkable resistance to corrosion renders it a favoured option for construction projects conducted in outdoor environments. Table 3.2 provides a summary of the material properties for the selected steel reinforcement, while table 3.3 details the cross sections of the construction elements along with their respective reinforcement information.

Table 3. 2: Summary of the material properties.

Materials	Material Properties	Value
	f_{yk}	275 N/mm^2
	Mass Density	7.85×10^{-9} tonne/mm^3
S275 steel	Young's Modulus	210 000 N/mm^2
	Poisson's Ratio	0.3
	Yield stress	275 N/mm^2

Table 3. 3: Summary of the steel reinforcement.

Structural Element	Dimension (mm)	Reinforcement
Column	40×40	8T3
Beam	31×75	4T3

3.4.3 Glulam type

Glulam, or glued laminated timber, is an engineered wood product composed of multiple layers of dimensioned lumber bonded together with durable, moisture resistant adhesives. Glulam offers superior strength, stability, and versatility compared to traditional solid timber, making it an ideal choice for timber framed structures. Given its prevalence and efficacy in multi-storey buildings, GL28h grade glulam has been selected for its balanced strength and stiffness characteristics. GL28h is commonly used in low rise buildings due to its optimal balance between strength, stiffness, and cost-effectiveness. The material properties of GL28h glulam are summarised in Table 3.4.

Table 3. 4: Summary of the material properties (Hasslacher Norica Timber, n.d.).

Materials	Material Properties	Value
GL28h	Bending Strength	28 MPa
	Tensile Strength (Parallel to the grain)	22.3 MPa
	Tensile Strength (Perpendicular to the grain)	0.5 MPa
	Compression Strength (Parallel to the grain)	28 MPa
	Compression Strength (Perpendicular to the grain)	2.5 MPa
	Shear Strength	3.5 MPa
	Young's Modulus (Mean – Parallel to the grain)	12600 MPa
	Young's Modulus (Fifth Percentile – Parallel to the grain)	10500 MPa
	Young's Modulus (Mean – Perpendicular to the grain)	300 MPa
	Shear Modulus	650 MPa
	Characteristic Density	460 kg/m^3
	Poisson's Ratio	0.35

3.4.4 Tensile resistance

In structural engineering, tensile strength plays a crucial role in determining the ability of materials to resist pulling or stretching forces. Significant differences in tensile strength become apparent when comparing materials that commonly used in construction, such as concrete, steel, and timber.

Concrete grade of C25/30 has significantly lower tensile strength, with mean tensile strength, f_{ctm} = 2.56 N/mm^2. This inherent weakness in tension necessitates reinforcement with materials like steel to enhance its tensile capacity and prevent cracking under tensile loading conditions.

Steel has characterised by its high yield strength of approximately 275 N/mm^2, stands out as one of the strongest materials in tension. Its exceptional tensile strength makes it well-suited for applications where high strength and ductility are required.

In contrast, glulam exhibits lower tensile strength values, typically demonstrating tensile strength of 22.3 N/mm^2 parallel to the grain and 0.5 N/mm^2 perpendicular to the grain. Despite its lower tensile strength compared to steel, glulam's good strength-to-weight ratio and sustainability make it a viable option for various structural applications.

Understanding the varying tensile strengths of materials is important for structural design and analysis, informing material selection and the design of structural elements to ensure adequate performance and safety under different loading scenarios.

3.4.5   Compression

In structural engineering, compression resistance refers to a material's ability to withstand compressive forces or stresses. The compression strength of materials such as concrete, glulam, and steel, is critical in designing structural elements to support loads and ensure stability.

Concrete grade of C25/30, a commonly used construction materials, exhibits significant compression strength with a yield stress of 25 N/mm^2. This high compression strength allows concrete to efficiently support vertical loads in structural elements such as columns and footings, providing stability to the overall structure.

In comparison, glulam demonstrates respectable compression strength values, with GL28h grade glulam exhibiting compression strength of 28 N/mm^2 parallel to the grain and 2.5 N/mm^2 perpendicular to the grain.

Steel also possesses notable compression strength, making it suitable for various structural elements subjected to compressive loads. However, it is important to note that steel is often used in combination with other materials, such as concrete and glulam, to achieve optimal structural performance and efficiency.

Understanding the compression resistance of materials is important for designing safe and efficient structural systems. By considering the compression strengths of concrete, glulam, and steel, engineers can select appropriate materials and design structural elements capable of withstanding the anticipated loads and ensuring the structural integrity of the building or infrastructure project.

3.5   Modelling

The initial stage in the modelling process involves defining geometry of the structure, which includes specifying dimensions and arranging components. To accomplish this, navigate to the **Parts** in the Model Tree and assign appropriate name of each part (**Beam, Column, Tenon**). Next, select the modelling space, type and base feature as shown in Figure 3.6. A **solid** shape and **extrusion** type are selected for glulam beam, column, and tenon. The approximate size is set to a value of **2000**.
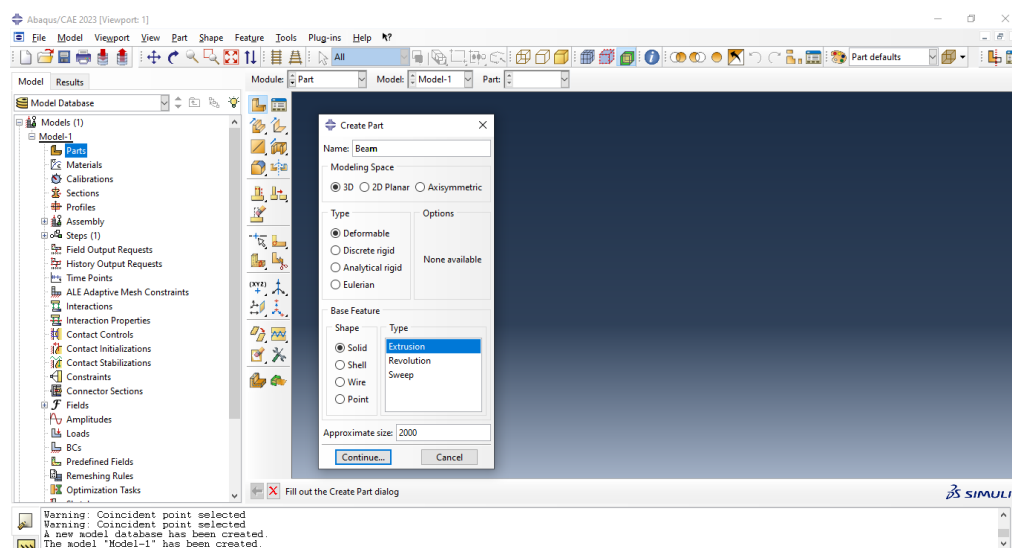
Figure 3. 6: Create Part dialog box for glulam model.

Next, utilise the sketching tools provided in the Sketcher toolbox on the left side of the window. For timber modelling, opt for the **Create Line: Rectangle (4 lines)** tool situated at the upper -right corner of the toolbox. This tool facilitates the creation of a two-dimensional rectangle. Enter the coordinates of the starting corner and the opposite corner in the prompt area,

ensuring they correspond to the desired length and width of the respective parts. Table 3.5 presents the coordinates for timber parts and their respective depths, while Figure 3.7 depicts the model of the beam. Repeat the aforementioned steps to construct the column and tenon. The extruded parts of the column and tenons are depicted in Figure 3.8, Figure 3.9, and Figure 3.10 respectively.

Table 3. 5: Coordinates and depth of the timber parts.

Parts	Starting Corner	Opposite Corner	Depth
Column	(0,0)	(40,40)	500
Beam	(0,0)	(40,75)	750
Tenon 15x15	(0,0)	(15,15)	15
Tenon 15x30	(0,0)	(15,30)	15
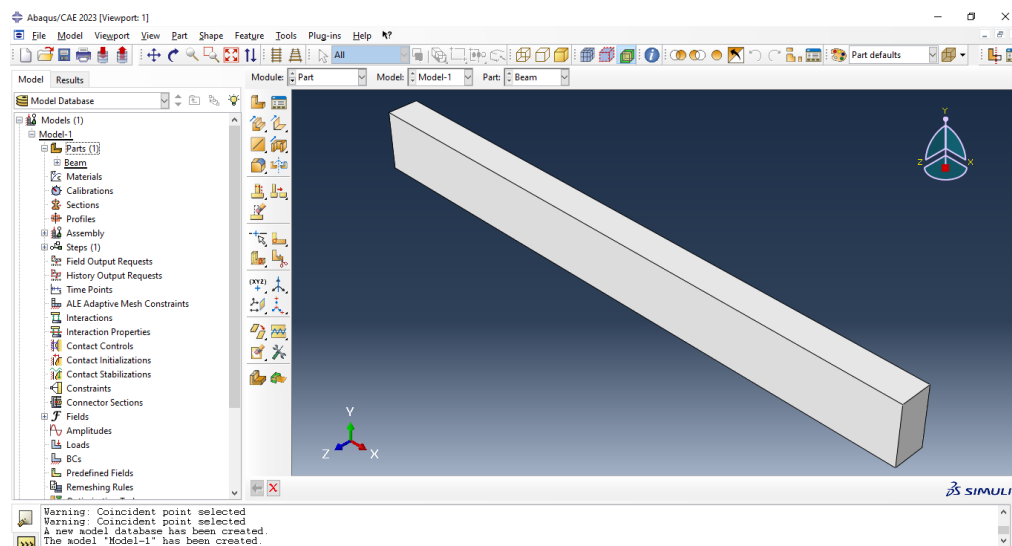
Figure 3. 7: Extruded glulam beam model.
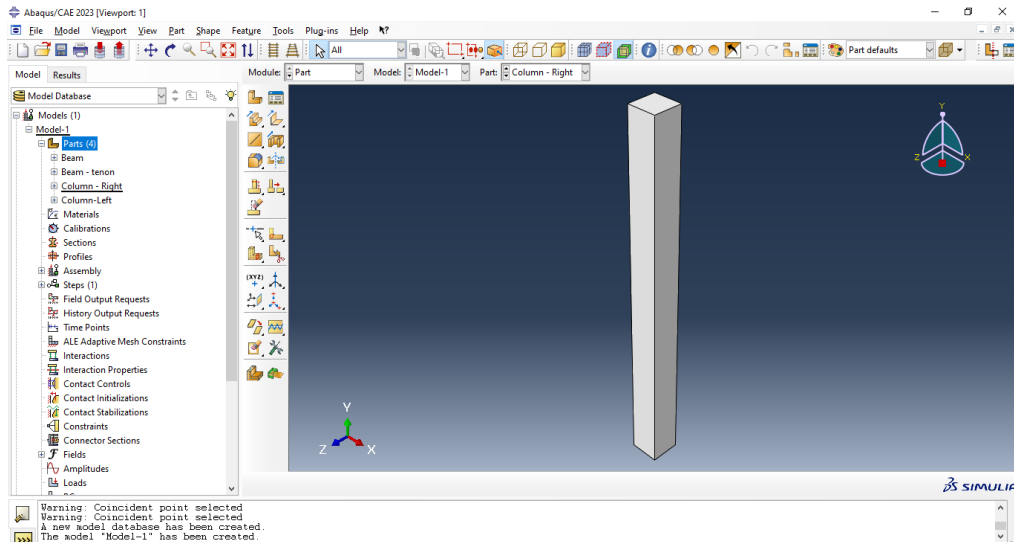
Figure 3. 8: Extruded glulam column model.
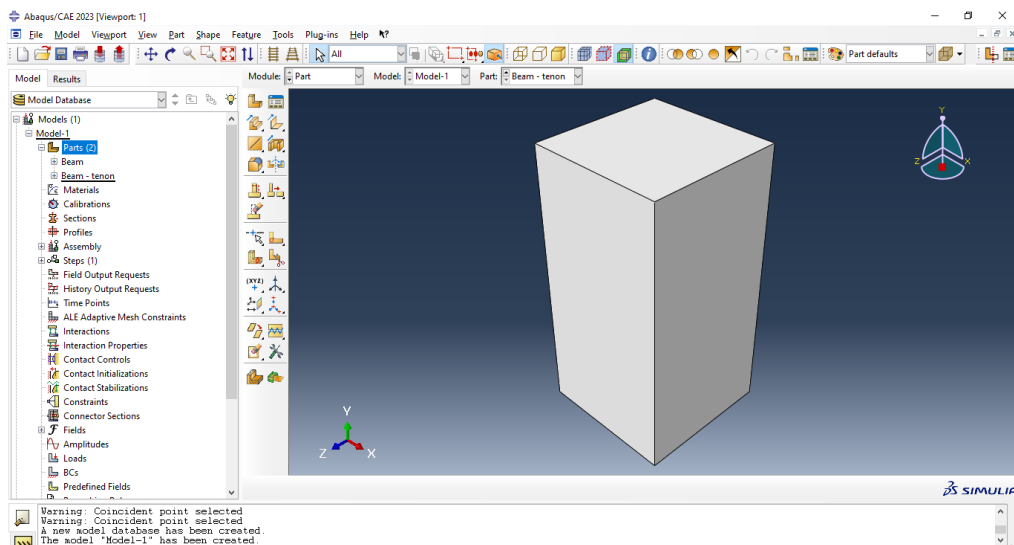
Figure 3. 9: Extruded glulam tenon of 15x30.
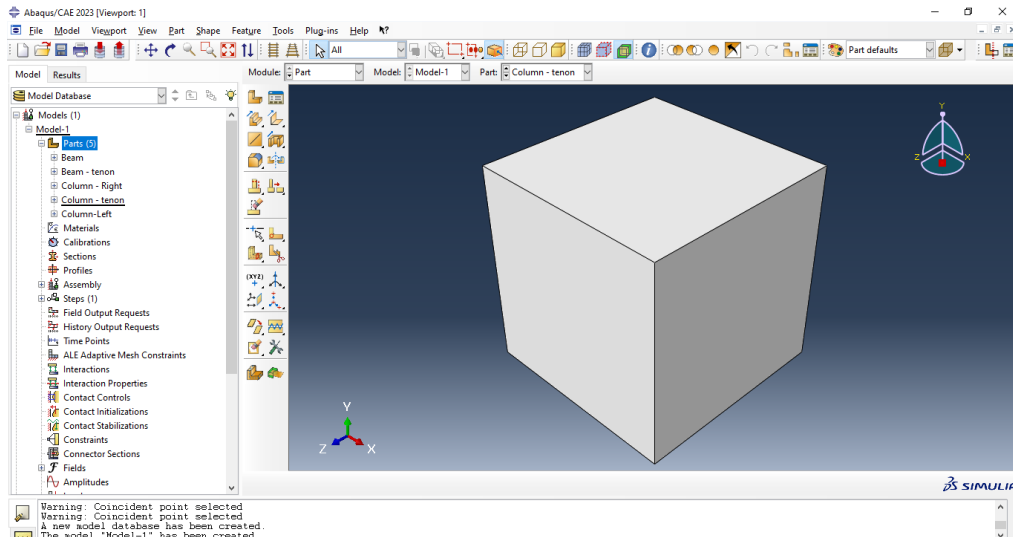
Figure 3. 10: Extruded glulam tenon of 15x15.

As the structure is purely glulam, no reinforcement or additional fasteners are required. The next step involves creating the materials. Click on **Materials** in the model tree; the part module will automatically switch to the property module, and the **Edit Material** dialog box will appear. Name the material as **Glulam** and input the values as stated in Table 3.4, as depicted in Figure 3.11.
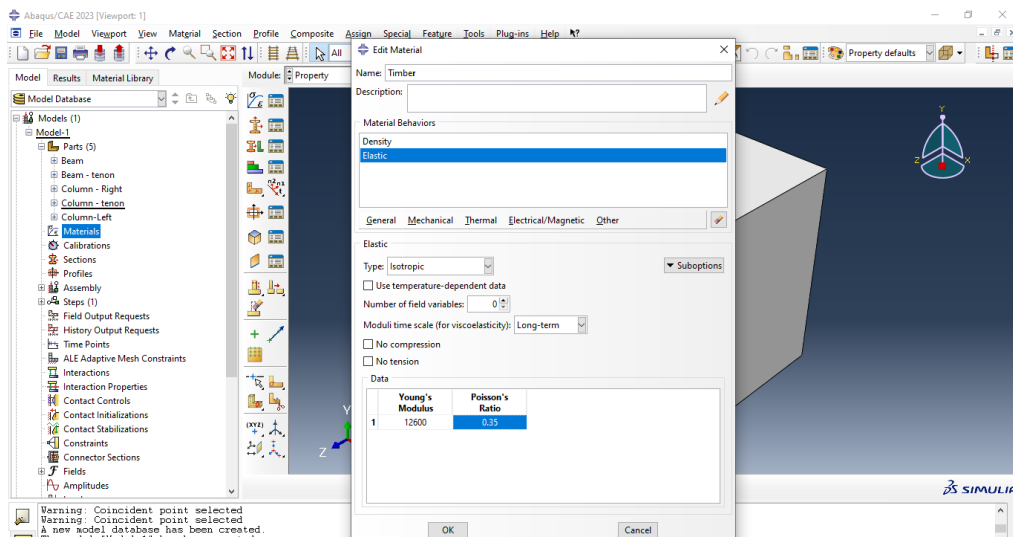
Figure 3. 11: Dialog box of Edit Material.

Next, proceed to define and assign the section properties. Click on **Sections** in the Model Tree, and the **Create Section** dialog box will appear, as

shown in Figure 3.12. Name the section as **Glulam CS** (Glulam Cross Section), select **Solid** as the category, and choose **Homogeneous** as the type. Then, click **Continue**. Figure 3.13 displays the Edit Section dialog box after clicking continue. Here, choose **Glulam** material for the timber section and click **OK**.
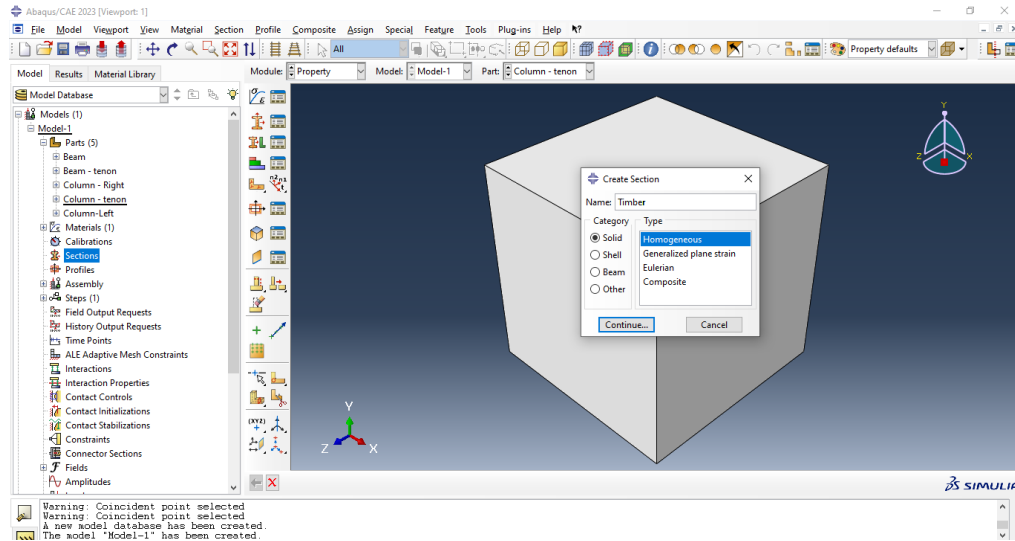
Figure 3. 12: Dialog box of Create Section for glulam.
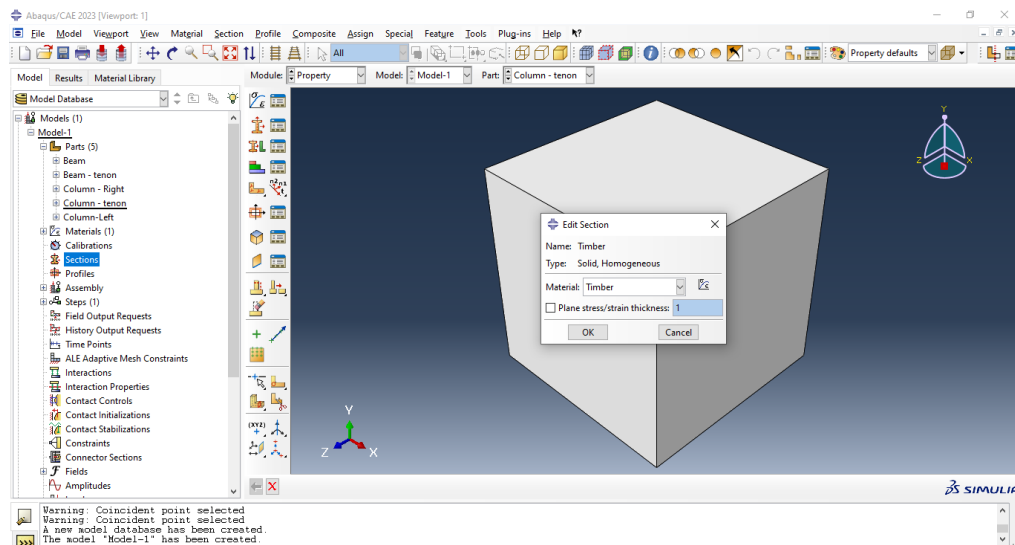
Figure 3. 13: Dialog box of Edit Section for glulam.

The next step involves **Section Assignments**. Expand the branch of the parts and continue expanding the beam. The Section Assignments option will appear in the list. Click on it and select the entire portion of the beam, as demonstrated in Figure 3.14. follow the prompts displayed in the prompt area

for guidance throughout the procedure. Click **DONE** after selecting the geometry. In the **Edit Section Assignment** dialog box, choose **Glulam CS**. After clicking **OK**, the colour of the model will change to green, indicating that the part has a section assignment, as depicted in Figure 3.15.
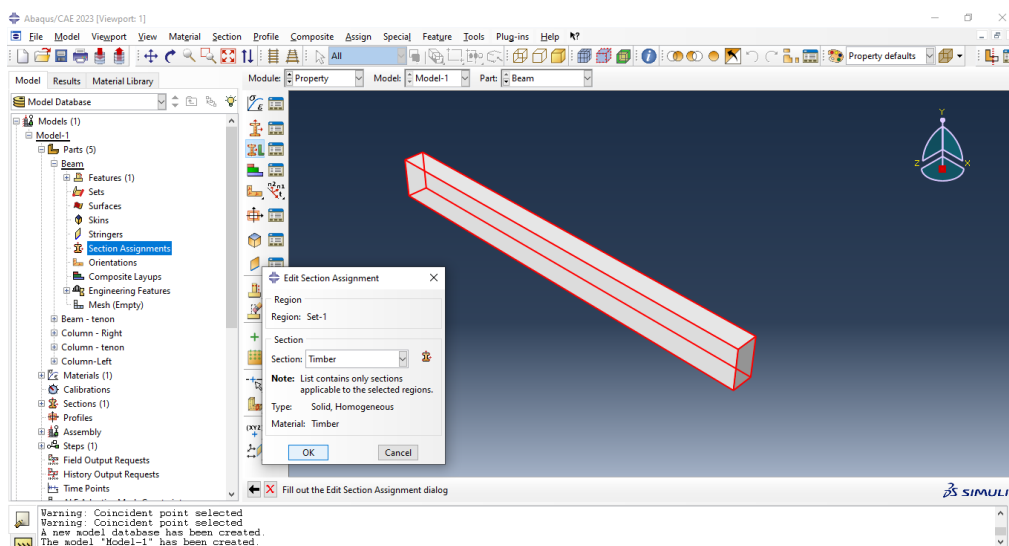
Figure 3. 14: Section assignment of the beam.
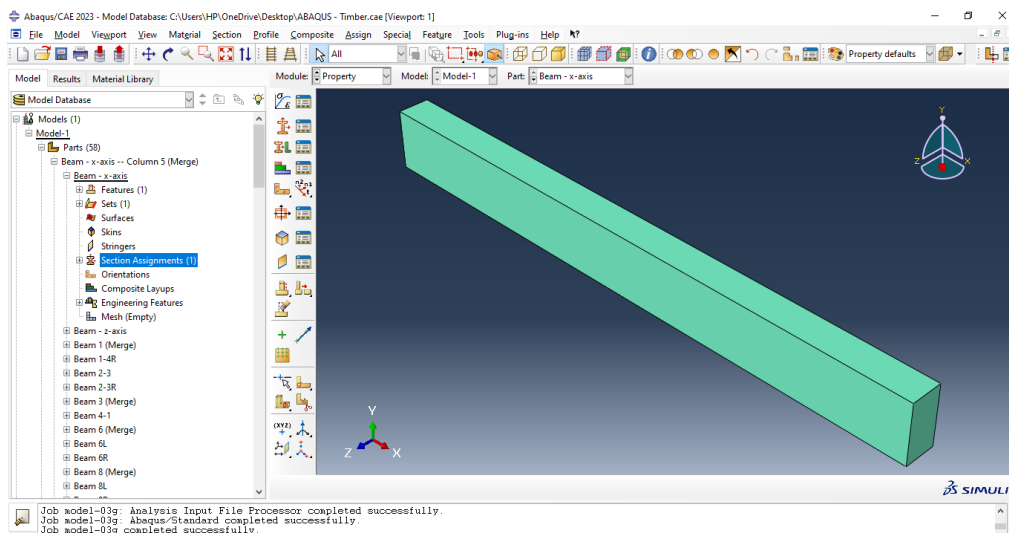
Figure 3. 15: Section assignment to the beam is completed.

Each previously created part not only possesses a distinct orientation based on its own coordinate system but also functions independently within the model. A model comprising only one assembly can be defined by generating instances of a part and establishing relationships among these instances within

a global coordinate system. There are two types of instances: Independent and dependent part instances. The distinction lies in how independent part instances are meshed separately, while the mesh of dependent part instances is connected to the mesh of the original part.

To define the assembly, navigate to the Model Tree and expand the **Assembly** section. Click on the **Instances** within the assembly. This action automatically switched to the Assembly module, and a dialog box for creating instances appears. Figure 3.16 illustrates the dialog box for creating instances. Select both components (Beam and Tenon) / (Column and Tenon), then click **OK**.
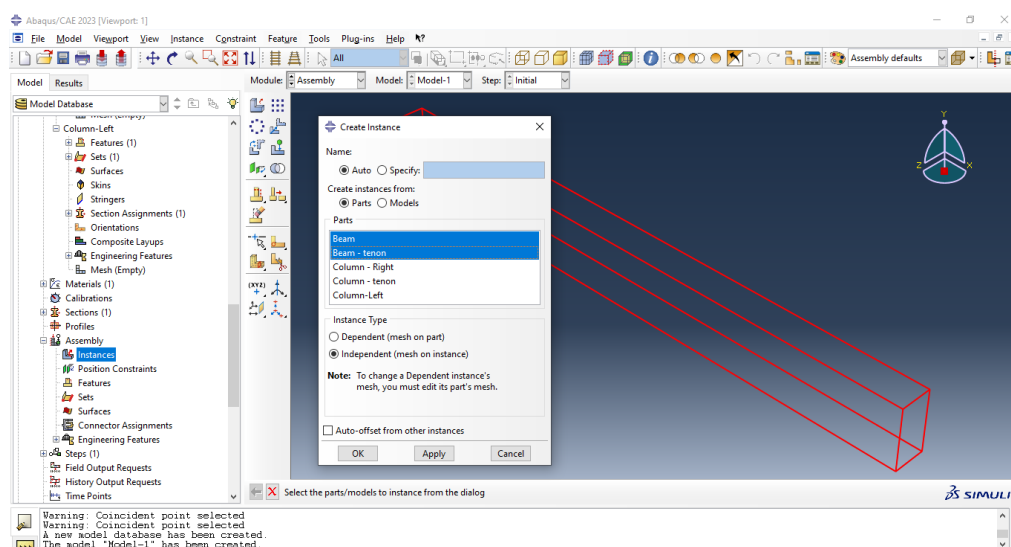
Figure 3. 16: Interface of creating a instance for beam.

After supressing the timber beam, column, and tenon, as there are mortises involved, proceed to click on **Merge/Cut Instance**. Name the part appropriately, for example, 'Column 1'. Click on **Cut Geometry,** as demonstrated in Figure 3.17. Next, select the instance to be cut, followed by selecting the instance that will perform the cut. Click **OK**, and the part will displace the column with mortises. Following the same procedure, click on **Merge /Cut Instance** again, and merge the column and tenon to become one part, as shown in Figure 3.18. The resulting view of the part after merging procedure is depicted in Figure 3.19.
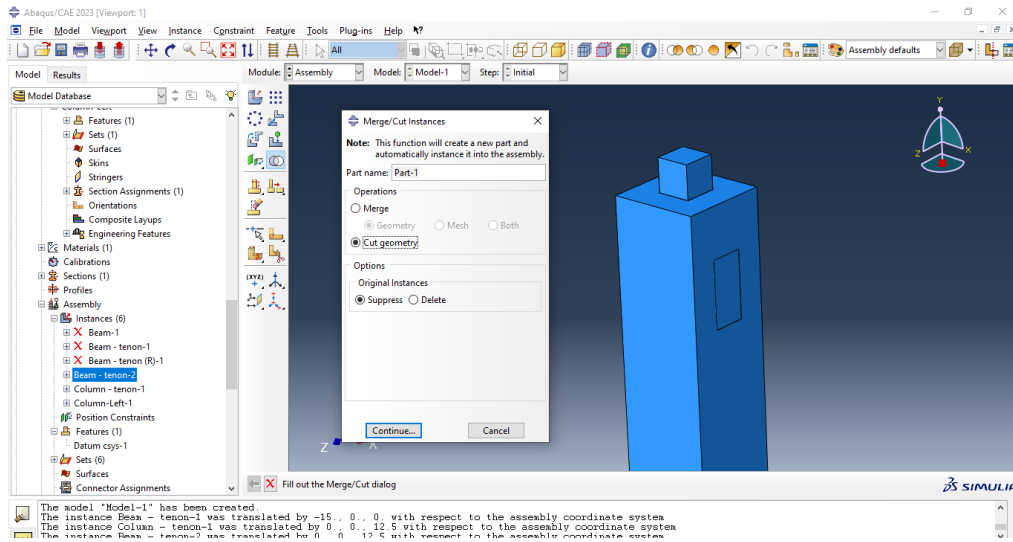
Figure 3. 17: Interface of creating Cut/Merge Instance for parts.
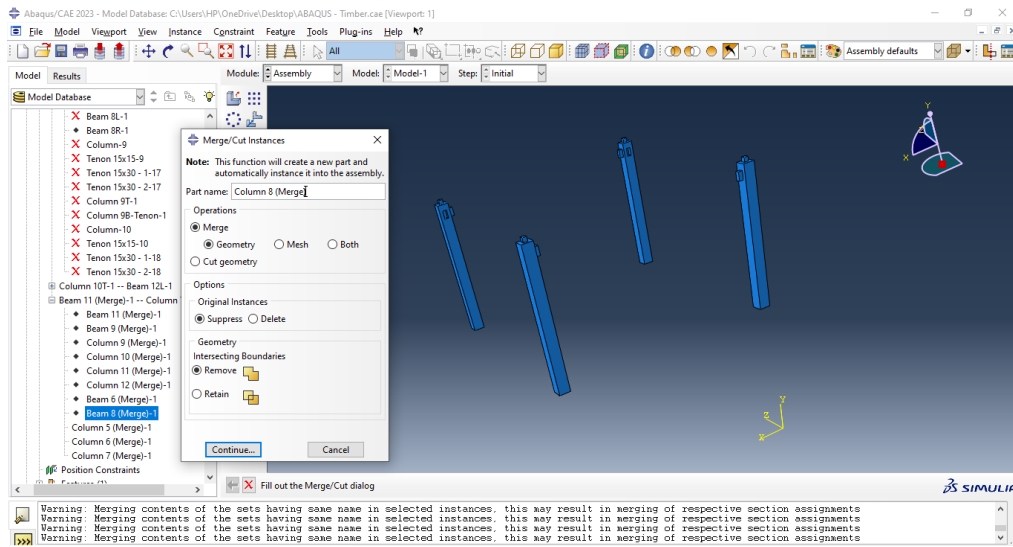
Figure 3. 18: Interface of creating Cut/Merge Instance for parts.
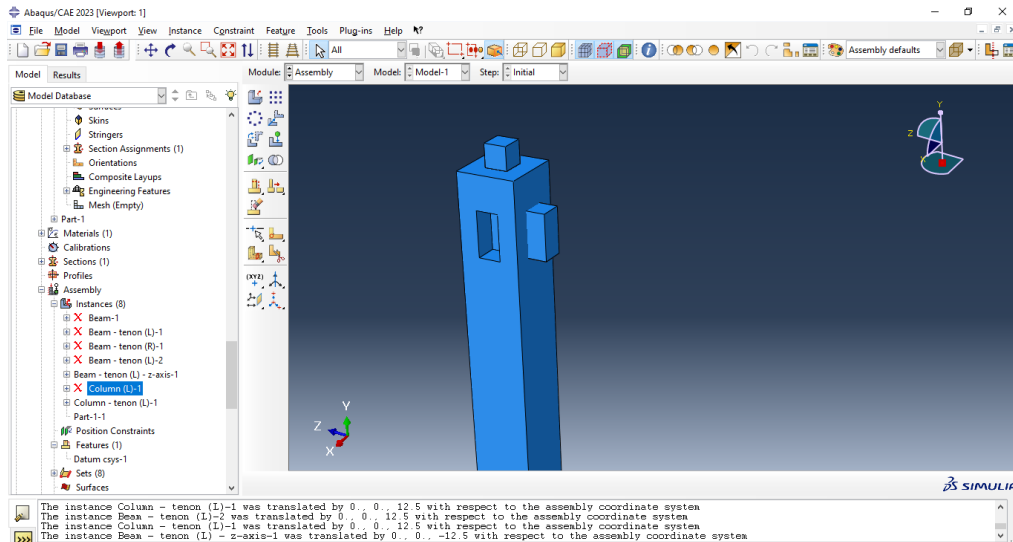
Figure 3. 19: Resulting view of a column after Cut/Merge Instance process.

Subsequently, select **Translate Instance** in the toolbox area to coordinate the parts. Two methods can be used are either inputting the coordinates of each part or using the global method by clicking on the point or node. Figure 3.20 illustrates the building after the Translate Instance process has been completed, aligning all parts appropriately. Finally, a complete building model has been designed.
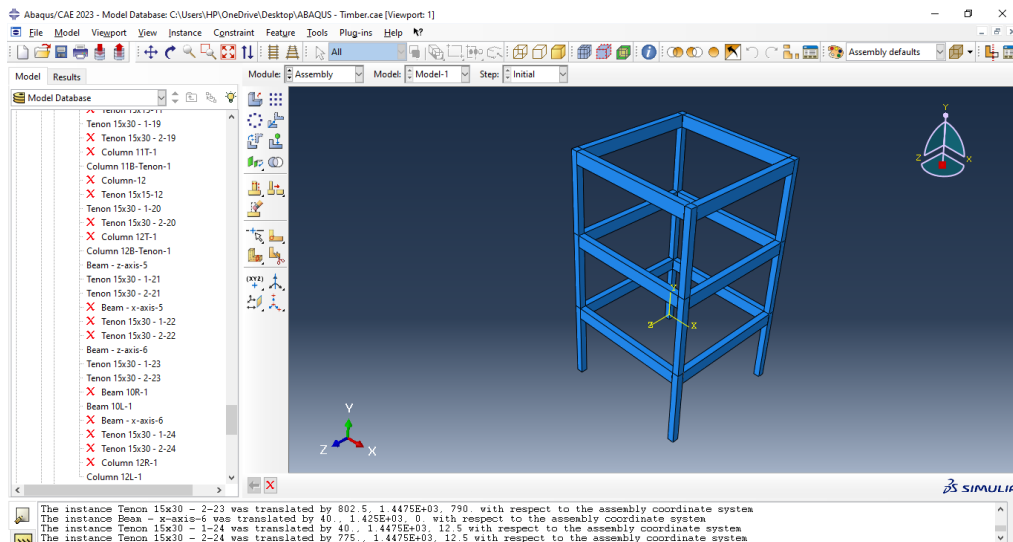
Figure 3. 20: Resulting view of glulam framed building after completing Translate Instance.

3.6   Boundary condition

After completing the creation of the model, the next step is to establish constraints. Begin by clicking **Constraint** in the model tree and locate the **RP** icon. Clicking on this icon enables the setting of a reference point. Nodes will automatically appear to facilitate this process, as illustrated in Figure 3.21. position the reference points accordingly, as demonstrated in Figure 3.22.
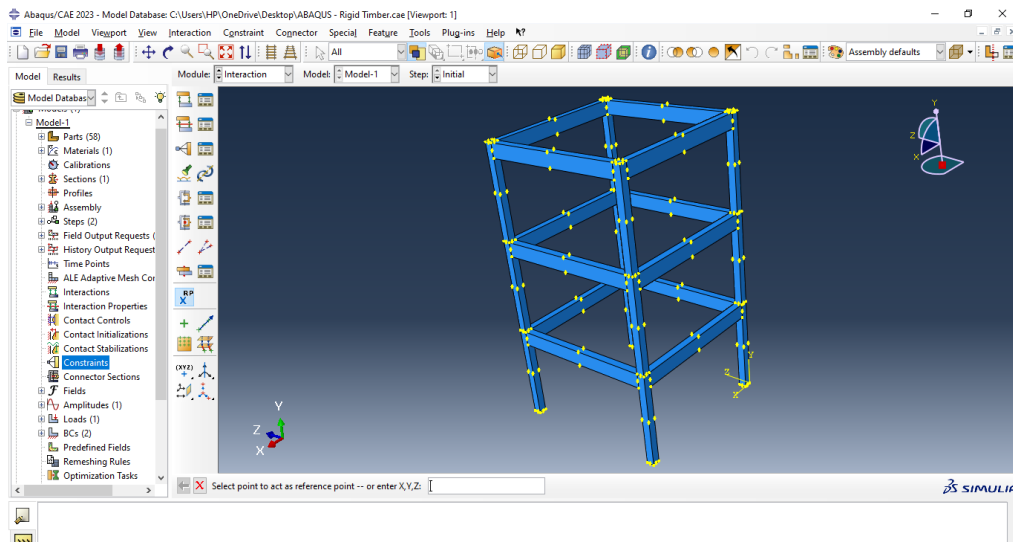
Figure 3. 21: Nodes for selecting reference point.
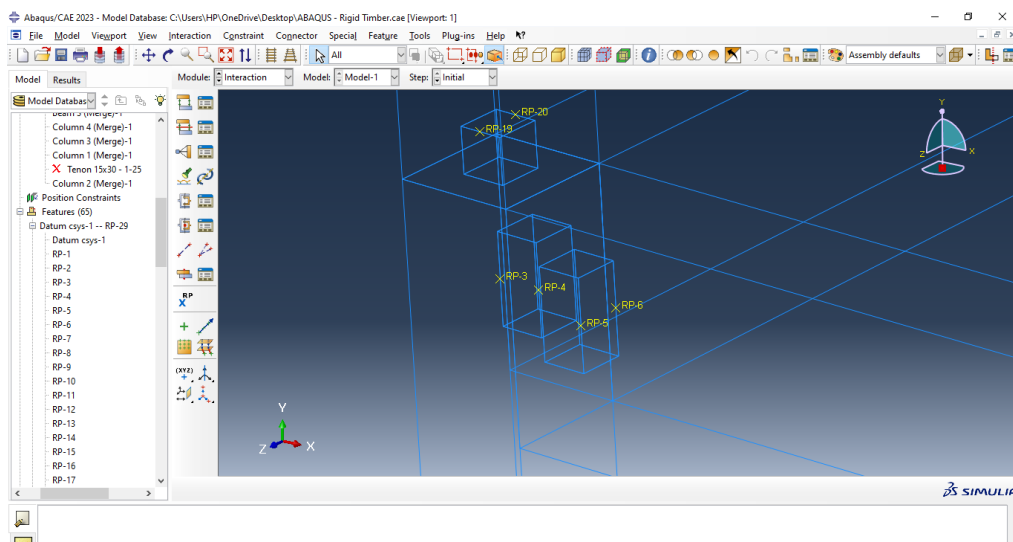
Figure 3. 22: Reference point location.

From this study, a rigid body model is employed. To initiate the creation of constraints, click on **Constraint** in the model tree, prompting the appearance

of the **Create Constraint** dialog box. Provide a suitable name for the constraint and select **Rigid Body** from the type list, as depicted in Figure 3.23. Subsequently, the **Edit Constraint** dialog box will appear. Here, choose the appropriate **Region Type** and select the reference point to establish the connection, as shown in Figure 3.24. Upon completion, the parts subjected to constraints will be displayed as depicted in Figure 3.25. Repeat these steps for the remaining parts of the model and will displayed as depicted in Figure 3.26.
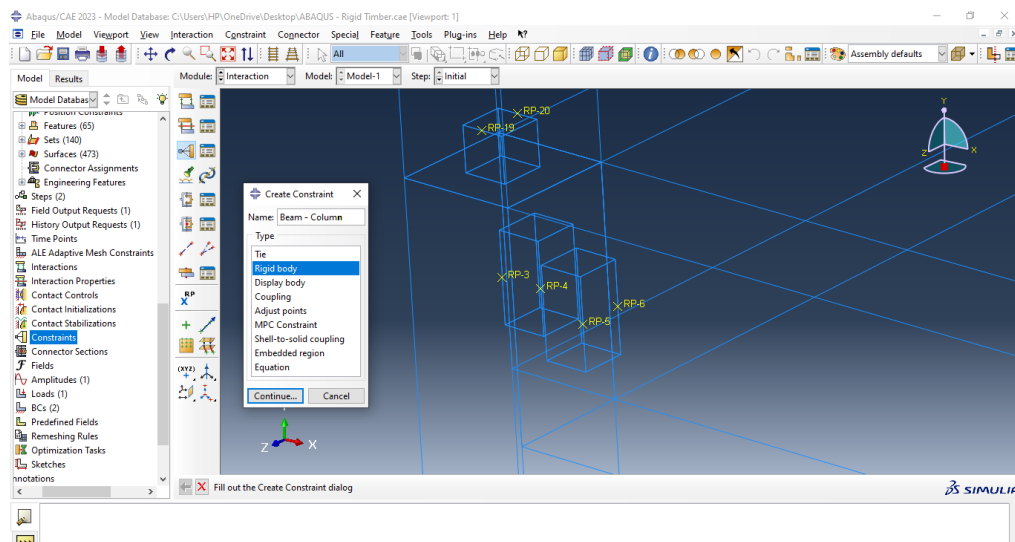
Figure 3. 23: Dialog box of Create Constraint.
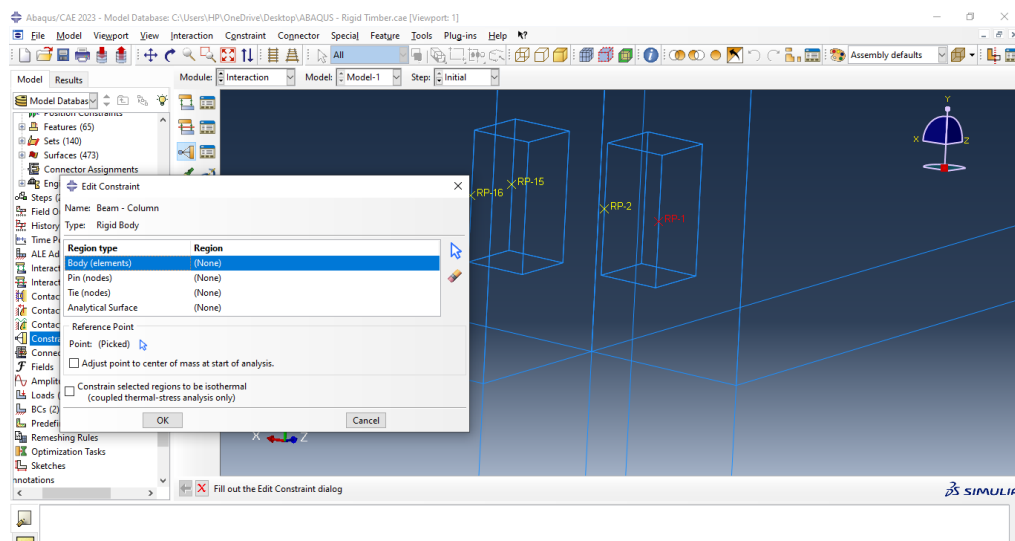
Figure 3. 24: Dialog box of Edit Constraint.
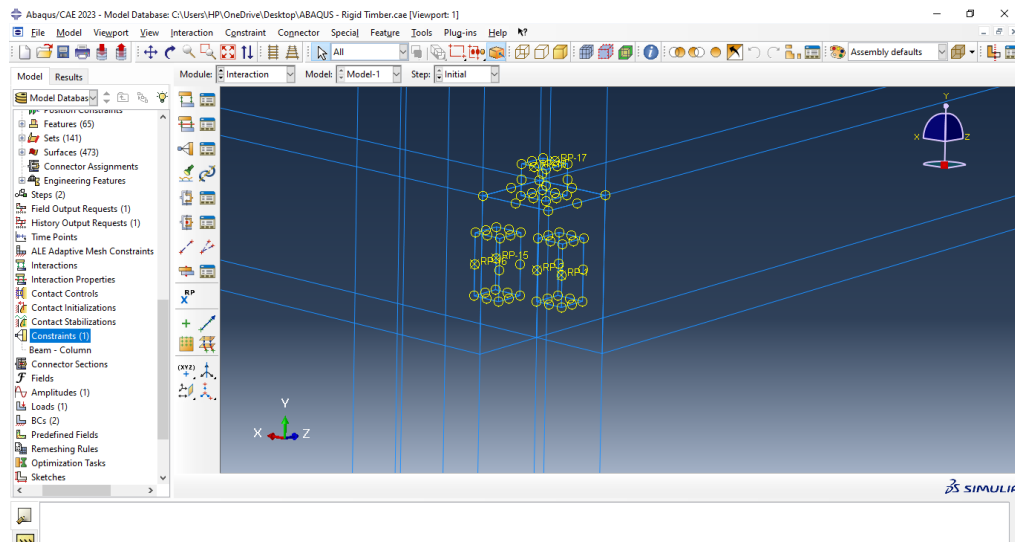
Figure 3. 25: Rigid constraint on the structure.
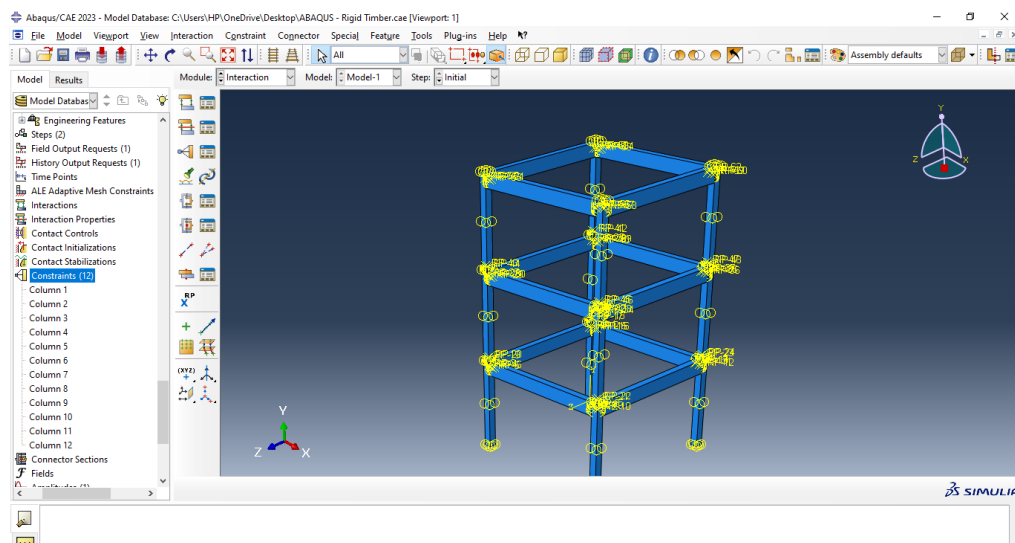
Figure 3. 26: Rigid constraint on the whole structure.

In this analysis, two steps are involved: the initial step and the analysis step. The initial step is automatically generated upon applying boundary conditions, while the analysis step requires the application of loads. Before creating the analysis step, it is necessary to define the earthquake amplitude. To create the earthquake amplitude, navigate to **Amplitude** in the Model Tree. In the Load module, a dialog box for creating the amplitude will appear. Rename the step to **EI Centro Earthquake**. Then, input the relevant data for the earthquake, such as time and amplitude, into the dialog box and click **OK**, as illustrated in Figure 3.27.
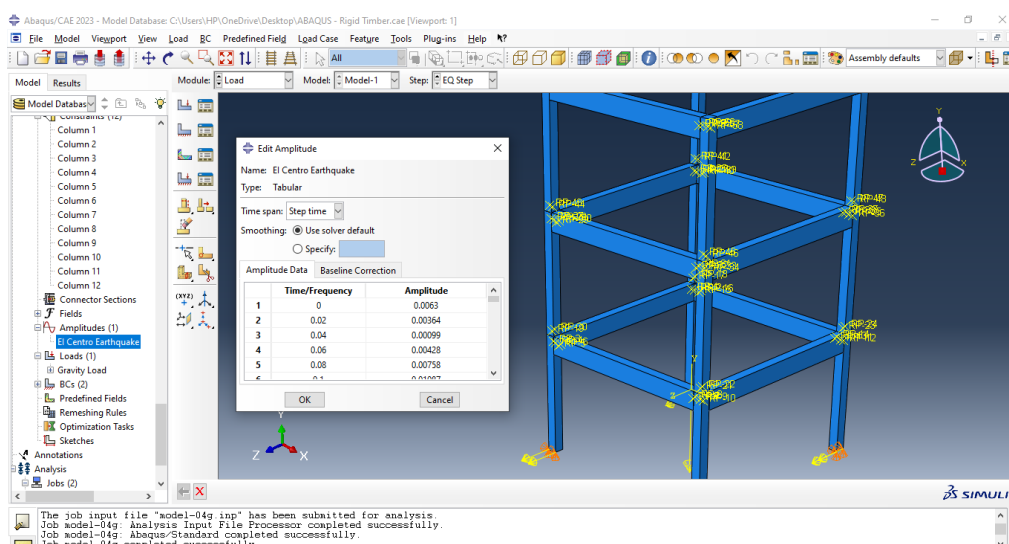
Figure 3. 27: Dialog box of Edit Amplitude.

Navigate to **Steps** in the Model Tree to generate a new step. In the Step module, a dialog box for creating will appear. Rename the step to **EQ Step** and select **Dynamic, Implicit** from the option in the lower section of the dialog box. After clicking **Continue**, as Edit Step dialog box will appear. In the **Edit Step** dialog box, adjust the time period to **3.118** and set the initial incremental size to **0.002**. Additionally, specify the maximum number of increments as **311800**, as illustrated in Figure 3.28 and Figure 3.29 respectively.
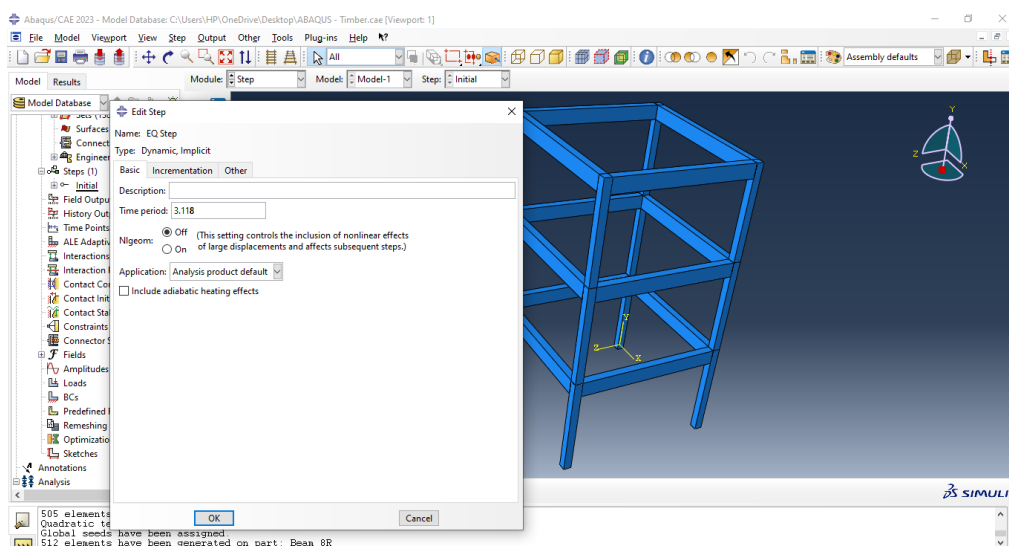
Figure 3. 28: Edit step by changing the time period.
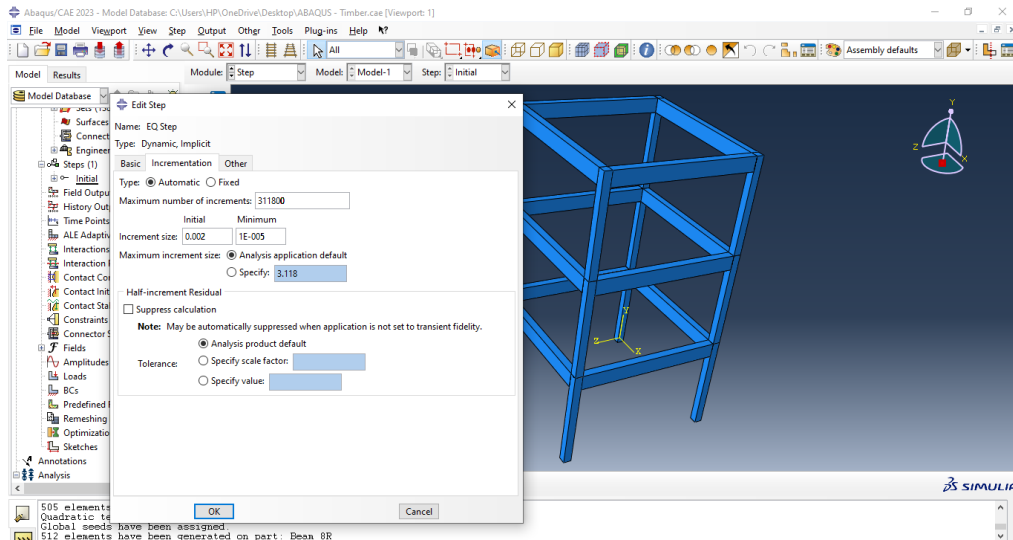
Figure 3. 29: Edit step by changing the value of incrementation.

To establish boundary conditions, navigate to **BCs** in the Model Tree, which triggers the appearance of the **Create Boundary Condition** dialog box, as depicted in Figure 3.30. Begin by naming the first boundary condition, such as **Fixed Support** and select **EQ Step**. Choose **Displacement/Rotation** from the **Types for Selected Step** list. Upon clicking **Continue**, designate the bottom surface of the column as the section where the boundary condition will be applied, as demonstrated in Figure 3.31.
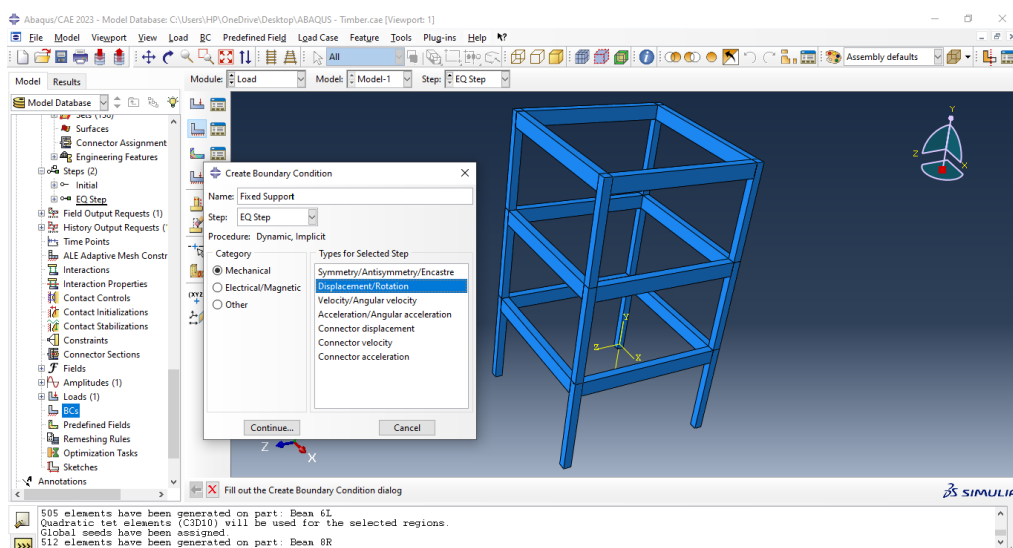
Figure 3. 30: Create Fixed Support boundary condition.
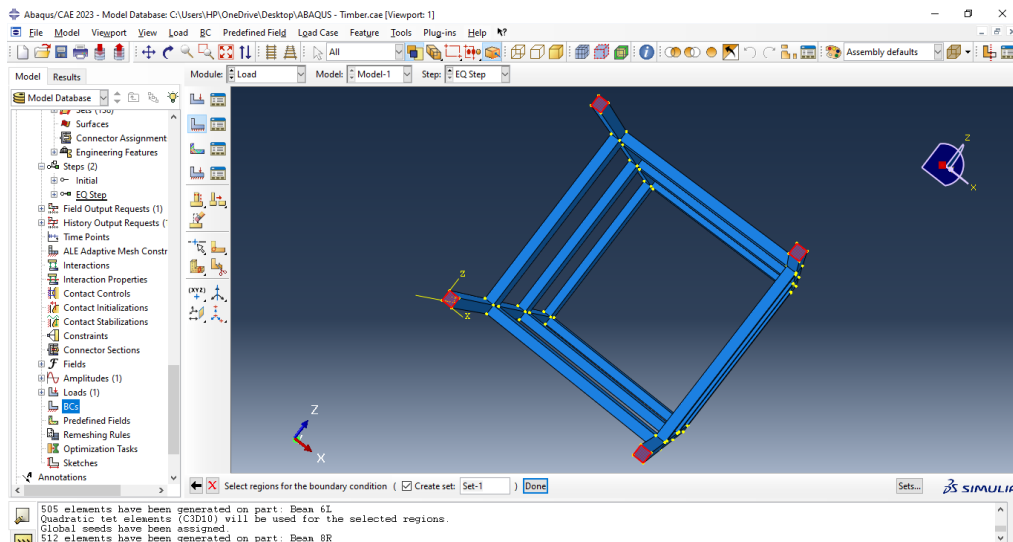
Figure 3. 31: Select the bottom surface of the column.

Subsequently, the Edit Boundary Condition dialog box will appear, as illustrated in Figure 3.32. Here, select U1 and U2 to define the displacement constraints, and click OK to finalise the boundary condition. The presence of arrowheads at the bottom of the column, as depicted in Figure 3.33, indicates the imposition of fixed support boundary conditions.
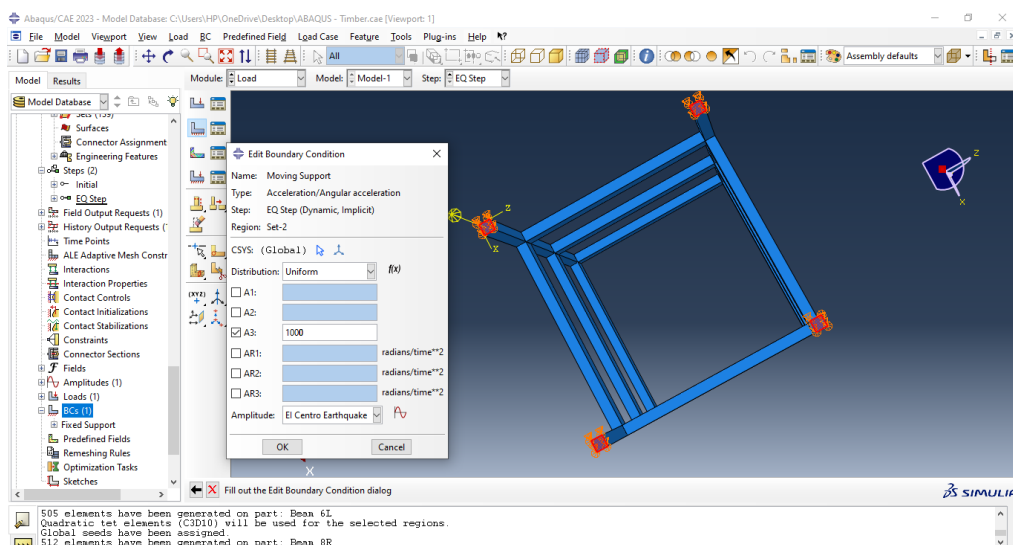
Figure 3. 32: Dialog box of Edit Boundary Condition.
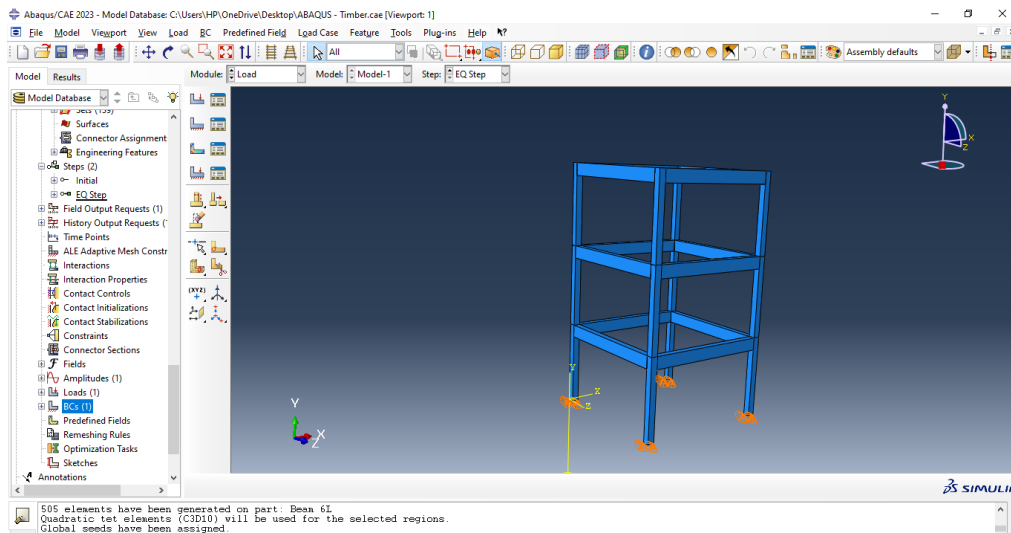
Figure 3. 33: Arrowheads at the bottom of the column.

3.7 Applied loads

Applying loads to the model is a crucial step in the analysis process. In this simulation, a gravity load is applied under the **EQ Step** created earlier. Navigate to the **Loads** section in the Model Tree, where a dialog box for creating a load will appear, as shown in Figure 3.34. Name the load **Gravity Load** and select **Gravity** as the type for the selected step. After clicking **Continue**, an **Edit Load** dialog box will appear, as shown in Figure 3.35. Enter a magnitude of **-9.807** for Component 2, representing the load in the y-direction.
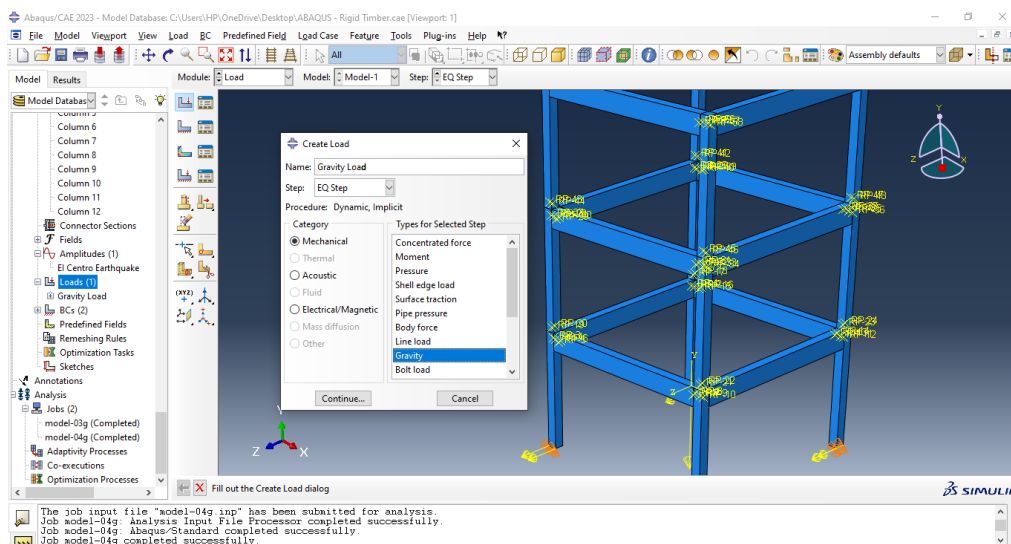
Figure 3. 34: Dialog box for creating gravity load.
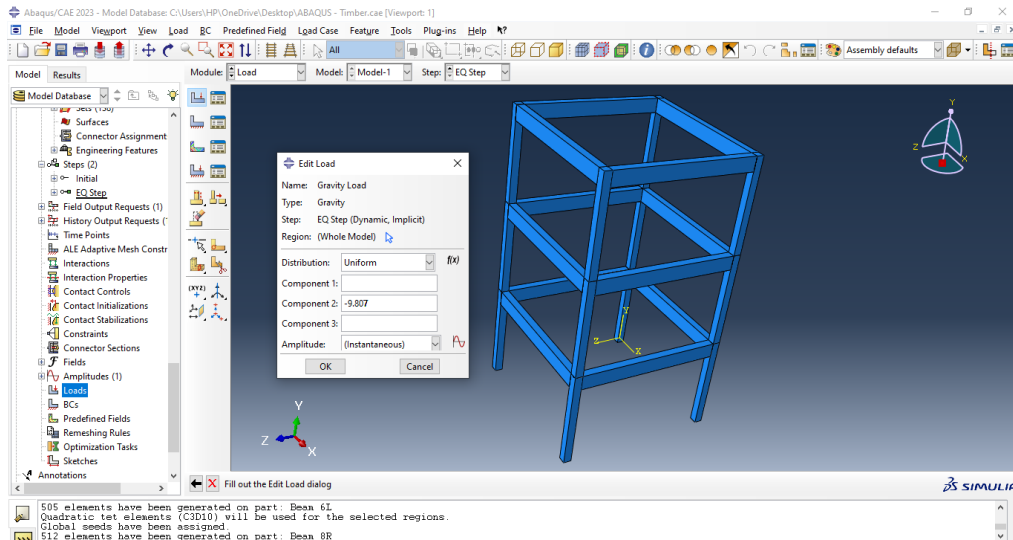
Figure 3. 35: Dialog box of Edit Load.

3.8 Creating job & setting

The meshing process is typically conducted after the model is completed. However, in this simulation, the mesh is created after the merge and cut process due to the specific characteristics of the model. Consequently, each part needs to be meshed individually. Begin by switching to the **Mesh** module and selecting **Seed-Instance** from the menu bar. After selecting the part as the region to be assigned **Global Seeds**, click Done in the prompt area. A dialog box for global seeds will appear, as shown in Figure 3.36. Insert a value of **40** as the approximate global size.
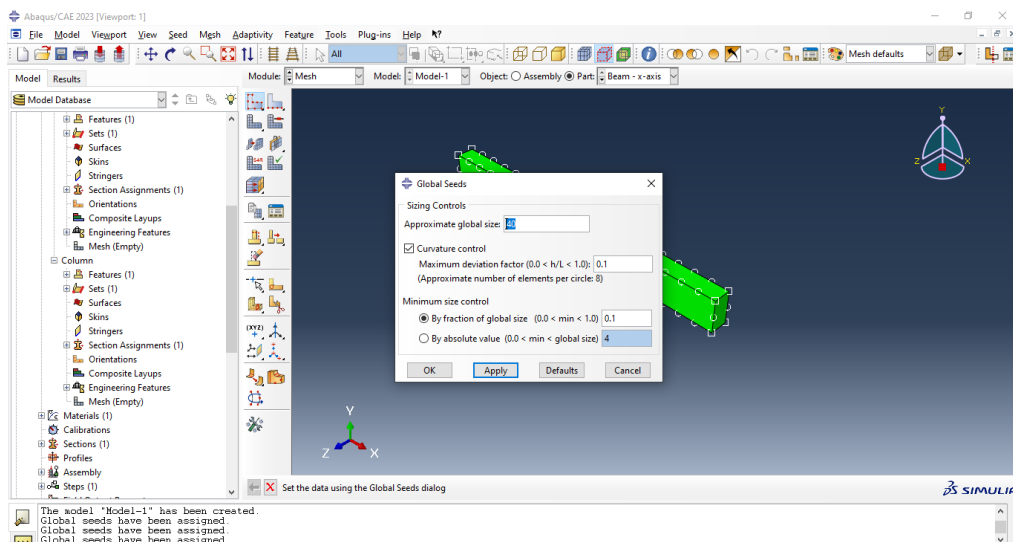
Figure 3. 36: Approximate global size of the model.

The next step is to select **Mesh – Element Type** from the menu bar and then choose the sections to be assigned element types. In the Element Type dialog box, assign the element types as depicted in Figure 3.37.
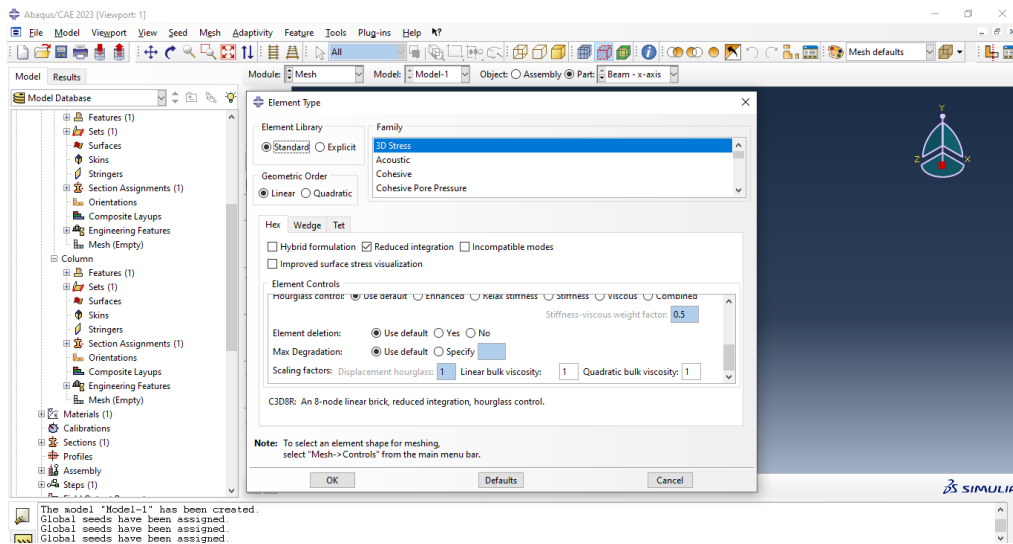
Figure 3. 37: Assign element type to the model.

Next, proceed to **Mesh – Control** and select the sections where mesh controls need to be applied. Click **Done** in the prompt area, and in the Mesh Controls dialog, select Hex as the element shape, as illustrated in Figure 3.38.
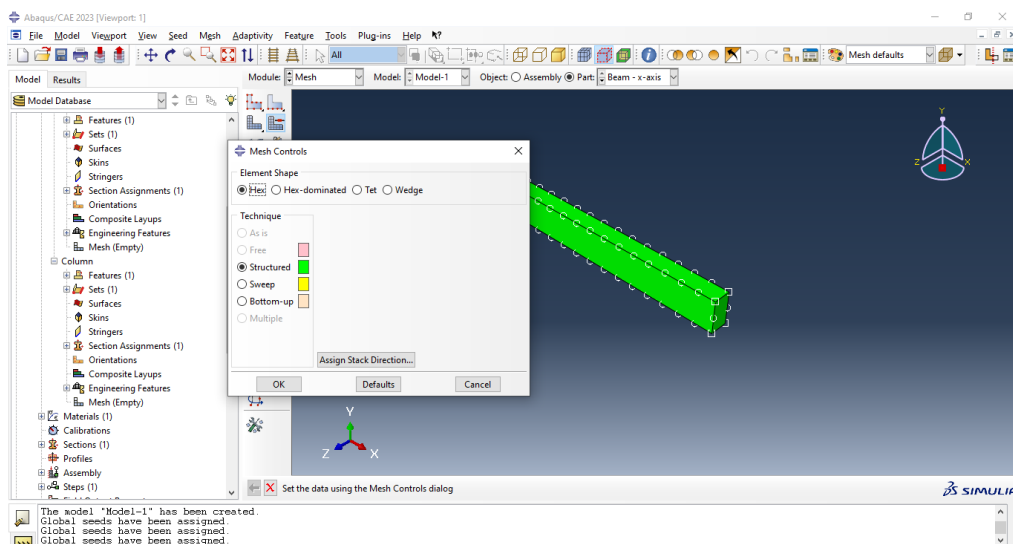
Figure 3. 38: Element shape for the model.

Lastly, navigate to **Mesh – Instance** in the menu bar and select the regions that need to be meshed. The resulting meshed part and model are depicted in Figure 3.39 and Figure 3.40 respectively.
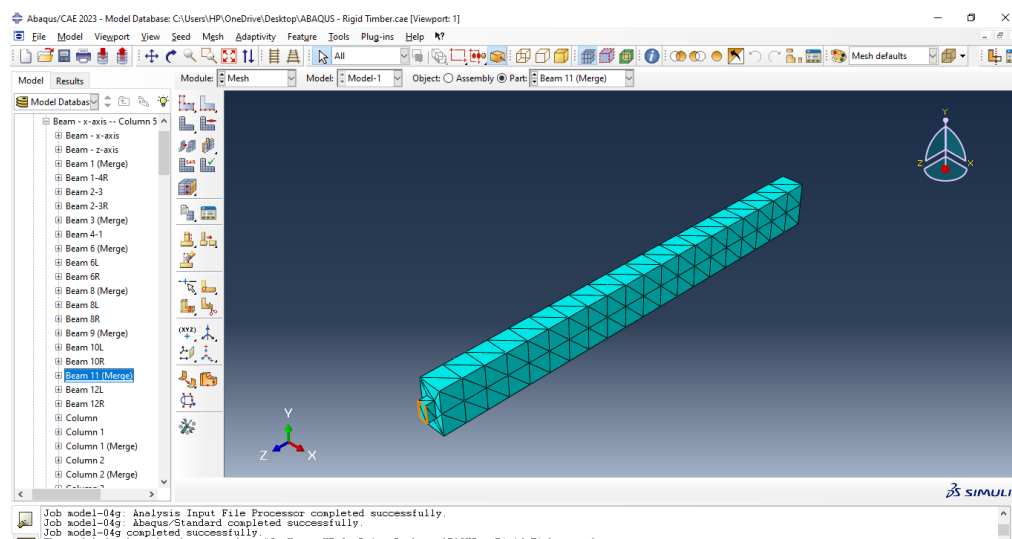
Figure 3. 39: Meshed part.
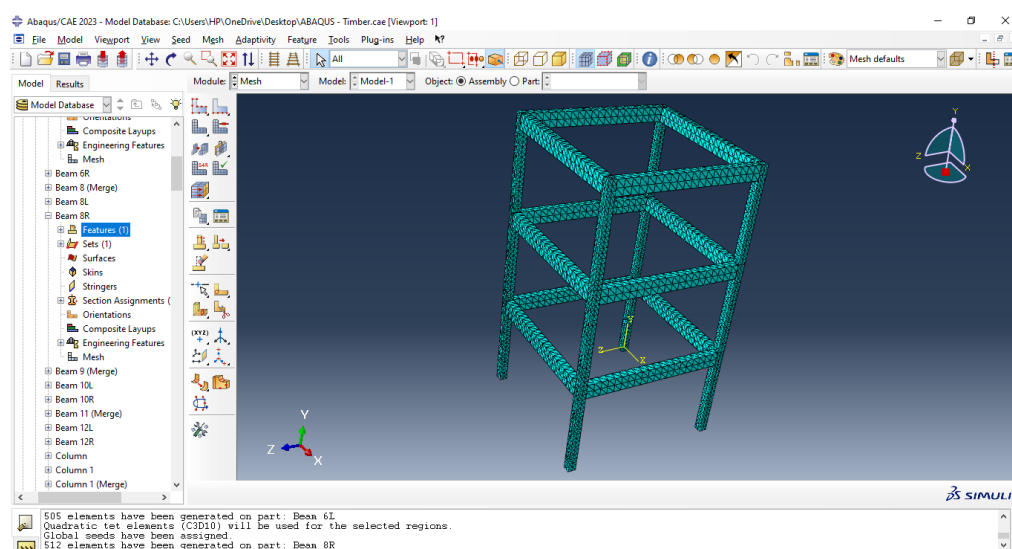
Figure 3. 40: Meshed model.

The final step is to analyse the **Job**. In the Job module, click on **Job** in the Model Tree and name the job as **model-03g** in the **Create Job** dialog box, as shown in Figure 3.41. Next right-click on the **Job** in the Model Tree and click **Submit**. Abaqus will then simulate the model based on the loadings and

boundary conditions provided. The job status will be displayed beside the job name after submitting the job. Different statuses include:

- Submitted: The job is being submitted for analysis.
- Running: The model is being analysed.
- Completed: The analysis is completed.
- Absorbed: There is an error during analysis.

During the analysis, the progress can be monitored by right-clicking on the **Job** in the Model Tree and clicking **Monitor**. The **Job Monitor** dialog box includes information such as job status, log, error, and message files, as shown in Figure 3.42.
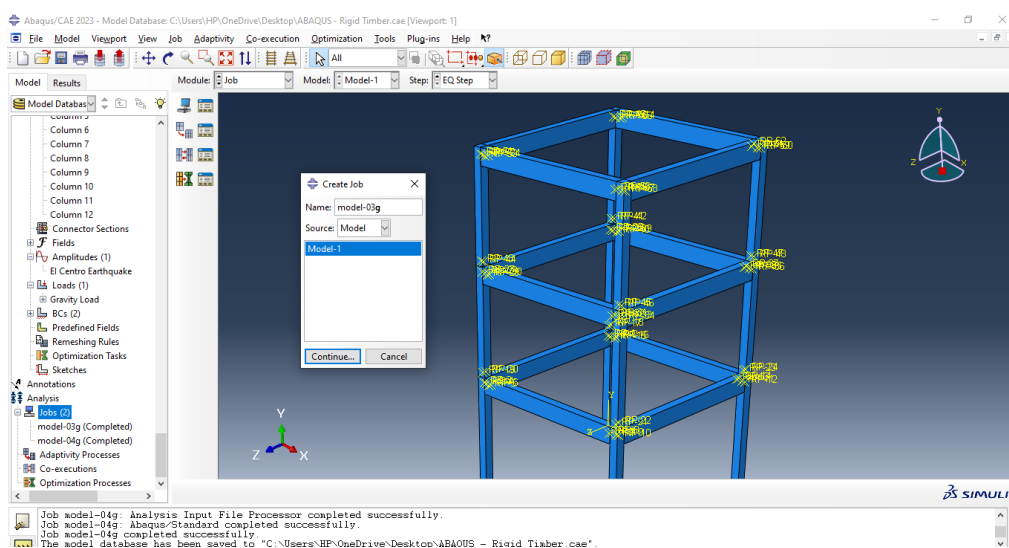
Figure 3. 41: Dialog box of Create Job.
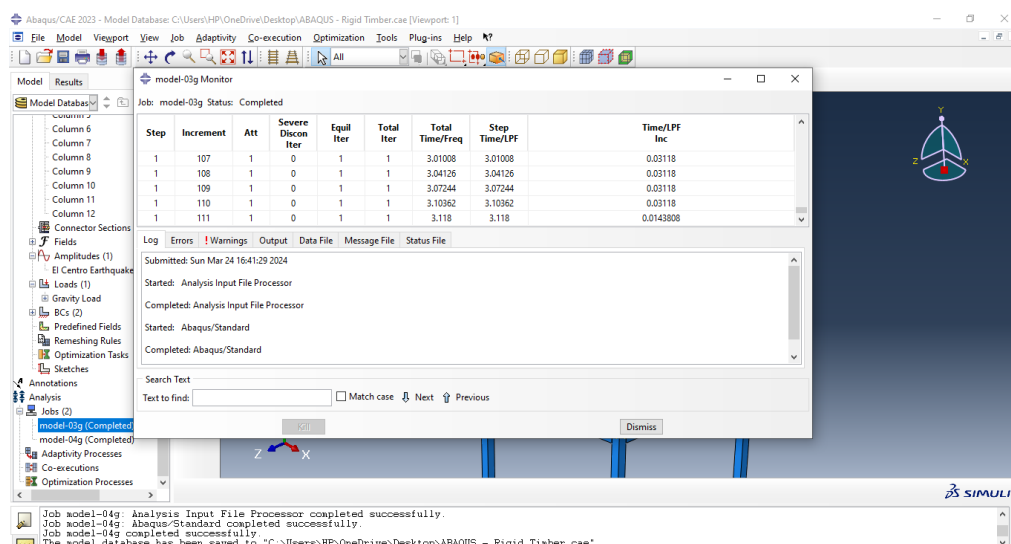
Figure 3. 42: Job details for the simulation of the model.

3.9   Summary of methodology

To summarise, the methodology for modelling concrete, glulam, and steel components within the structural framework, along with the simulation procedure, is elucidated. The process involves detailing the structural properties and dimensions of each material, including their respective mechanical behaviours under various loading conditions. The chapter provides a comprehensive guide to the modelling techniques and simulation procedures utilised to investigate the seismic behaviours of the glulam framed structures with mortise and tenon design.

CHAPTER 4

RESULTS AND DISCUSSIONS

4.1 Introduction

In this chapter, the results and discussions are intricated to the objectives of this study, which aim to delve into the seismic behaviour of glulam framed structures featuring mortise and tenon design, pinpoint stress concentration areas during seismic events, and conduct a comparative assessment of the seismic performance between timber and reinforced concrete (RC) building.

The analysis conducted in this chapter reveals the seismic response of the glulam framed structure with mortise and tenon joinery, providing valuable insights into its behaviour under earthquake loading conditions. By examining parameters such as global deflection, Von Mises stress distribution, and orientations of principal stresses, the study offer a comprehensive understanding of how the glulam framed responds to seismic forces and how the unique mortise and tenon design influences its performance.

Furthermore, the evaluation of stress concentration areas within glulam structures during earthquakes can fulfil the objective of assessing stress distribution and concentration areas. This analysis enables a deeper understanding of the structural vulnerabilities and informs potential design enhancements to mitigate stress concentrations and enhance the overall seismic resistance of glulam framed structures.

Moreover, the comparative assessment conducted in this chapter allows for a robust evaluation of the strengths and weaknesses of glulam structures in comparison to RC buildings concerning their seismic performance. By comparing the seismic responses of glulam and RC buildings under similar loading conditions, the study provides valuable insights into the relative advantages and limitations of each structural system, thereby aiding in structural design and construction practices.

4.2 Global deflection

Based on the displacement results for glulam framed structures subjected to different PGAs, several important observations can be made. The result for glulam structures have depicted in Table 4.1. At lower PGA levels, such as 0.1g to 0.5g, the displacements remain relatively low, ranging from 6.02e-06 mm to 3.01e-05 mm, indicating minimal structural deformation. This suggests that the glulam structures exhibit good resistance to seismic loading at these PGA levels, consistent with their intended seismic performance objectives. However, PGA increases, particularly beyond 0.5g, the displacements in the glulam structures escalate significantly, reaching 4.21e-05 mm at 0.7g, 5.42e-05 mm at 0.9g, and 6.02e-05 mm at 1.0g. These larger displacements signify greater structural deformation and potential vulnerability to seismic forces, highlighting areas where improvements in design and material selection may be necessary to enhance seismic resistance.

In contrast, the concrete buildings display negligible displacement at 0.1g, indicating robust resistance to low-intensity seismic events. However, as the PGA increases, the displacements in concrete structures escalate rapidly, reaching 1.91e+00 mm at 0.1g, 1.59e+00 mm at 0.16g, 1.76e+00 mm at 0.5g, 1.81e+00 mm at 0.7g, and 1.83e+00 mm at 0.9g. This rapid increase in displacement underscores the brittle nature of concrete under high seismic loading, where it exhibits limited ductility compared to glulam. Additionally, the high load bearing capacity of concrete structures is evident, allowing them to withstand seismic forces up to a certain threshold before experiencing substantial deformation.

Furthermore, it is important to consider the implications of these displacement patterns on the overall seismic performance of both structural systems. While glulam framed structures demonstrate resilience and flexibility at the lower PGA levels, they may require additional measures to mitigate displacement and ensure stability under stronger seismic events. Conversely, concrete buildings exhibit robustness and high load bearing capacity but are prone to significant displacement and potential brittleness under extreme seismic forces. This comparative analysis underscores the importance of understanding how different structural systems respond to varying seismic

intensities and informs the evaluation of their seismic performance strengths and weaknesses. Additionally, the results for both structures have been collected at critical time points of 2.2 seconds, where the highest amplitude level during the seismic event occurred. This time point is considered critical for analysis as it represents the peak response of the structures to seismic forces. This is illustrated in Figure 4.1 and 4.2, which provide graphical representations of the displacement responses of the glulam and concrete structures, respectively.

Table 4. 1:Displacement results for timber framed and concrete structure.

PGA	Glulam (mm)	Concrete (mm)
0.1g	6.02E-06	1.91E+00
0.16g	9.63E-06	1.59E+00
0.5g	3.01E-05	1.76E+00
0.7g	4.21E-05	1.81E+00
0.9g	5.42E-05	1.83E+00
1.0g	6.02E-05	3.55E+00
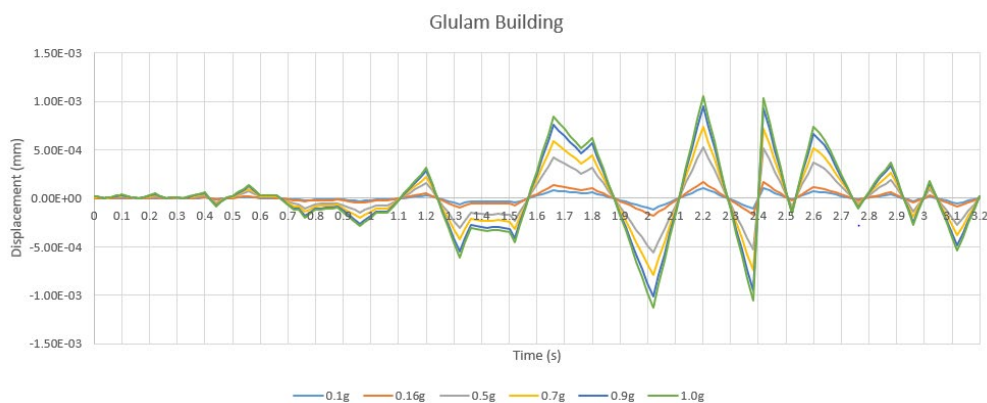
Figure 4. 1: Displacement vs Time for glulam building according to El Centro.
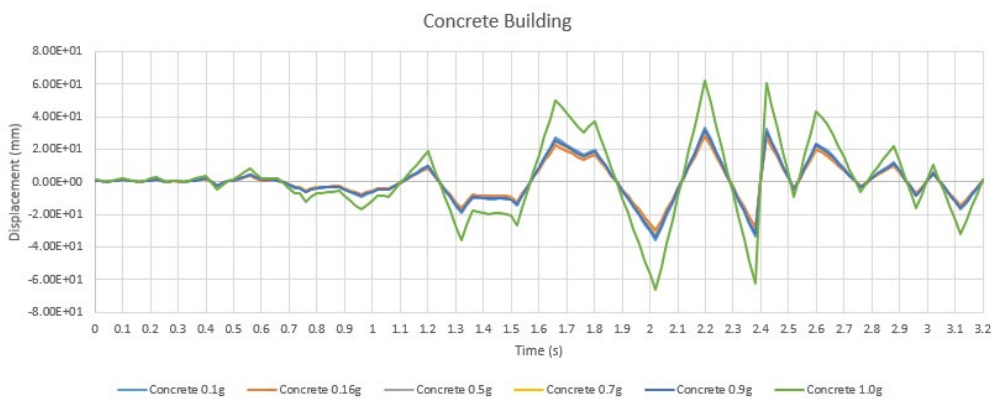
Figure 4. 2: Displacement vs Time for concrete building according to El Centro.
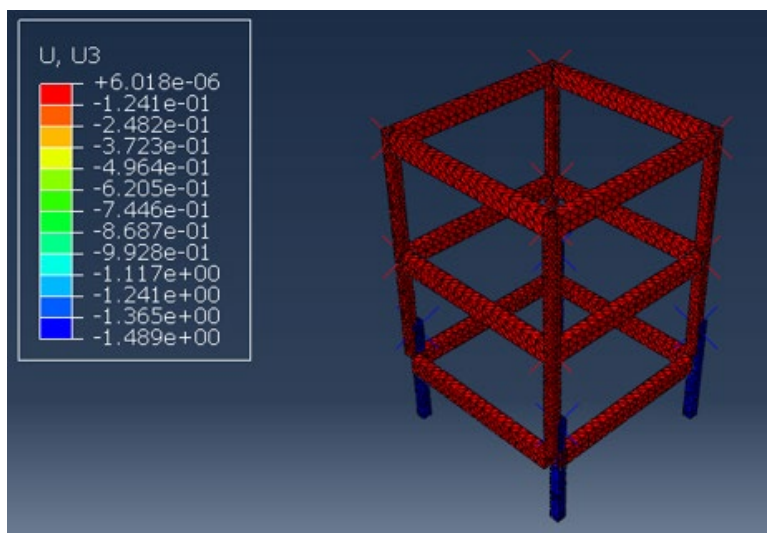
(a)
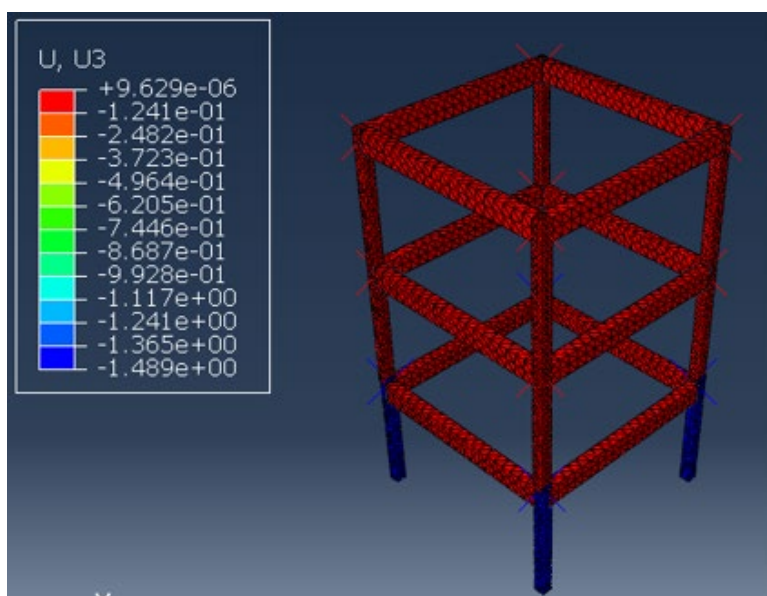
(b)
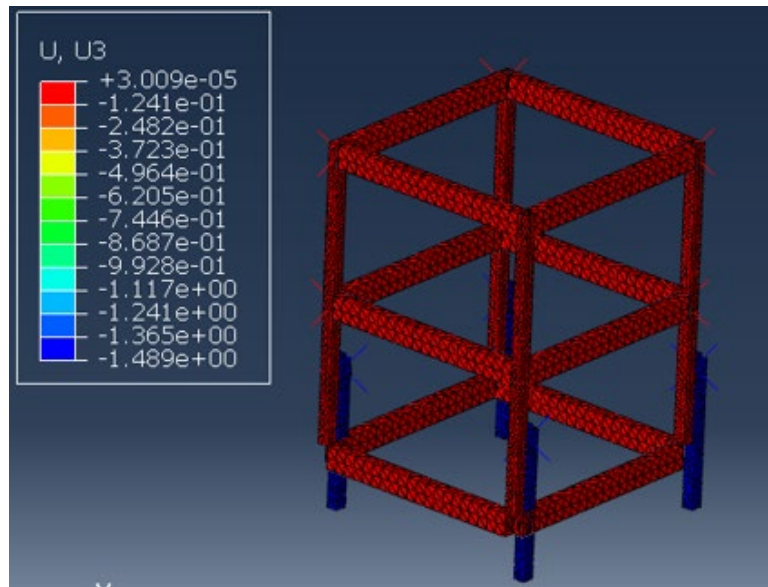
(c)
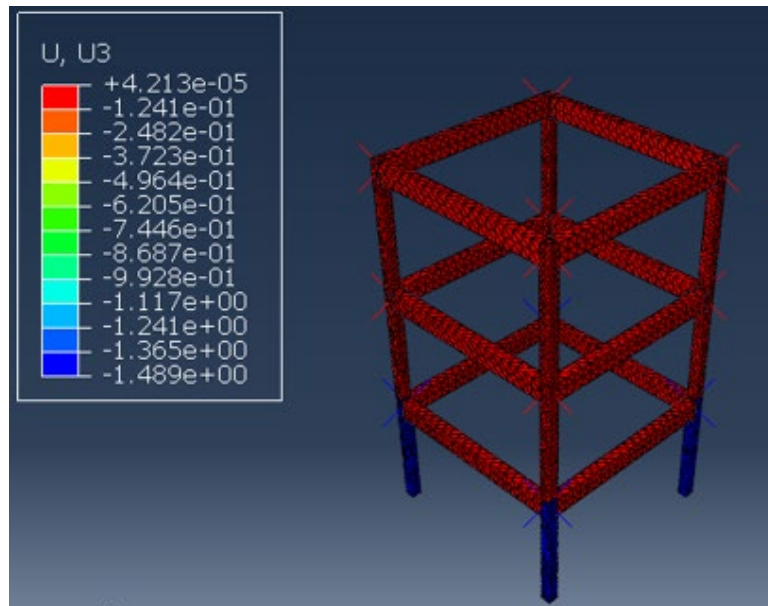
(d)
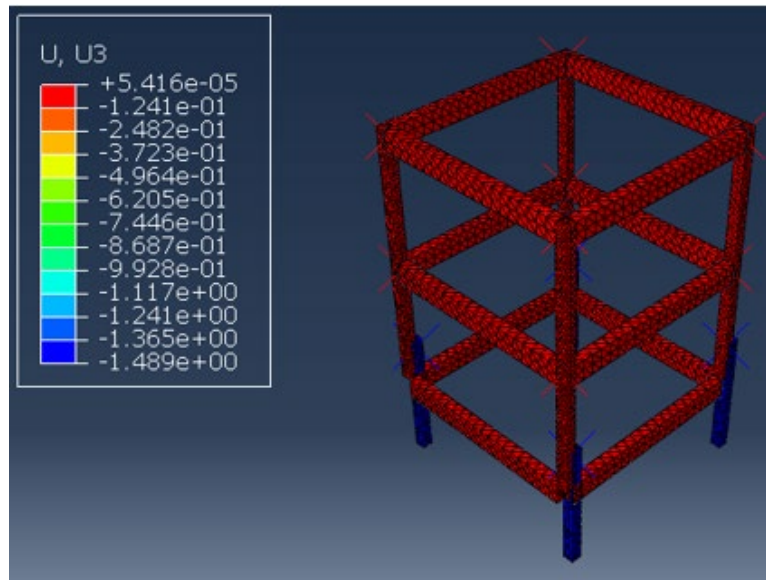
(e)
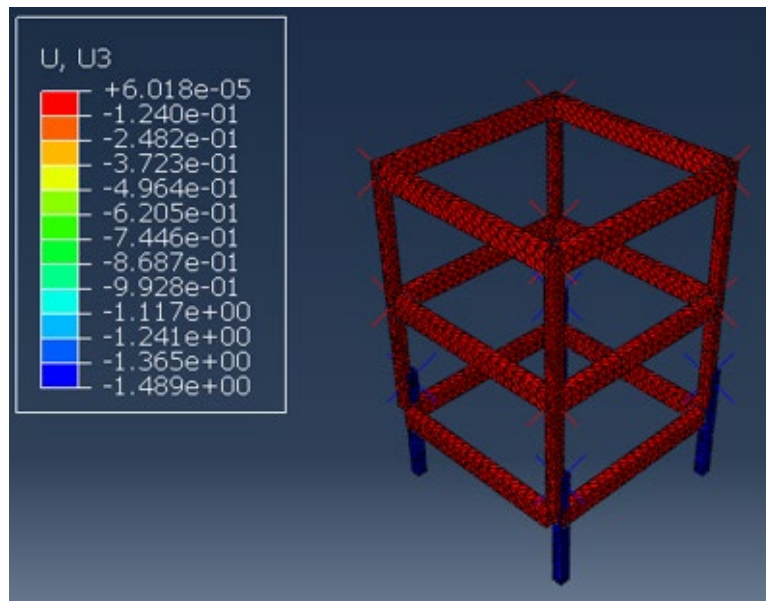
(f)
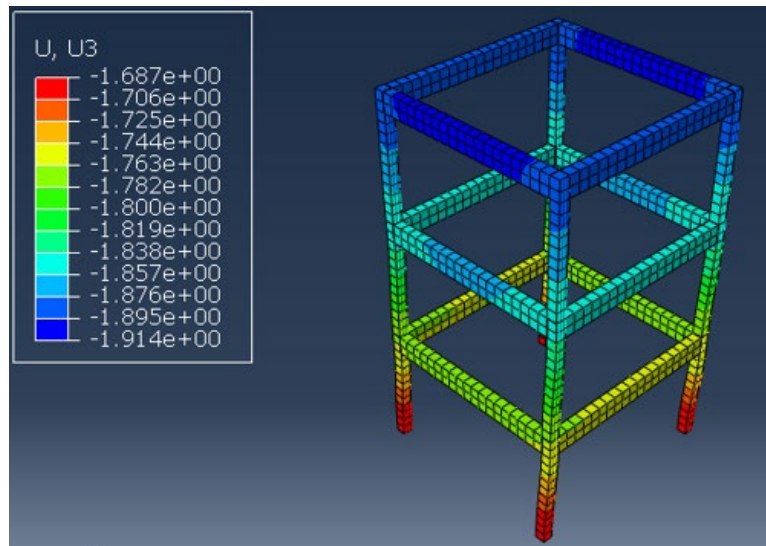
(g)
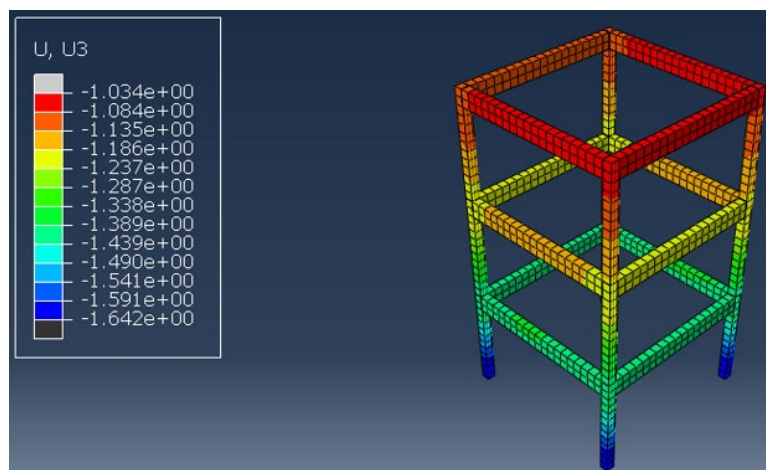
(h)
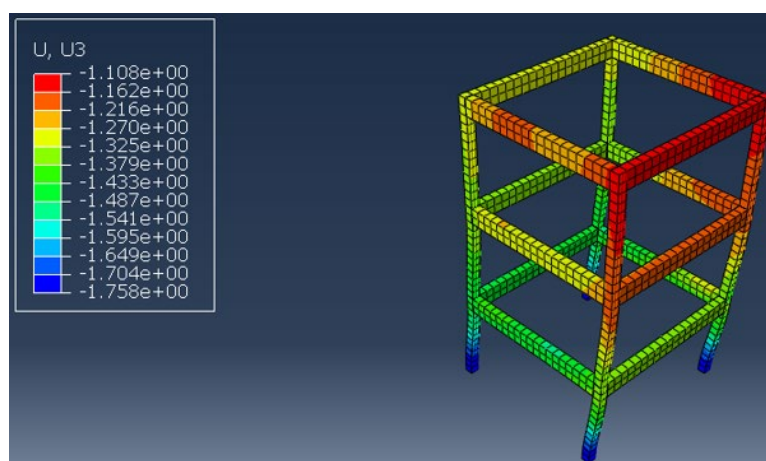
(i)
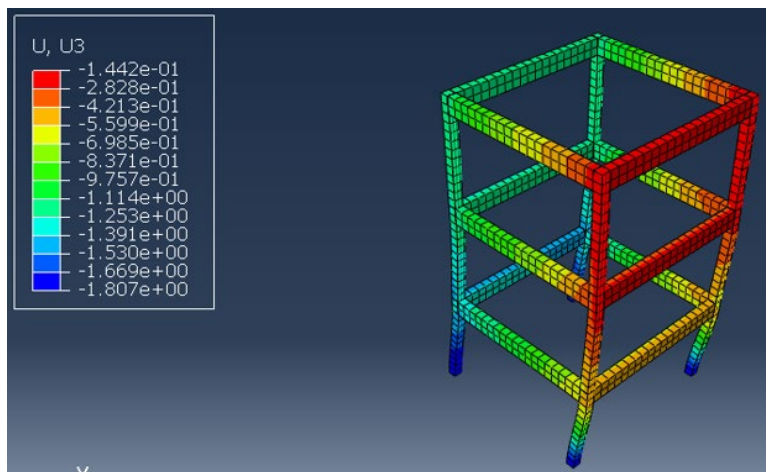
(j)
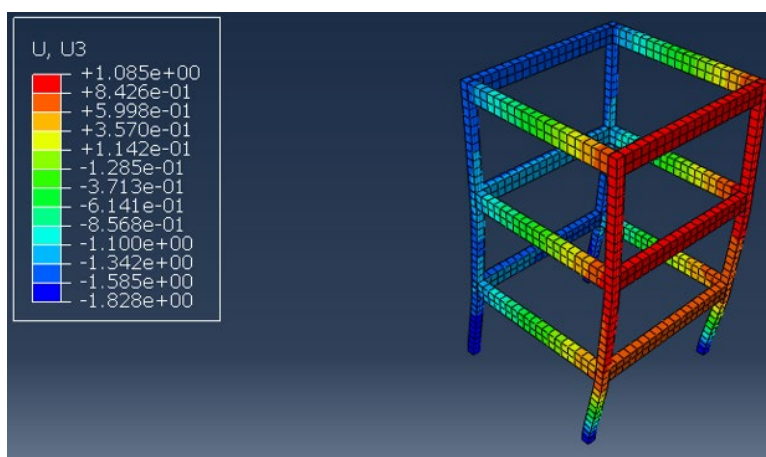
(k)
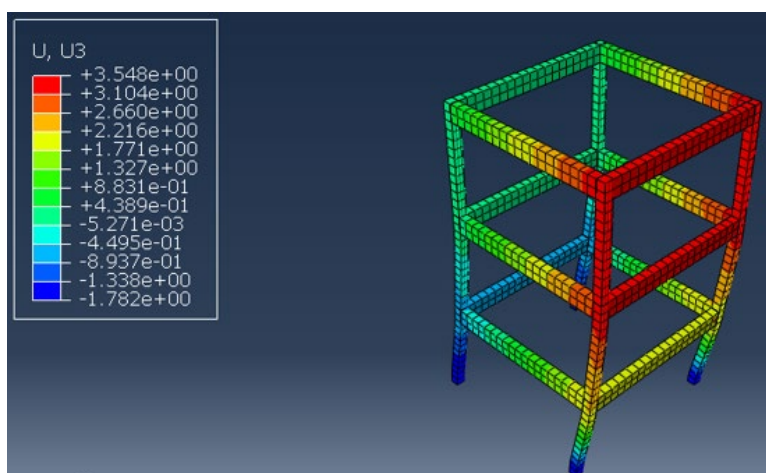
(l)

4.3   Von mises stress

Based on the von Mises stress results obtained for glulam framed structures and concrete buildings subjected to various PGA levels, significant insights into

their seismic behaviour can be gleaned. The results are depicted in Table 4.2. At the lower PGA levels below 0.5g, glulam structures exhibit negligible stress indicating their robust resistance to seismic loading, which corresponds well with the study's aim to evaluate mortise and tenon designs for seismic performance. However, as the PGA surpasses 0.5g, stress levels within glulam structures begin to escalate, underscoring potential areas of vulnerability, emphasising the need for further investigation to pinpoint stress concentration areas during earthquakes. This aspect of the analysis directly addresses the objective of identifying weaknesses in timber structures' seismic performance and informs potential avenues for improvement.

Conversely, concrete buildings display relatively low stress levels at lower PGAs but experience a rapid increase in stress as the PGA exceed 0.5g, signalling potential structural deformation and brittleness under extreme seismic forces. This comparative analysis highlights the strengths and weaknesses of each structural system, with glulam structures demonstrating flexibility and concrete buildings showcasing high load bearing capacity.

Table 4. 2: Von Mises stress result for both structures.

PGA	Glulam (N/mm^2)	Concrete (N/mm^2)
0.1g	1.54E-12	1.68E-02
0.16g	2.47E-12	8.23E+00
0.5g	4.67E-12	2.15E+01
0.7g	6.68E-12	2.19E+01
0.9g	7.76E-12	2.10E+01
1.0g	9.11E-12	2.20E+01

(a)

(b)

(c)

(d)

(e)

(f)

(g)

(h)

(i)

(j)

(k)

(l)
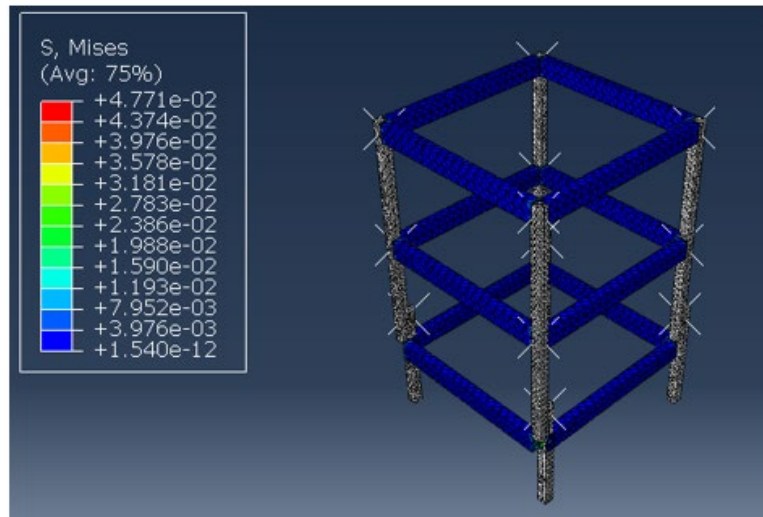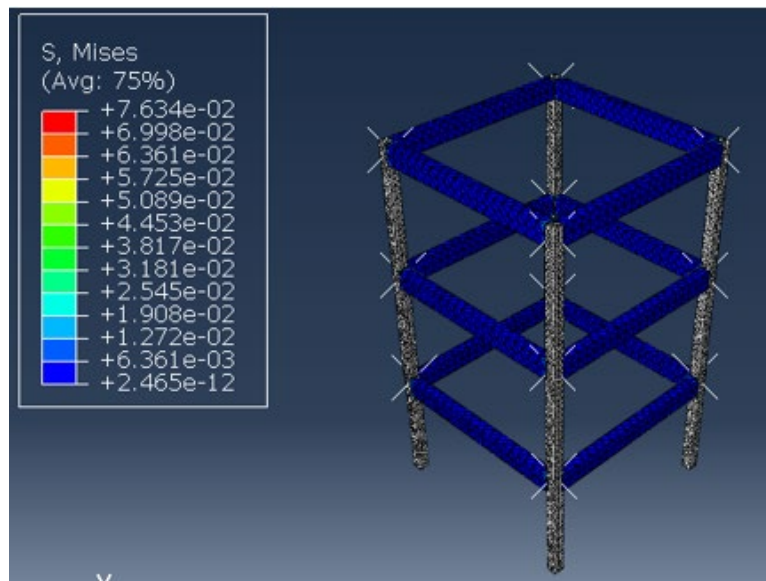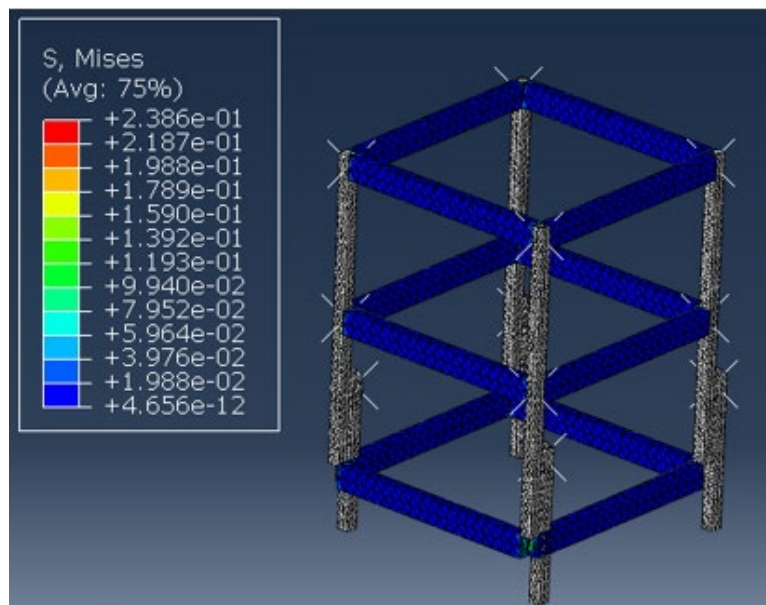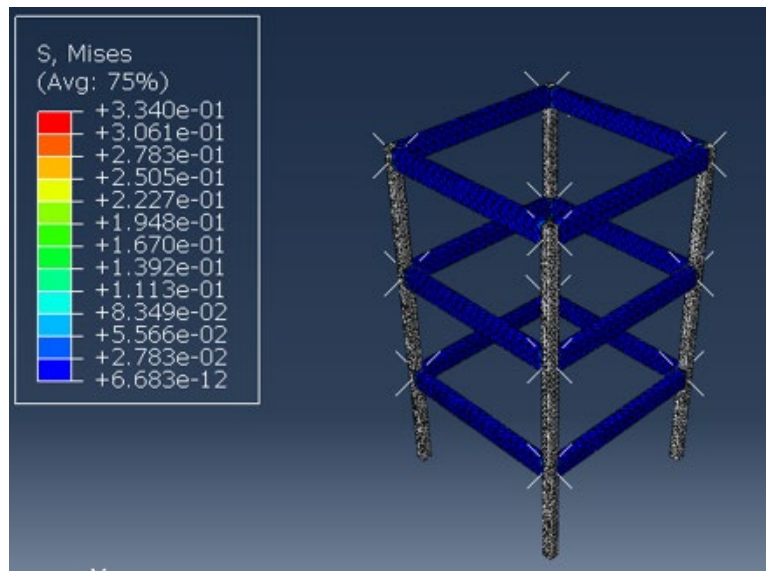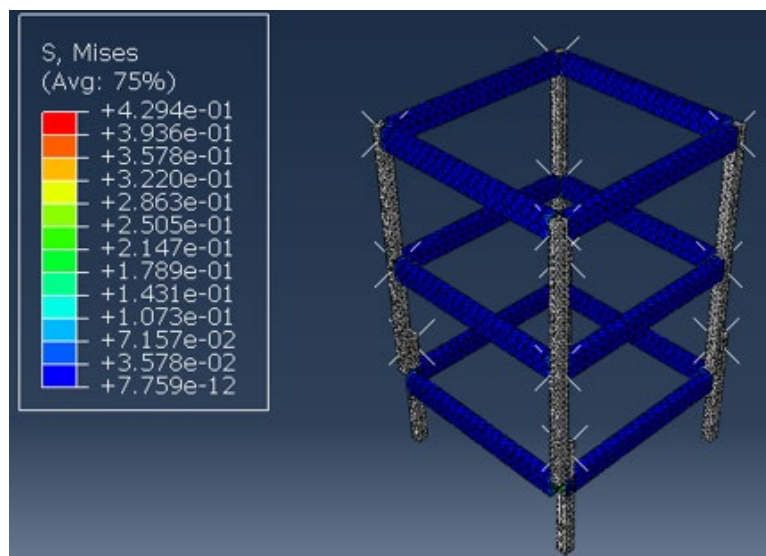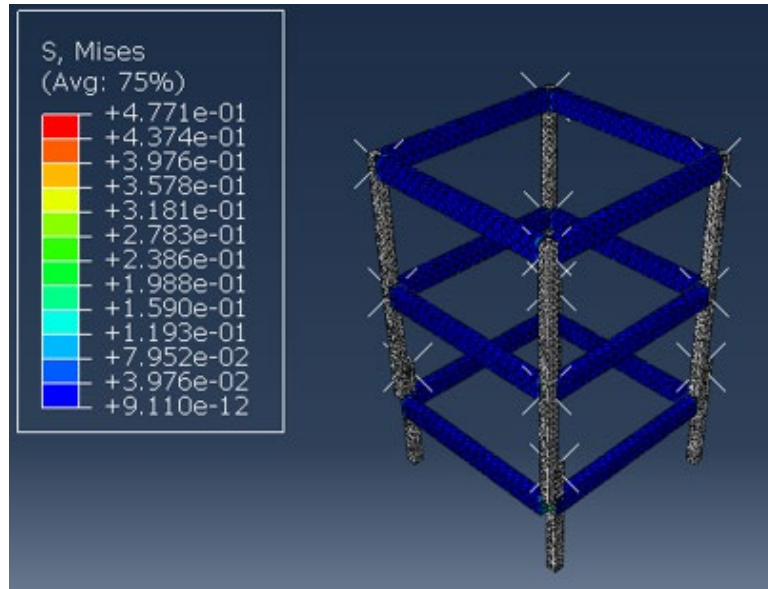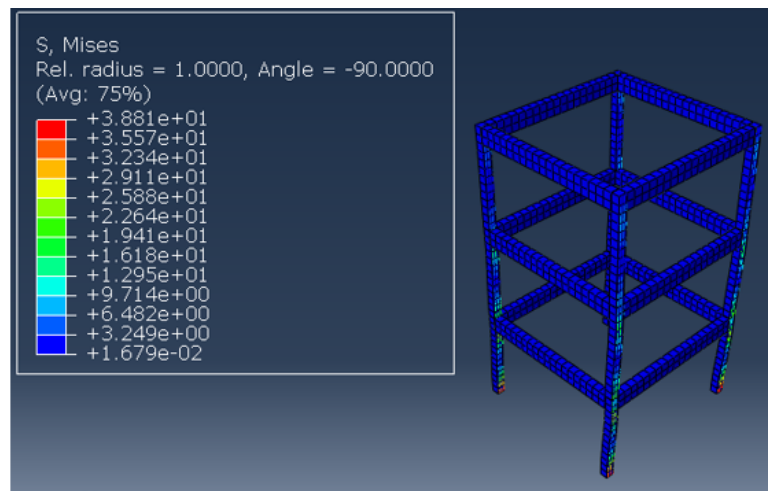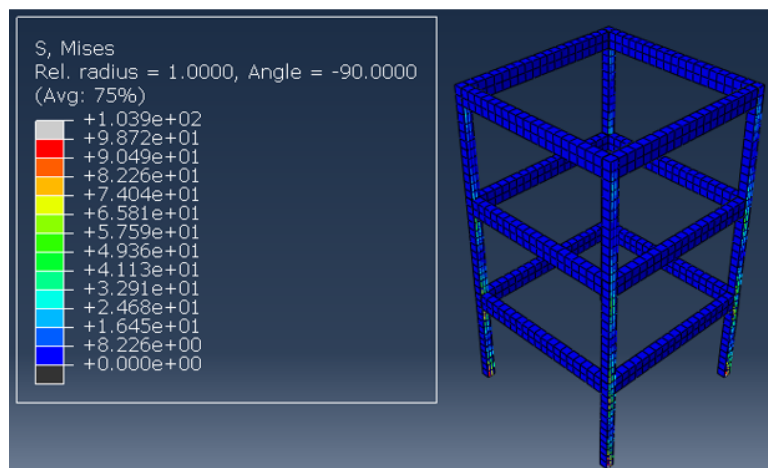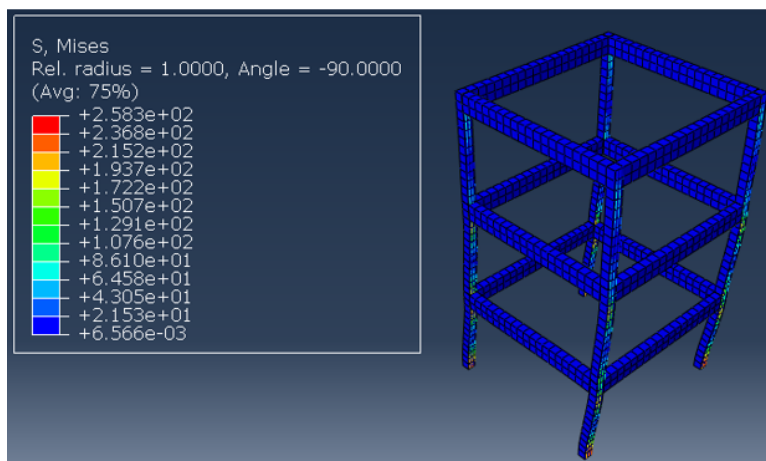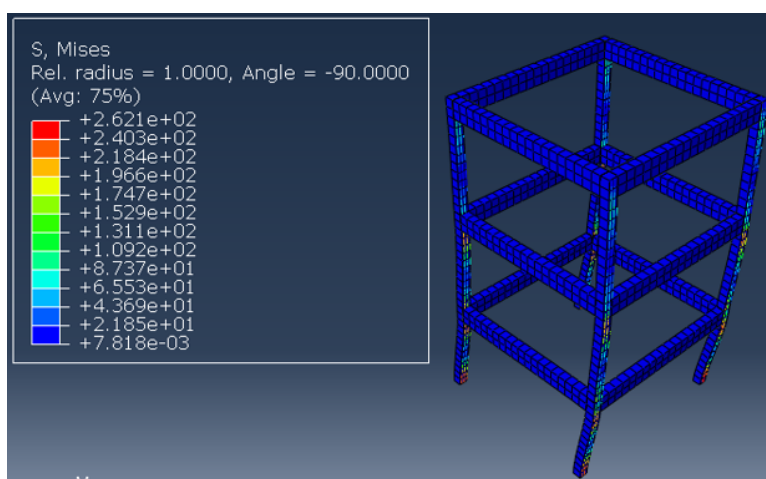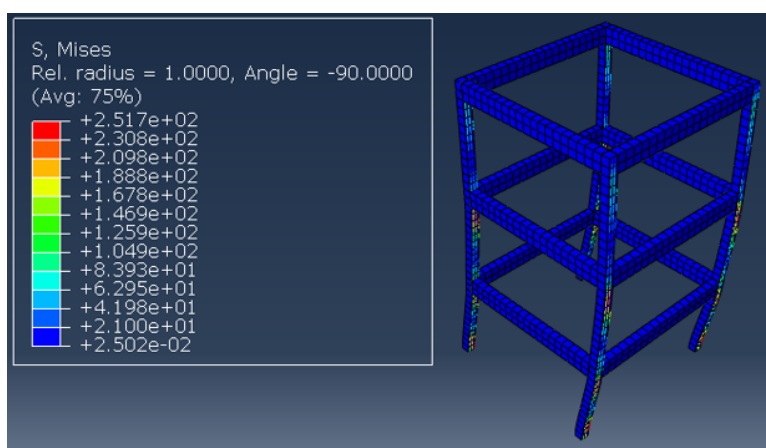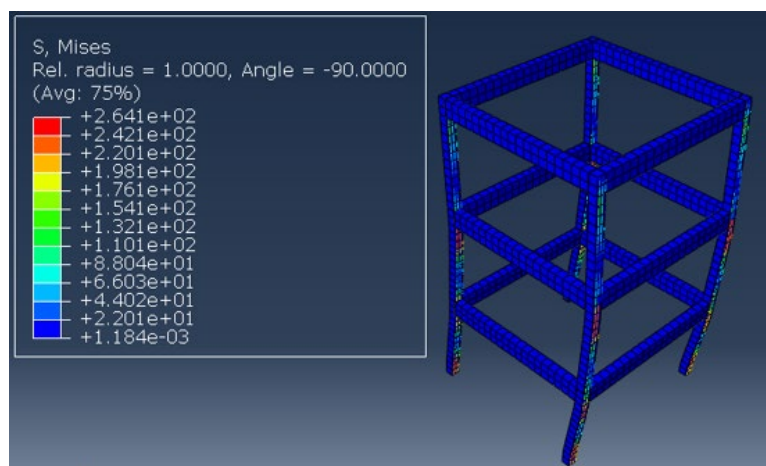
4.4　Principal stress

The principal stress results in the x-direction for glulam framed structures and concrete buildings at various PGA levels offer valuable insights into their seismic behaviour, particularly regarding shear stress, as shown in Table 4.3. Glulam structures exhibit relatively low principal stress values at lower PGAs, indicating minimal shear stress and suggesting robust resistance to seismic loading in the x-direction. However, as the PGA increases beyond 0.5g, principal stress levels in glulam structures escalate, signifying heightened shear stress and potential vulnerability to seismic forces. This highlights the importance of further investigation into shear stress concentration areas to enhance the seismic resilience of glulam framed structures.

In contrast, concrete buildings display higher principal stress values in the x-direction at lower PGAs, reflecting greater shear stress levels and potential susceptibility to seismic loading. As the PGA surpasses 0.5g, principal stress levels in concrete buildings continue to increase significantly, indicating substantial shear stress and potential structural deformation. This underscores the brittle nature of concrete under high seismic loading and emphasises the need for reinforcement strategies to mitigate shear stress concentration and enhance seismic resistance.

The comparison of principal stress results between glulam framed structures and concrete buildings highlights the contrasting behaviour of the two structural systems under seismic loading conditions. While glulam structures demonstrate resilience and flexibility with minimal shear stress at lower PGA s,

concrete buildings exhibit higher shear stress levels and increased vulnerability to seismic forces. This comparative analysis underscores the importance of understanding shear stress distribution and its implications for structural performance, informing strategies for optimising both glulam framed structures and concrete buildings for enhanced seismic resilience, particularly in x-direction.
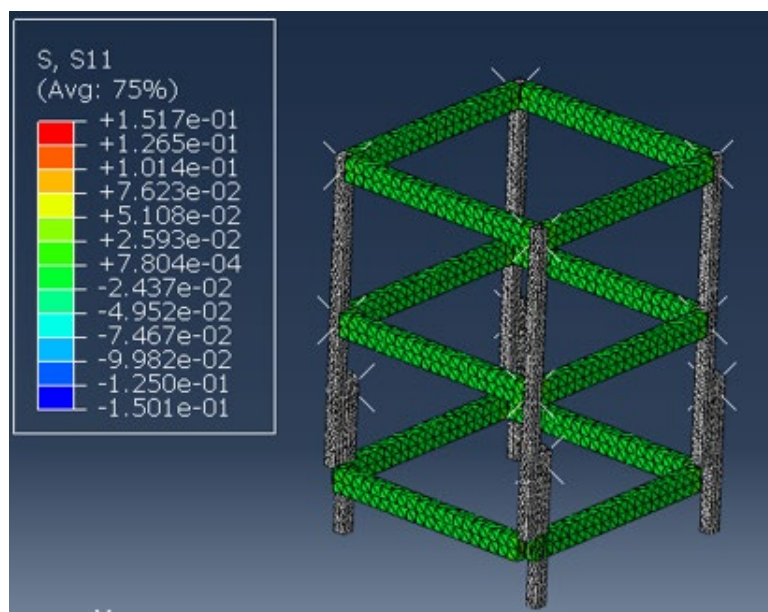
Table 4. 3: Principal stress in x-direction.

PGA	Glulam (N/mm²)	Concrete (N/mm²)
0.1g	1.56E-04	8.85E-01
0.16g	8.30E-03	2.83E+00
0.5g	2.59E-02	5.45E+01
0.7g	3.63E-02	4.59E+01
0.9g	4.67E-02	4.42E+01
1.0g	5.19E-02	4.28E+01

(a)

(b)

(c)

(d)
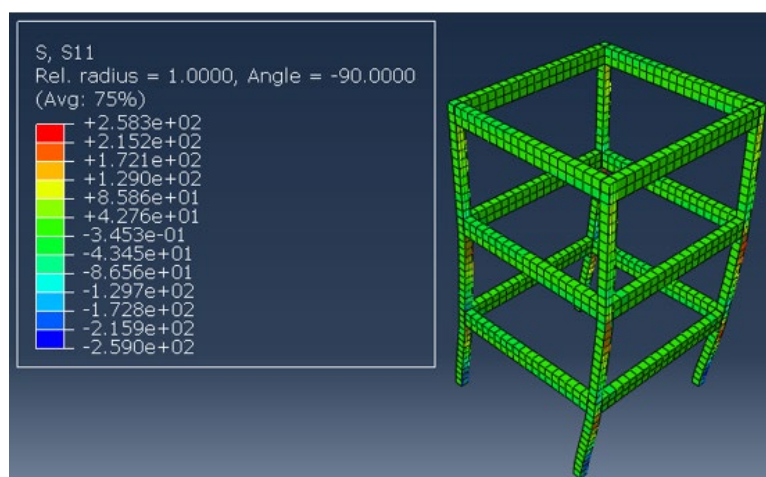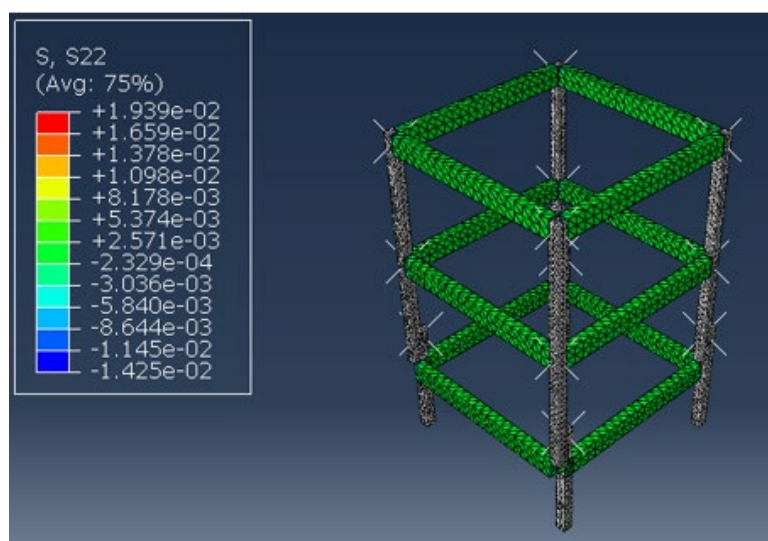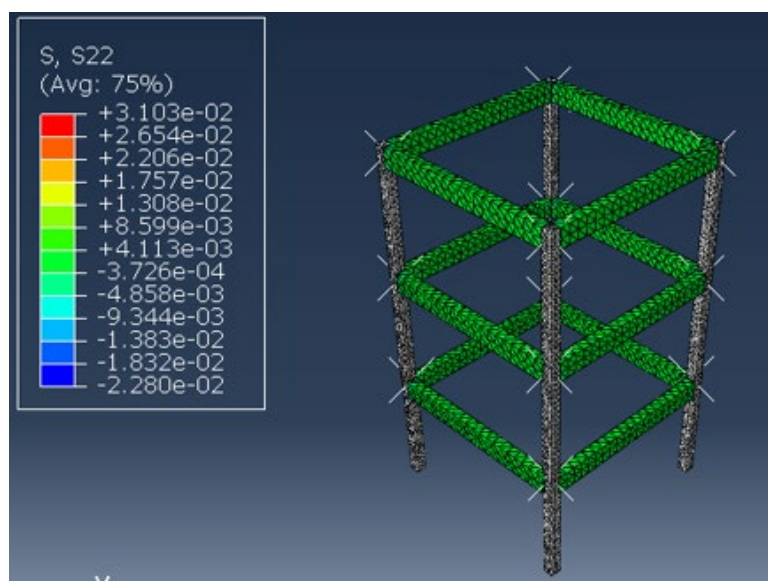

(e)

(f)

(g)

(h)

(i)

(j)

(k)

(l)
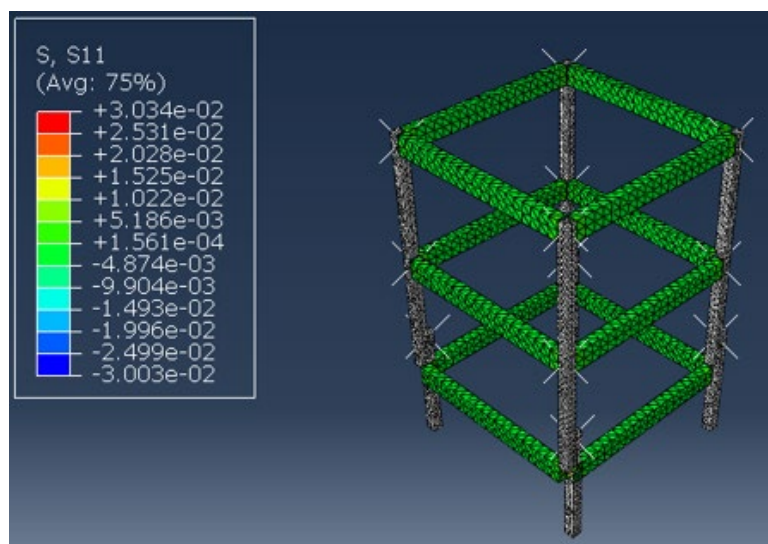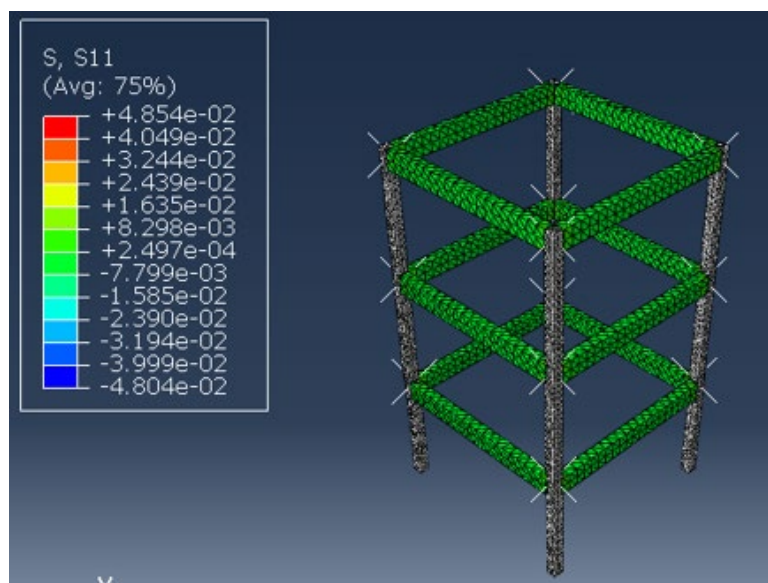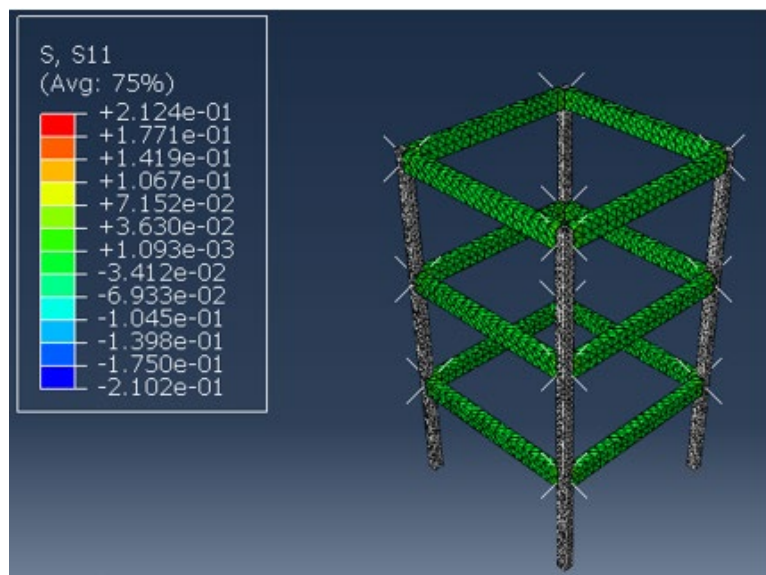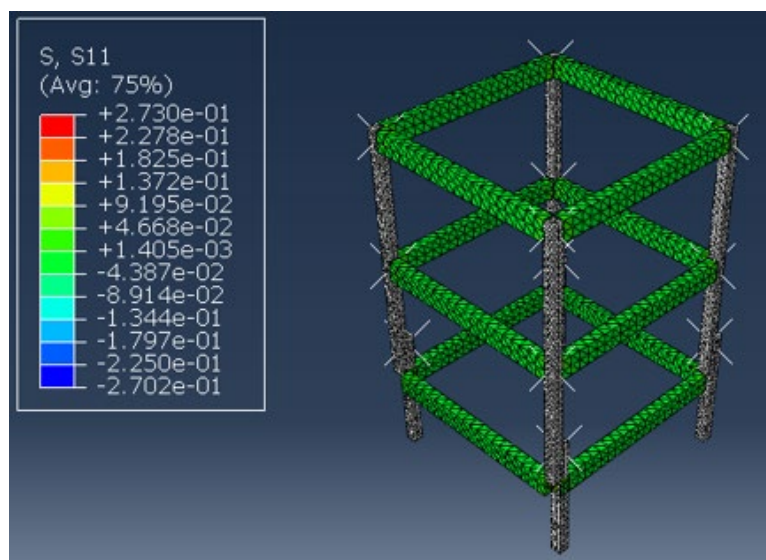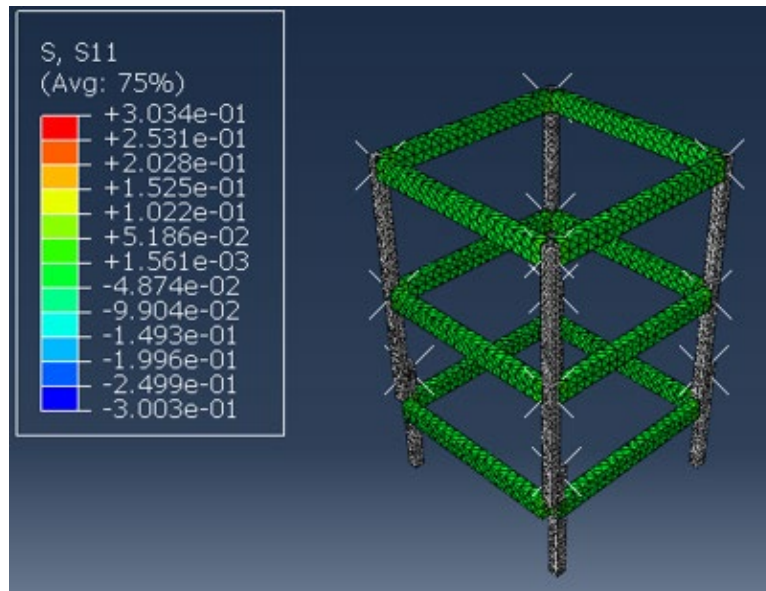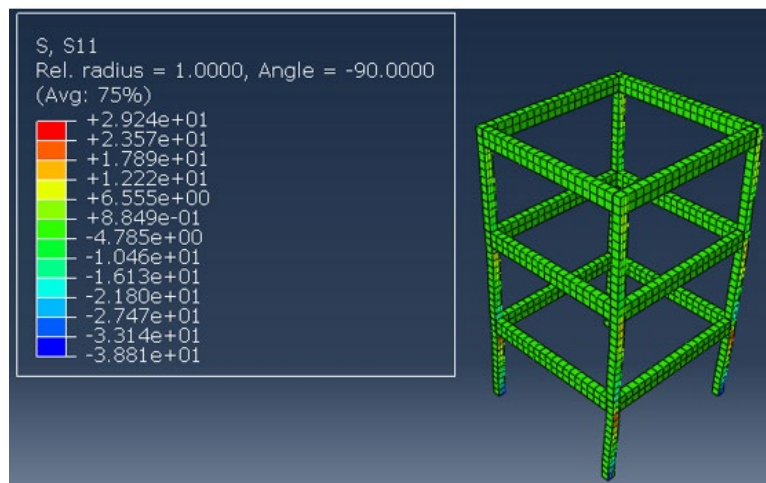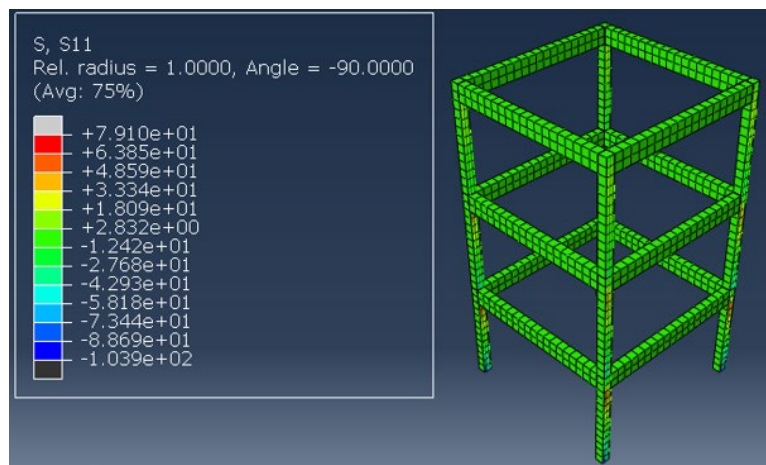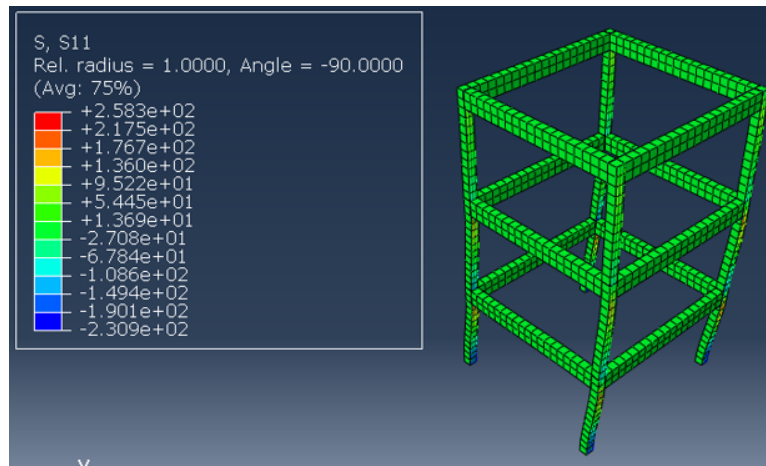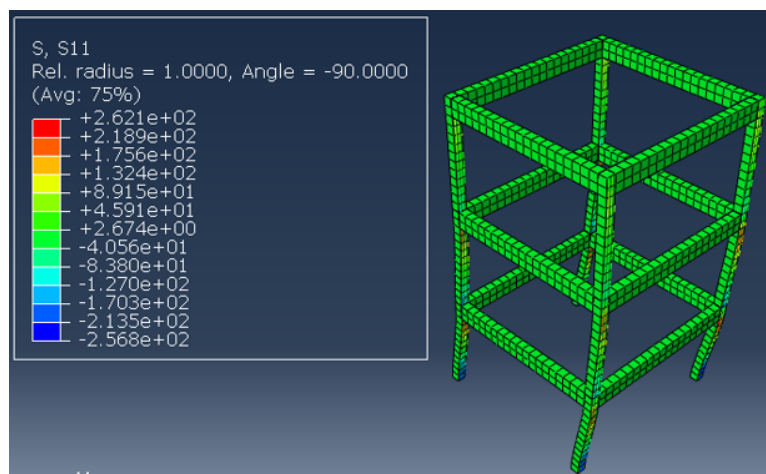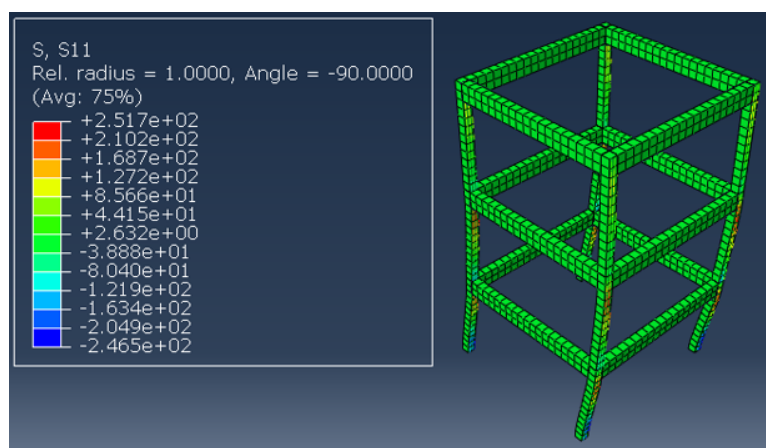
Table 4.4 presents the principal stresses observed in the y-direction for glulam framed and concrete structures, specifically obtained from beams. Glulam structures exhibit relatively low principal stress values at lower PGAs, indicating minimal tension and compression stress and robust resistance to seismic loading. However, as the PGA increases beyond 0.5g, principal stress levels escalate, signifying heightened tension and compression stress and potential vulnerability to seismic forces. Conversely, concrete buildings display higher principal stress values at lower PGAs, reflecting greater tension and compression stress levels and susceptibility to seismic loading. As the PGA surpasses 0.5g, principal stress levels in concrete buildings continue to increase significantly, indicating substantial tension and compression stress and potential structural deformation. This comparison highlights the differing behaviour of the two structural systems and underscores the importance of understanding tension and compression stress distribution for optimising seismic resilience.

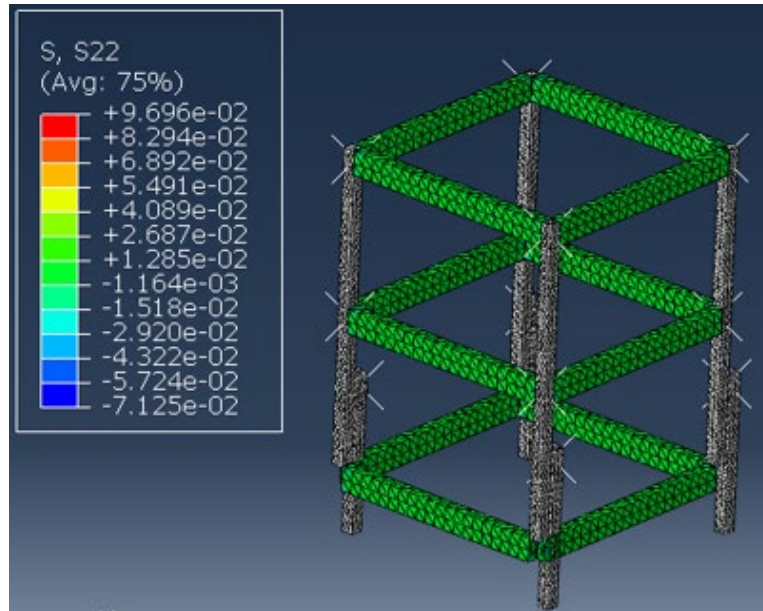Table 4. 4: Principal stress in y-direction.

PGA	Glulam (N/mm^2)	Concrete (N/mm^2)
0.1g	5.37E-03	5.24E-02
0.16g	8.60E-03	3.78E-01
0.5g	2.69E-02	1.02E+00
0.7g	3.76E-02	1.64E+00
0.9g	4.84E-02	1.98E+00
1.0g	5.37E-02	2.03E+00

(a)

(b)

(c)
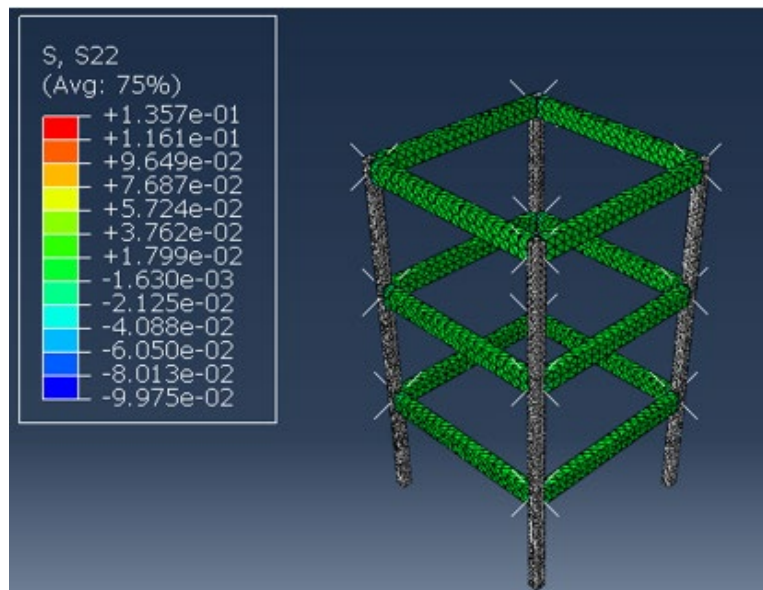
(d)
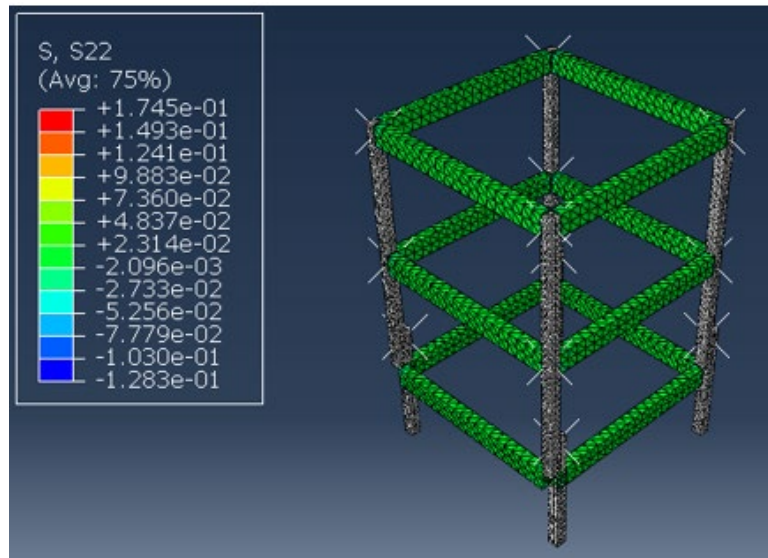
(e)
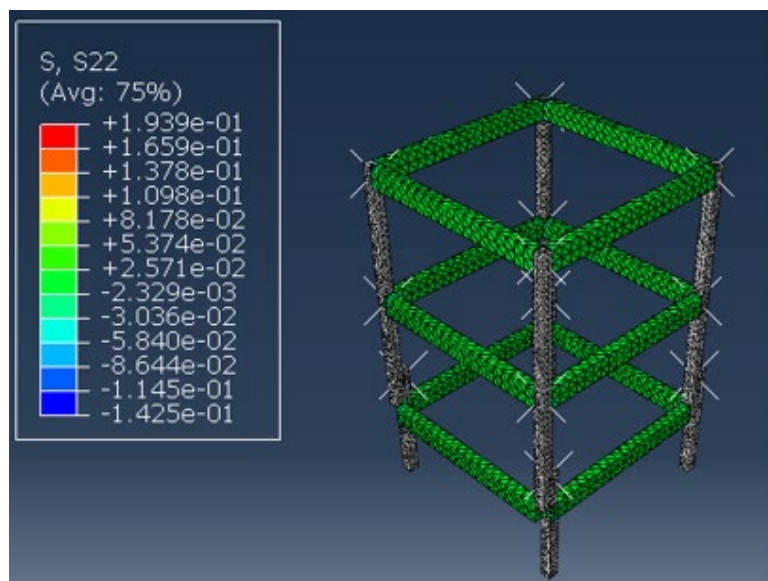
(f)
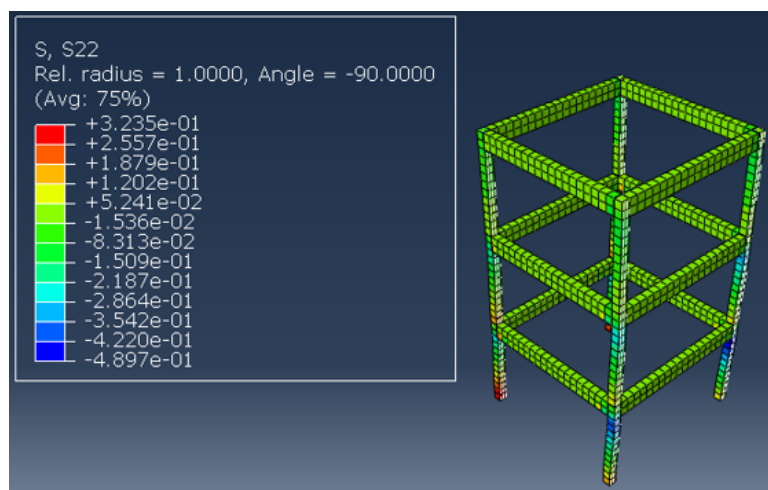
(g)
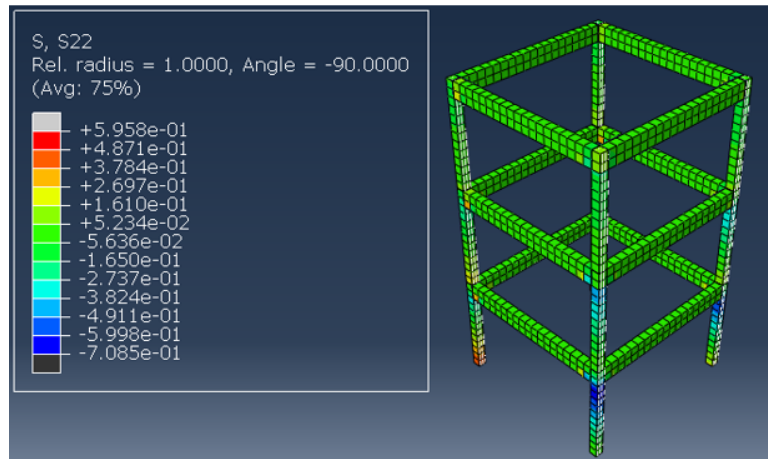
(h)

(i)

(j)

(k)

(l)

Table 4.5 presents the principal stresses observed in the z-direction for glulam framed and concrete structures, obtained specifically from beams for direct comparison. Glulam structures exhibit relatively low principal stress 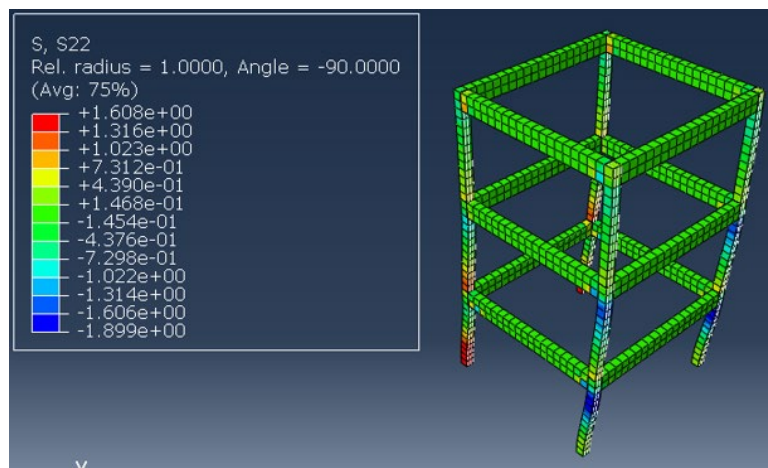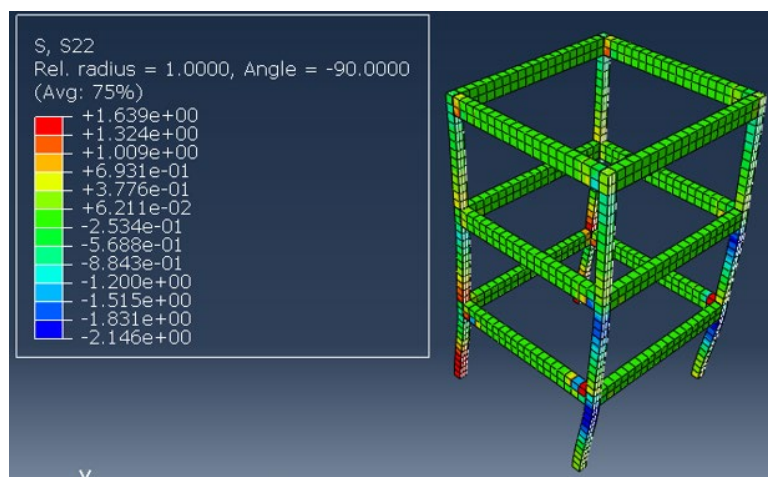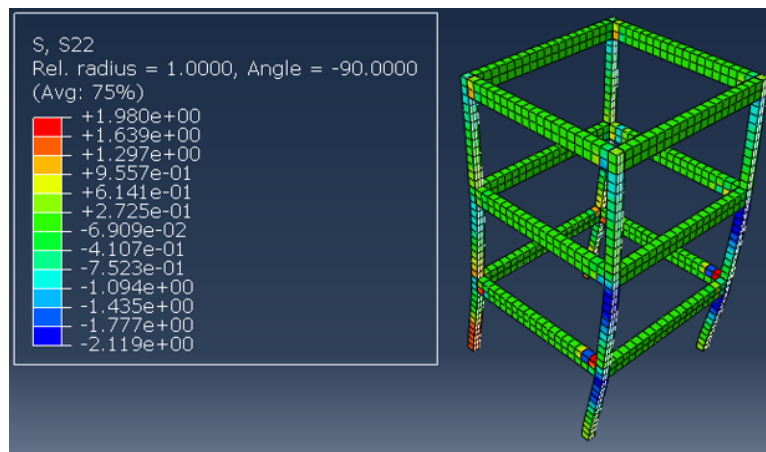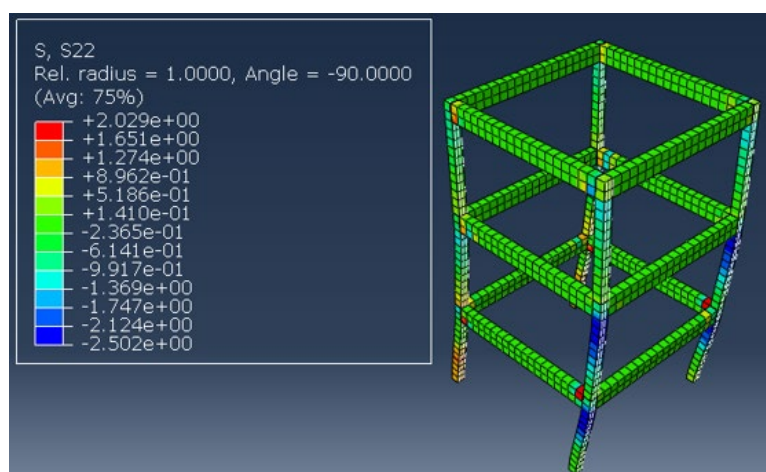values at lower PGAs, indicating minimal stress in z-direction and robust resistance to seismic loading. However, as the PGA increases beyond 0.5g, principal stress levels escalate, signifying heightened stress in the z-direction and potential vulnerability to seismic forces.

In contrast, concrete buildings display higher principal stress values at lower PGAs, reflecting greater stress in the z-direction and susceptibility to seismic loading. As the PGA surpasses 0.5g, principal stress levels in concrete buildings continue to increase significantly, indicating substantial stress in the z-direction and potential structural deformation. This comparison underscores

the importance of understanding stress distribution in the z-direction for optimising seismic resilience in both structural systems.

Table 4. 5: Principal stress in z-direction.

PGA	Glulam (N/mm^2)	Concrete (N/mm^2)
0.1g	4.02E-03	1.75E-01
0.16g	6.44E-03	2.93E-01
0.5g	2.01E-02	5.41E-01
0.7g	2.82E-02	1.52E+00
0.9g	3.62E-02	2.22E+00
1.0g	4.02E-02	2.19E+00

(a)

(b)

(c)

(d)

(e)

(f)

(g)

(h)

(i)

(j)

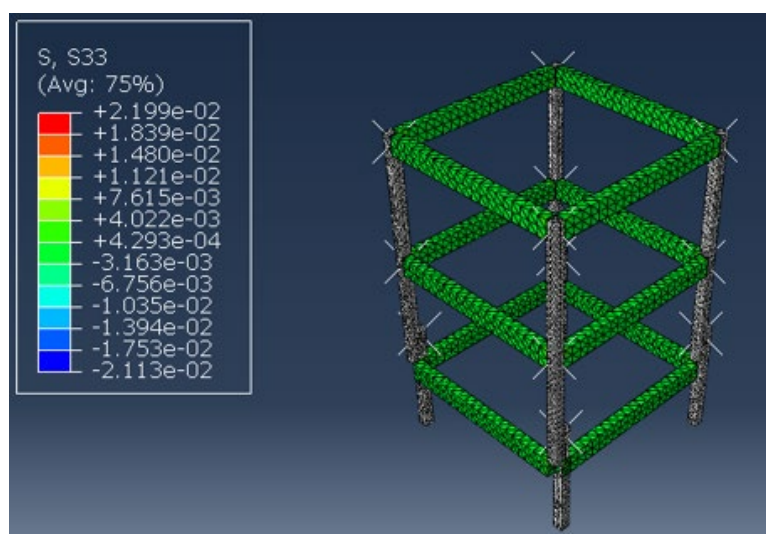(k)

(l)
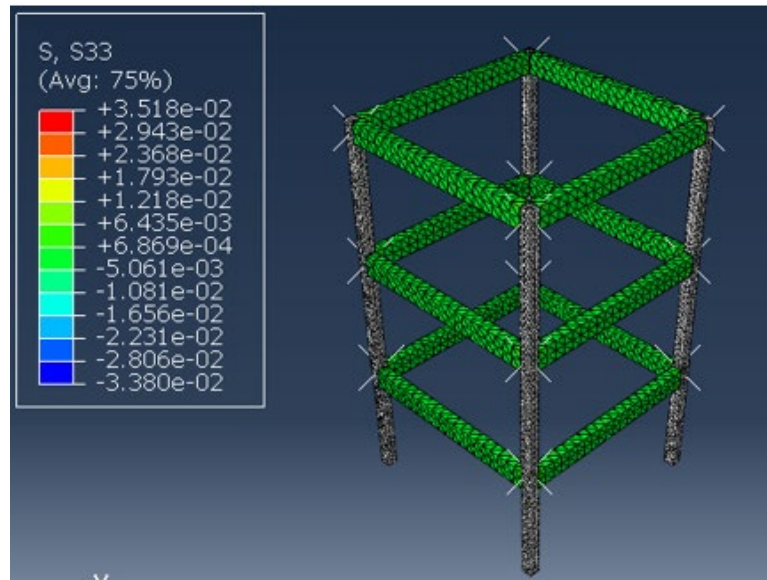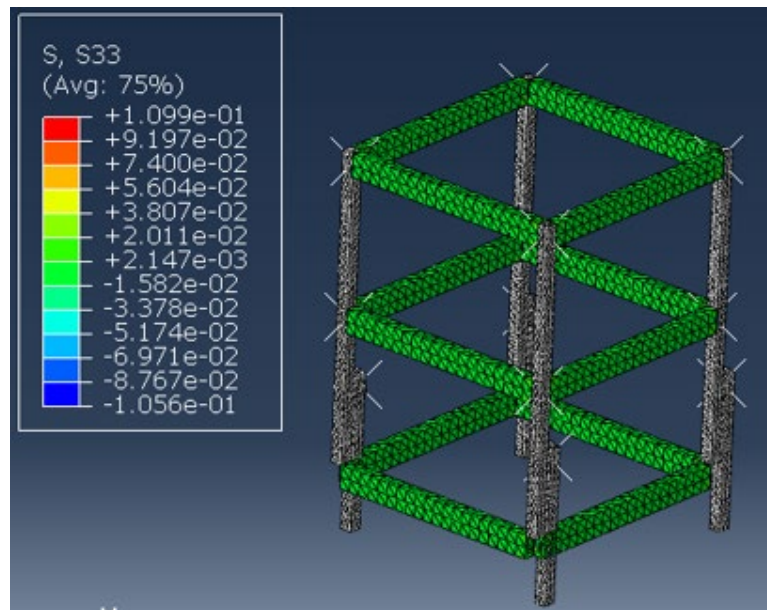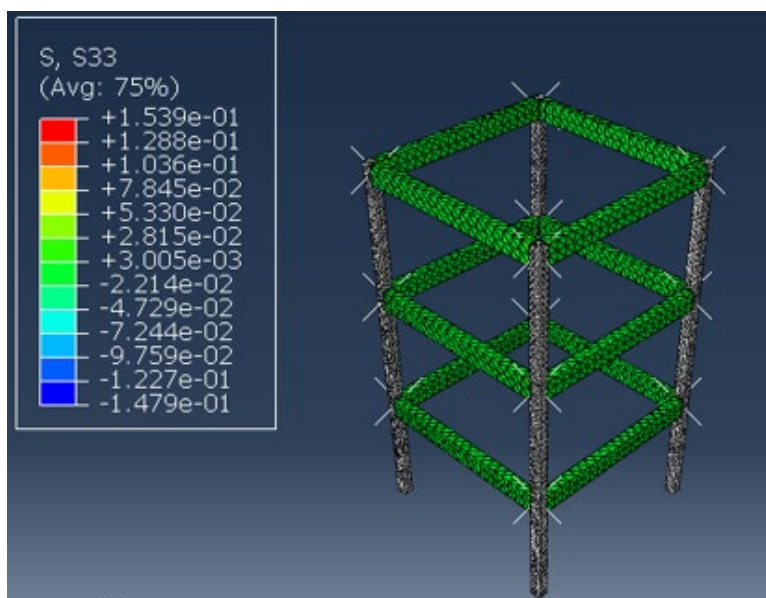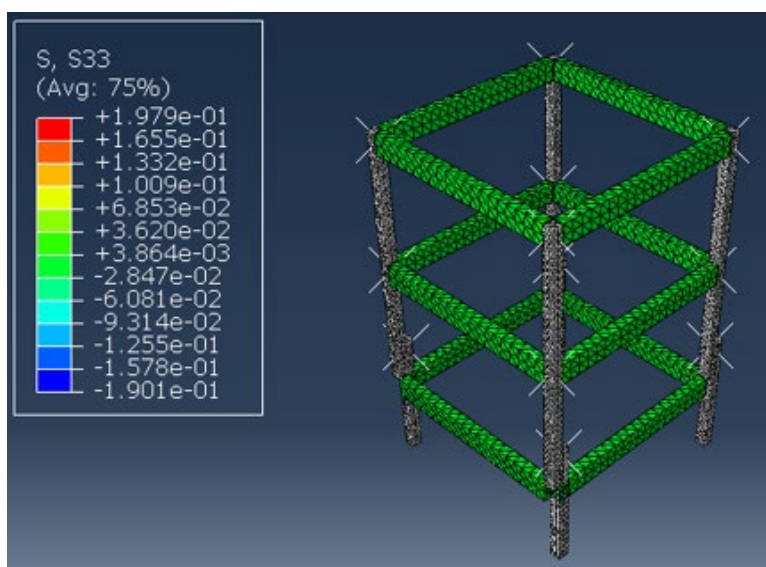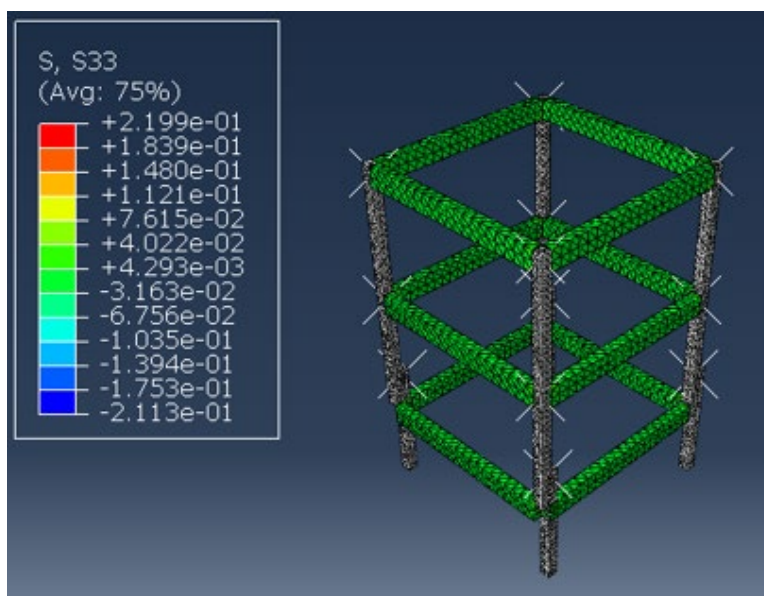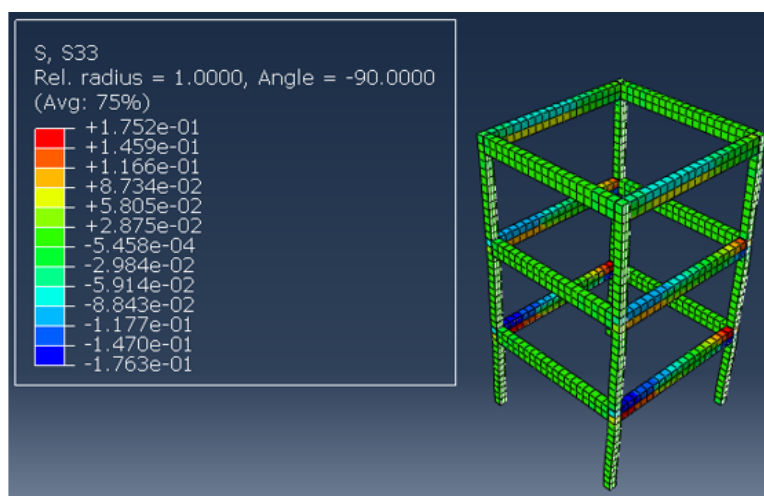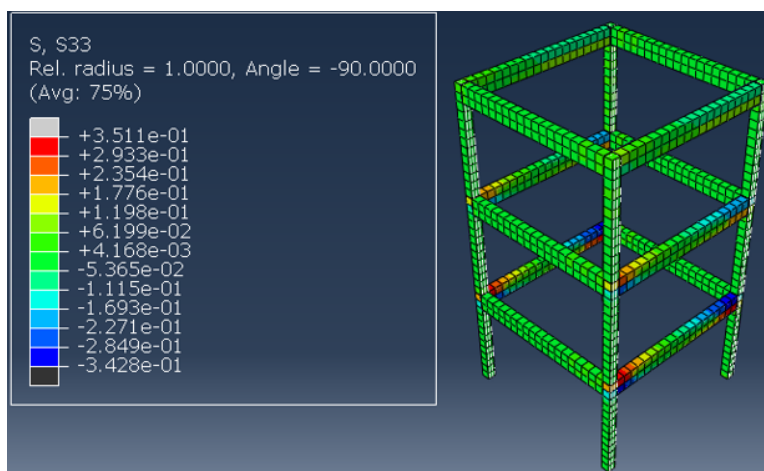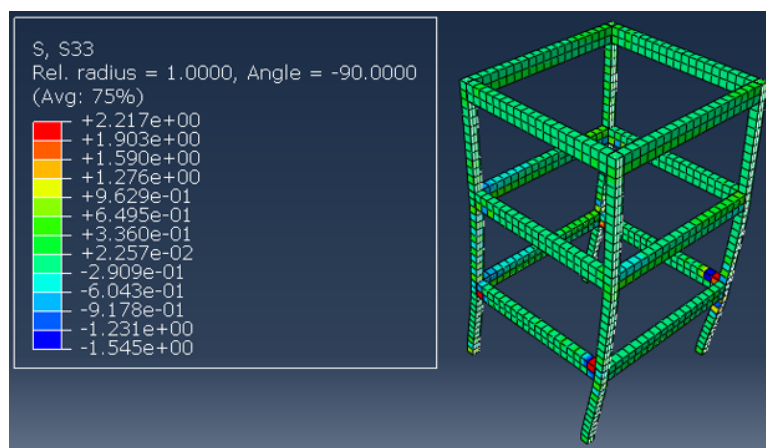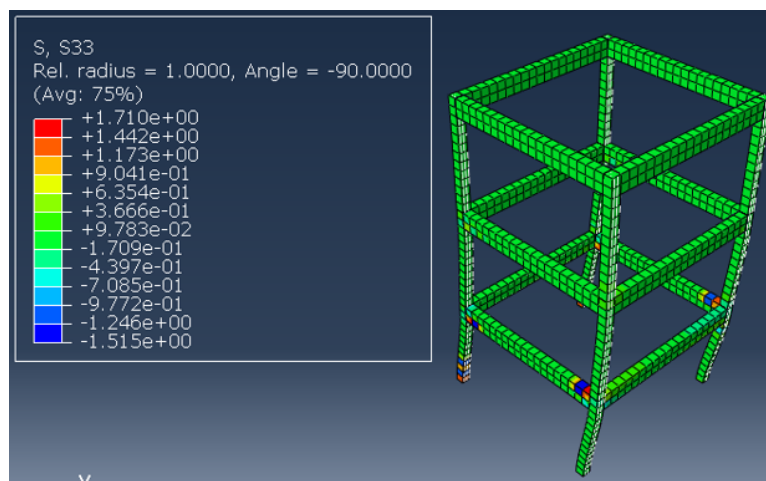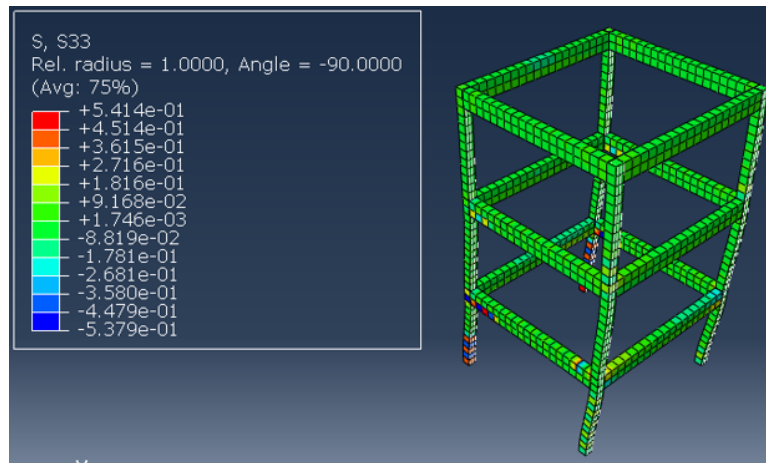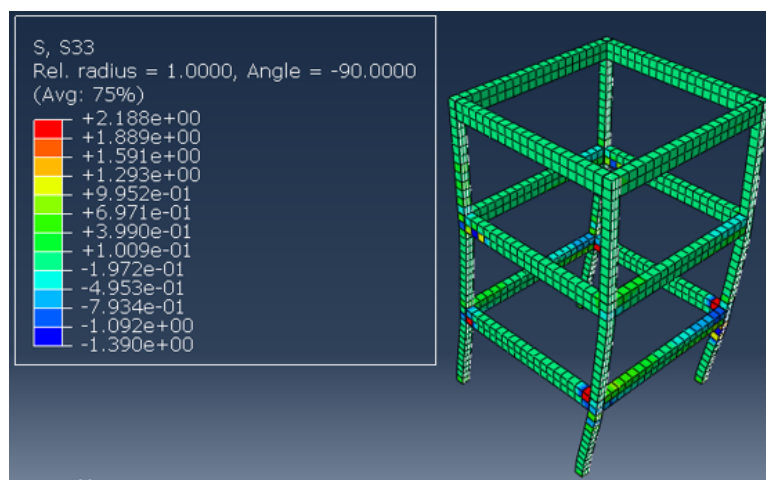
4.5 Summary

In summary, the seismic performance of glulam framed structures and concrete buildings was evaluated through analyses of displacement, von Mises stress, and principal stresses in the x-, y-, and z-directions. Glulam structures exhibited minimal displacement at lower PGAs, indicating good resistance to seismic loading, whereas concrete buildings displayed negligible displacement at low PGAs. However, as PGA levels increased, both types of structures experienced significant deformation, with glulam structures showing relatively lower displacement compared to concrete.

Additionally, glulam structures demonstrated lower stress levels in the x- and z-directions compared to concrete buildings, suggesting potential advantages in terms of structural integrity and resilience. However, stress levels increased significantly in glulam structures as PGA levels rose, indicating areas of vulnerability and the need for further investigation into stress concentration areas during earthquakes.

Conversely, concrete buildings exhibited higher stress levels across all directions, underscoring their brittleness under seismic loading conditions. These findings emphasise the importance of understanding the behaviour of different structural systems under varying seismic intensities to inform design enhancements and improve overall seismic resilience.

CHAPTER 5

CONCLUSIONS AND RECOMMENDATIONS

5.1 Conclusions

In conclusion, this study has investigated the seismic behaviour of glulam framed structures compared with concrete structures, with the objective of assessing their seismic performance and identifying areas for improvement. By analysing displacement, von Mises stress, and principal stresses in the x-, y-, and z-directions, significant insights have been gleaned into the structural response of both glulam and concrete structures to seismic loading. The results indicate the resilience of glulam structures to low-intensity seismic events, with minimal displacement observed at lower PGAs. However, as the PGA levels increased, both glulam and concrete structures experienced substantial deformation and stress escalation, highlighting vulnerabilities under higher seismic forces. These findings underscore the importance of informed design decisions and mitigation strategies to enhance the seismic resistance of buildings, particularly in seismic-prone areas. By addressing these challenges, engineers can contribute to the development of safer and more resilient structures capable of withstanding seismic events and ensuring the safety of occupants and communities.

5.2 Recommendations for future work

While this study provides valuable insights into the seismic behaviour of glulam framed structures, the limitations suggest areas for future research. To address the oversimplification of real-world seismic events inherent in finite element analysis assumptions, future studies should prioritise experimental testing to validate simulation results. Additionally, efforts should be made to refine numerical models used for seismic analysis, considering the simplified boundary conditions in current finite element models. Future research should also focus on accounting for variations in foundation types, soil properties, and building configurations to provide a more comprehensive understanding of

structural responses to seismic forces. These recommendations aim to enhance the accuracy and reliability of seismic analysis in glulam framed structures.

REFERENCES

Acmartin, n.d. *Los Angeles city hall seismic rehabilitation and renovation.* [online] Available at: <https://www.acmartin.com/portfolio/la-city-hall-seismic-rehabilitation-and-renovation> [Accessed 12 December 2023]

Alih, S. and Vafaei, M., 2019. Performance of reinforced concrete buildings and wooden structures during the 2015 Mw 6.0 Sabah earthquake in Malaysia. *Engineering Failure Analysis*. 102, pp. 351-368.

Anand, P., 2016. *Base isolation system: outline on principles, types, advantages & applications.* [online] Available at: <https://civildigital.com/base-isolation-system-outline-on-principles-types-advantages-applications/> [Accessed 12 December 2023]

Arnold, M. H., n.d. *The Tohoku disaster: responding to Japan's 3/11 earthquake, tsunami, and nuclear accident.* [PowerPoint slides]. Harvard Kennedy School. https://www.hks.harvard.edu/sites/default/files/centers/research-initiatives/crisisleadership/files/Tohoku%20Disaster_Taubman%20Center_20 12%2011%2014_red_web_Part%202.pdf

BBC, n.d.. *Causes And Impact Of An Earthquake.* [online] Available at: <https://www.bbc.co.uk/bitesize/guides/zg9h2nb/revision/5#:~:text=Disease%20may%20spread.,damage%20caused%20by%20the%20earthquake.> [Accessed 7 June 2023]

Bin M. and Hamid A., n.d.. Analysis of existing high-rise reinforced concrete structures in Malaysia subjected to earthquake and wind loadings.

Birketts Bog Mats, n.d. *Timber in construction: a history.*[online] Available at: <https://www.birkettsbogmats.com/timber-in-construction-a-history/#:~:text=Early%20Use%20of%20Timber%20in,Mesolithic%20period%20(Stone%20Age).> [Accessed 15 December 2023]

British Geological Survey, 2008. *Earthquakes.* [online] Available at: <http://earthquakes.bgs.ac.uk/education/eq_guide/eq_booklet_what_is.htm> [Accessed 6 June 2023]

BYJU's, n.d.. *Deformation of solids.* [online] Available at: < https://byjus.com/physics/solid-deformation/> [Accessed 3 March 2024]

Charles, C., Michel, B., Greg, M., Roberto, L., and Alistair, F., 2011. Steel structures damage form the Christchurch earthquake series of 2010 and 2011. *Bulletin of the New Zealand Society for Earthquake Engineering*. 44(4).

Construction Plus Asia, 2016. *Glulam from Malaysian hardwood.* [online] Available at: < https://www.constructionplusasia.com/my/glulam-from-malaysian-hardwood/> [Accessed 10 April 2024]

Dan, S., 2023. *What are mortise-and-tenon joints used for?*. [online] Available at: <https://www.familyhandyman.com/article/mortise-and-tenon-joint/> [Accessed 15 December 2023]

David, M., 2019. Seismic risk assessments and due diligence studies. [online] Available at: <https://www.sgh.com/insight/seismic-risk-assessments-and-due-diligence-studies/> [Accessed 10 January 2024]

Eduardo, S., 2021. *Is mass timber a good choice for seismic zones?*. [online] Available at: <https://www.naturallywood.com/blog/is-mass-timber-a-good-choice-for-seismic-zones/#:~:text=Wood%20as%20a%20structural%20material,the%20moment%20of%20its%20fracture.> [Accessed 15 December 2023]

Faisal, F., Zaini, S. and Selokumar, T., 2020. Evaluation of cost analyses for earthquake resistant reinforced concrete buildings based on Malaysian National Annex to Eurocode 8. *Lecture Notes in Civil Engineering*. 53, pp. 1485-1492.

GCSE Geography, n.d.. *The Sichuan Earthquake – An Example Of An Earthquake Disaster In An LEDC.* [online] Available at: < https://www.coolgeography.co.uk/GCSE/AQA/Restless%20Earth/Earthquakes/Sichuan.htm#:~:text=A%20total%20of%205%20million,was%20put%20at%20%2475%20million.> [Accessed 7 June 2023]

Hamid, N., Razak, S., Sanik, M., Mokhtar, M., Sahat, S., Kaamin, M. and Ramli M., 2019. Application of seismic resisting systems for building construction in Malaysia. *International Journal of Recent Technology and Engineering*. 8(2 Special Issue 2), pp. 71-75.

Hasslacher Norica Timber, n.d. *Glued laminated timber*. [online] Available at: <https://www.hasslacher.com/glue-laminated-timber> [Accessed 10 April 2024]

Irwan Adiyanto, M. and Majid, T, 2014. Seismic design of two storey reinforced concrete building in Malaysia with low class ductility. pp. 27-46.

John, P.R., 2024. Richter scale. [online] Available at: < https://www.britannica.com/science/Richter-scale> [Accessed 22 March 2024]

Jorge, L., Ehsan, H., Umar, A. S., Mohammed, S., Annie, A. and Tom, L., 2023. Application of machine learning-based algorithms to predict the stress-strain curves of additively manufactured mild steel out of its microstructural characteristics. *Results in Engineering*. 20(2023) 101587.

Kang, L., 2022. *Finite element analysis of tuned mass damper*. Universiti Tun Hussein Onn Malaysia. pp. 281-290.

Kumar, A. A., 2023. *What are the types of frame structures in construction?*. [online] Available at: <https://www.getpowerplay.in/resources/blogs/what-are-the-types-of-frame-structures-in-

construction/#:~:text=Frame%20structures%20can%20be%20made,result%20 from%20the%20applied%20loading.> [Accessed 20 February 2024]

Looi, D., Lam, N. and Tsang, H., 2021. Developing earthquake-resistant structural design standard for Malaysia based on Eurocode 8: challenges and recommendations. *Standards*. 1(2), pp. 134-153.

Lupoi, A. and Greco, A., 2022. *Bridge safety, maintenance, management, life-cycle, resilience and sustainability*. London: CRC Press.

Malay Mail, 2015. *Sabah earthquake a 2015 shock for the nation*. [online] Available at: <https://www.malaymail.com/news/malaysia/2015/12/24/sabah-earthquake-a-2015-shock-for-the-nation/1029201> [Accessed 7 June 2023]

Manjip, S., Chandra, K. K., Arjun, K. G., and Sunil, D., 2021. Post-earthquake damage assessment of traditional masonry buildings: A case study of Bhaktapur municipality following 2015 Gorkha (Nepal) earthquake. *Engineering Failure Analysis*. 123(2021), 1350-6307.

Meena, R., n.d. *Seismic bracing: a comprehensive guide to earthquake protection for your building*. [online] Available at: <https://www.littlepeng.com/single-post/seismic-bracing-a-comprehensive-guide-to-earthquake-protection-for-your-building#:~:text=Seismic%20bracing%20works%20by%20providing,that%20 occur%20during%20an%20earthquake.> [Accessed 12 December 2023]

Michael, G., 2017. *The mechanism and applications of a tuned mass damper (TMD)*. [online] Available at: <https://bsbgroup.com/blog/the-mechanism-and-applications-of-tuned-mass-damper-tmd#:~:text=A%20Tuned%20Mass%20Damper%20(TMD)%2C%20also%20 called%20a%20%22,earthquake%20or%20high%20winds%20hit.> [Accessed 12 December 2023]

Muthuveerappan, A. L. and Sivarajan, S., 2023. Finite element analysis of process parameters influences on deformation and von mises stress in drilling. *Materials Today: Proceedings*. 2214-7853.

Nanako, R., Aaron, O., and Chiho, O., 2024. Disrupted sense of place and infrastructure reconstruction after the Great East Japan Earthquake and Tsunami. *Progress in Disaster Science*. 22 (2024) 100322.

Nandona, G., 2022. *A review on the analysis of building with different types of bracings*. International Journal for Science Technology and Engineering. Vol. 10, Iss:3, pp. 215-218.

Okada, T., Umino, N. and Hasegawa, A., 2012. Hypocenter distribution and heterogeneous seismic velocity structure in and around the focal area of the 2008 Iwate-Miyagi Nairiku Earthquake, NE Japan – possible seismological evidence for a fluid driven compressional inversion earthquake. *Earth, Planets and Space*, 64(9), pp. 717-728.

Onder, P. and Mehmet, F. A., 2023. The effect of errors in structural system design on the structure damaged in 2023 Turkey earthquakes: A case study. *Engineering Failure Analysis*. 157, 1350-6307.

Ondrej, 2022. *ETABS*. [online] Available at: <https://wiki.csiamerica.com/display/etabs/Home> [Accessed 2 February 2024]

Pantelis, L., 2020. *Principal stresses and stress invariants*. [online] Available at: < https://www.pantelisliolios.com/principal-stresses-and-invariants/> [Accessed 3 March 2024]

Pishva, K., 2016. *Earthquake short term and long term effect*. [onine] Available at: <https://prezi.com/ydjd7uvlsuxj/earthquake-short-term-and-long-term-effect/> [Accessed 7 June 2023]

Raden, B. A. A. and Ibnu, P. R., 2023. *Alternatif desain struktur Gedung rumah sakit universitas islam malang dengan base isolator tipe friction pendulum system (FPS)*. Jurnal Teknik ITS. Vol.12, Iss:1.

Rahul, J., Surjya, K., and Shiv, B. S., 2017. 5 – Numerical modelling methodologies for friction stir welding process. *Computational Methods and Production Engineering*, 2017, pp. 125-169.

Roumen, M., S. E., and P. E., 2023. San Francisco – Oakland bay bridge. [online] Available at: <https://www.structuremag.org/?p=25700> [Accessed 12 December 2023]

Samsung C&T Global PR Manager, 2017. *Strong and steady: building quake-resistant structures*. [online] Available at:<https://news.samsungcnt.com/en/features/engineering-construction/2017-12-strong-steady-building-quake-resistant-structures/#:~:text=Another%20iconic%20skyscraper%20that's%20well,so%20through%20advanced%20structural%20support.> [Accessed 12 December 2023]

Sarah, E, 2015. *A local Sabahan on the earthquake aftermath that you're probably unaware of*. [online] Available at: <https://vulcanpost.com/289811/local-sabahan-earthquake-aftermath-youre-probably-unaware/> [Accessed 7 June 2023]

Simone, W., 2022. *Using wood for good-how timber can help fight climate change*. [online] Available at: <https://www.creatingtomorrowsforests.co.uk/blog/using-wood-for-good-how-timber-can-help-fight-climate-change#:~:text=For%20a%20more%20detailed%20description,it%20decays%20or%20is%20burned.> [Accessed 15 December 2023]

Simscale, 2023. What is von mises stress?. [online] Available at: < https://www.simscale.com/docs/simwiki/fea-finite-element-analysis/what-is-von-mises-stress/> [Access 3 March 2024]

Simulia, n.d. Abaqus. [online] Available at: <https://www.3ds.com/products/simulia/abaqus> [Accessed 2 February 2024]

Skymet Weather Team, 2017. Earthquake: relation between magnitude and intensity decoded. [online] Available at: <https://www.skymetweather.com/content/weather-news-and-analysis/earthquake-relation-between-magnitude-and-intensity-decoded/> [Accessed 7 January 2024]

Southern Pine, 2023. *Why use wood-frame construction in seismic, high-wind zones?*. [online] Available at: <https://www.southernpine.com/why-use-wood-frame-construction-in-seismic-high-wind-zones/#:~:text=Wood%2Dframe%20construction%20performs%20exceptionally,that%20provide%20redundant%20load%20paths.> [Accessed 15 December 2023]

Sovester, H. and Adiyanto, M., n.d. Seismic performance of reinforced concrete school buildings in Sabah.

Swiss Seismological Service, n.d. *Causes of earthquakes in general*. [online] Available at: <http://www.seismo.ethz.ch/en/knowledge/things-to-know/causes-of-earthquakes/general/> [Accessed 6 June 2023]

Tanja, K. and Marijana, H., 2017. Rapid seismic risk assessment. *International Journal of Disaster Risk Reduction*, 24(2017), pp. 348-360.

Uchida, N. and Matsuzawa, T., 2011. Coupling coefficient, hierarchical structure, and earthquake cycle for the source area of the 2011 off the Pacific coast of Tohoku earthquake inferred from small repeating earthquake data. *Earth, Planets and Space*, 53(7), pp. 675-679.

USGS, n.d. What are the effects of earthquakes?. [online] Available at: <https://www.usgs.gov/programs/earthquake-hazards/what-are-effects-earthquakes#:~:text=The%20effects%20from%20earthquakes%20include,%2C%20and%20less%20commonly%2C%20tsunamis.> [Accessed 22 December 2023]

USGS, n.d. *What is an earthquake and what causes them to happen?*. [online] Available at: <https://www.usgs.gov/faqs/what-earthquake-and-what-causes-them-happen#:~:text=The%20tectonic%20plates%20are%20always,the%20shaking%20that%20we%20feel.> [Accessed 6 June 2023]

USGS, n.d. *Where do earthquakes occur?*. [online] Available at: <https://www.usgs.gov/faqs/where-do-earthquakes-occur#:~:text=The%20world's%20greatest%20earthquake%20belt,our%20planet's%20largest%20earthquakes%20occur.> [Accessed 22 December 2023]

Vasudha, J., 2021. *A study of the 2004 Indonesian tsunami: the effects on GDP growth and tourism post-disaster.* [Unpublished Bachelor thesis]. Scripps College.

Volcano Hazards Program, n.d. The modified Mercalli intensity (MMI) scale assigns intensities as. [online] Available at: <https://www.usgs.gov/media/images/modified-mercalli-intensity-mmi-scale-assigns-intensities> [Accessed 10 January 2024]

Wang, P., 2020. *Mortise and tenon structure of T-shaped wall constructional column and construction method.*

Wilde Pdsvision, n.d. Ansys structural analysis. [online] Available at: <https://wildeanalysis.co.uk/software/design-simulation/ansys/structures/> [Accessed 2 February 2024]

World Vision, 2023. 2023 Turkey and Syria earthquake: facts, FAQs, and how to help. [online] Available at: <https://www.worldvision.org/disaster-relief-news-stories/2023-turkey-and-syria-earthquake-faqs#:~:text=courtesy%20of%20USGS)-,How%20many%20people%20were%20affected%20by%20the%20earthquake%20in%20Turkey,in%20need%20of%20urgent%20aid.> [Accessed 7 June 2023]

World Vision, 2023. Haiti earthquake: facts, FAQs, and how to help. [online] Available at: <https://www.worldvision.org/disaster-relief-news-stories/haiti-earthquake-facts#:~:text=Striking%20near%20Petit%2DTrou%2Dde,capital%2C%20claiming%20approximately%20300%2C000%20lives.> [Accessed 7 June 2023]

Wu, G., Zhang, K., Wang, C., & Li, X., 2023. Nucleation mechanism and rupture dynamics of laboratory earthquakes at different loading rates. *Appl. Sci.* 13(22), 12243.

Yena Engineering BV, 2023. *Choosing the right structural steel.* [online] Available at: <https://www.linkedin.com/pulse/choosing-right-structural-steel-yenaengineering#:~:text=S275%20steel%20is%20known%20for,choice%20for%20outdoor%20construction%20projects.> [Accessed 10 April 2024]

Yukutake Y., Takeda T. and Obara K., 2008. Fine fault structure of a moderate earthquake in the 2007 earthquake sequence of Northern Mie, Japan. pp. 981-985.

APPENDICES

Damage Grade	EMS-98 [4]	Representative buildings
D0: None damage	–	
D1: Slight damage		
D2: Moderate damage		
D3: Heavy damage		
D4: Very heavy damage		
D5: Destruction		

Appendice A: Buildings of different damage grade.
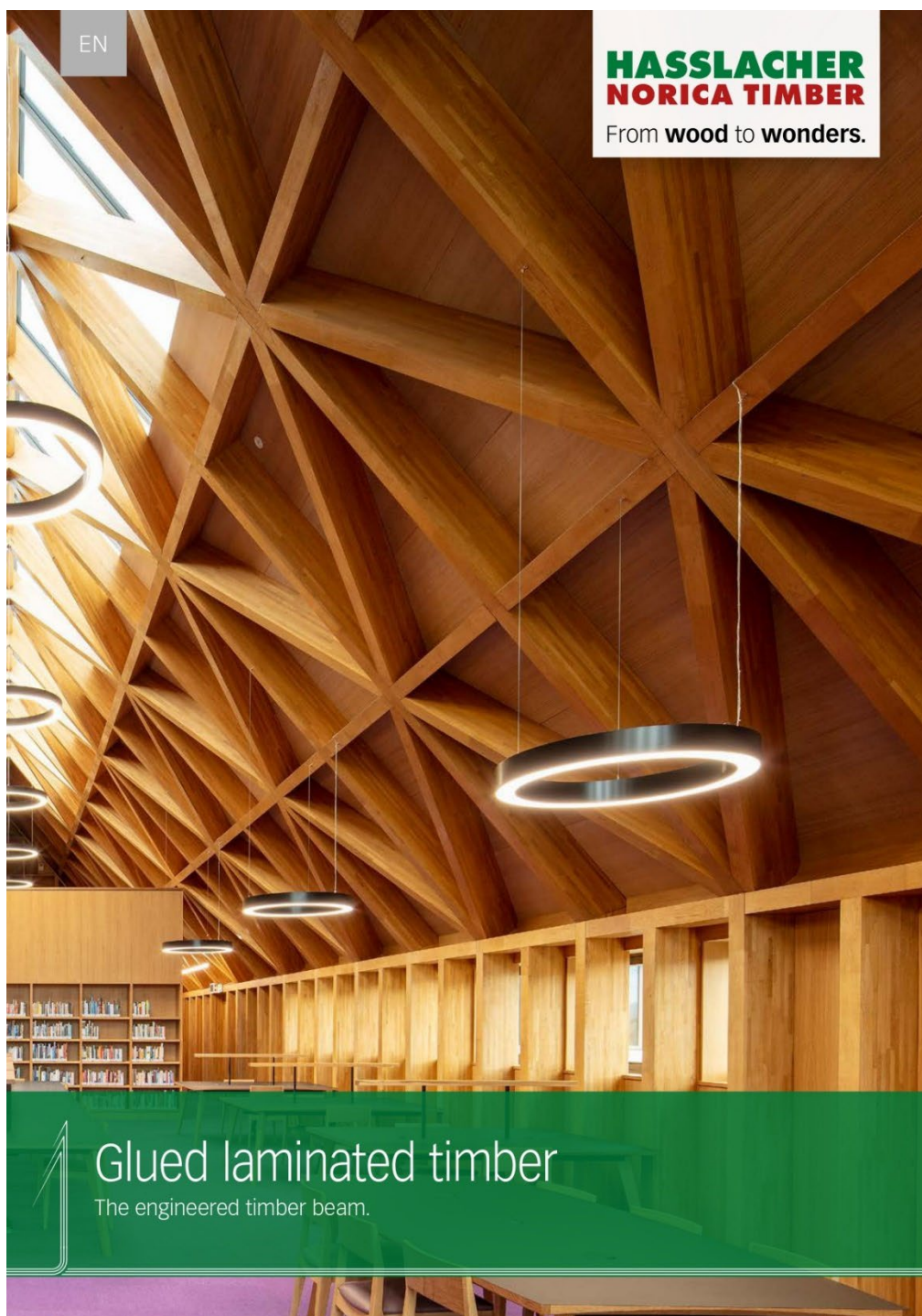
Appendice B: Catalog of Glued Laminated Timber.

07
Mechanical properties

Glued Laminated Timber – Mechanical properties

characteristic strength and stiffness properties for homogeneous glued laminated timber

Strength class		GL20h	GL24h	GL28h	GL30h	GL32h
Bending strength	$f_{m,g,k}$	20	24	28	30	32
Tensile strength	$f_{t,0,g,k}$	16	19.2	22.3	24	25.6
	$f_{t,90,g,k}$			0,5		
Compressive strength	$f_{c,0,g,k}$	20	24	28	30	32
	$f_{c,90,g,k}$			2.5		
Shear strength	$f_{v,g,k}$			3.5		
Rolling shear strength	$f_{r,g,k}$			1.2		
Modulus of elasticity	$E_{0,g,mean}$	8,400	11,500	12,600	13,600	14,200
	$E_{0,g,05}$	7,000	9,600	10,500	11,300	11,800
	$E_{90,g,mean}$			300		
	$E_{90,g,05}$			250		
Shear modulus	$G_{g,mean}$			650		
	$G_{g,05}$			540		
Rolling shear modulus	$G_{r,g,mean}$			65		
	$G_{r,g,05}$			54		
Density	$\rho_{g,k}$	340	385	425	430	440
	$\rho_{g,mean}$	370	420	460	480	480

Characteristic strength and stiffness properties for combined glued laminated timber

Strength class		GL24c	GL28c	GL30c	GL32c
Bending strength	$f_{m,g,k}$	24	28	30	32
Tensile strength	$f_{t,0,g,k}$	17	19.5	19.5	19.5
	$f_{t,90,g,k}$		0.5		
Compressive strength	$f_{c,0,g,k}$	21.5	24	24.5	24.5
	$f_{c,90,g,k}$		2.5		
Shear strength	$f_{v,g,k}$		3.5		
Rolling shear strength	$f_{r,g,k}$		1.2		
Modulus of Elasticity	$E_{0,g,mean}$	11,000	12,500	13,000	13,500
	$E_{0,g,05}$	9,100	10,400	10,800	11,200
	$E_{90,g,mean}$		300		
	$E_{90,g,05}$		250		
Shear modulus	$G_{g,mean}$		650		
	$G_{g,05}$		540		
Rolling shear modulus	$G_{r,g,mean}$		65		
	$G_{r,g,05}$		54		
Density	$\rho_{g,k}$	365	390	390	400
	$\rho_{g,mean}$	400	420	430	440

Appendice C: Mechanical properties of Glulam.